AER/AGS Open File Report 2015-10

Alberta Energy Regulator

Turtle Mountain Field Laboratory, Alberta (NTS 82G): 2014 Data and Activity Summary

AGS
ALBERTA GEOLOGICAL SURVEY

AER/AGS Open File Report 2015-10

Turtle Mountain Field Laboratory, Alberta (NTS 82G): 2014 Data and Activity Summary

D.E.Wood, D.K. Chao and T.C. Shipman

Alberta Energy Regulator
Alberta Geological Survey

February 2016

ISBN 978-1-4601-0151-3

Wood, D.E., Chao, D.K. and Shipman, T.C. (2016): Turtle Mountain Field Laboratory, Alberta (NTS 82G): 2014 data and activity summary; Alberta Energy Regulator, AER/AGS Open File Report 2015-10, 91 p.

Published February 2016 by:
Alberta Energy Regulator
Alberta Geological Survey
4th Floor, Twin Atria Building
4999 – 98th Avenue
Edmonton, AB T6B 2X3
Canada

Tel: 780.638.4491
Fax: 780.422.1459
E-mail: AGS-Info@aer.ca
Website: www.ags.gov.ab.ca

Contents

Tables

Figures

Acknowledgements

We acknowledge the following colleagues and collaborators who have contributed either to the operation, maintenance, or studies of the Turtle Mountain monitoring system during 2014:

- J. Warren (Alberta Energy Regulator, Alberta Geological Survey, Edmonton, AB)
- C. Froese (Alberta Energy Regulator, Alberta Geological Survey, Edmonton, AB)
- A. Kao (Alberta Energy Regulator, Calgary, AB)
- J. Guo (Alberta Energy Regulator, Calgary, AB)
- G. Bjorgan (NavStar Geomatics Ltd., Kelowna, BC)
- C. Rivolta (Ellegi srl, Milano, Italy)
- D. Leva (Ellegi srl, Milano, Italy)
- I. Binda Rosetti (Ellegi srl, Milano, Italy)
- S. Alberti (Ellegi srl, Milano, Italy)
- O. Hungr (Geotechnical Research Inc., West Vancouver, BC)
- J. Aaron (Geotechnical Research Inc., West Vancouver, BC)
- M. Jaboyedoff (University of Lausanne, Lausanne, Switzerland)
- F. Humair (University of Lausanne, Lausanne, Switzerland)
- J. Farrugia (Alberta Energy Regulator, Alberta Geological Survey, Edmonton, AB)
- R. Dokht (Alberta Energy Regulator, Alberta Geological Survey, Edmonton, AB)
- J. Yusifbayov (Alberta Energy Regulator, Alberta Geological Survey, Edmonton, AB)
- R. Rinaldi (Randy Rinaldi Welding Ltd., Frank, AB)
- J. Pawluck (Randy Rinaldi Welding Ltd., Frank, AB)
- D. Cox (Cox Electric, Blairmore, AB)
- Municipality of Crowsnest Pass Council Members (Crowsnest Pass, AB)
- Frank Slide Interpretive Centre Staff (Crowsnest Pass, AB)

The authors also wish to acknowledge the technical review and layout completed by editor A. Dalton. A special thanks to M. Grobe who carried out the scientific review, providing many improvements to the report.

Abstract

Since 2005, Turtle Mountain has been the site of ongoing monitoring and research focused on understanding the structure and kinematics of movements of the unstable eastern slopes. As this site provides a rich dataset and optimal conditions for the application of new and evolving warning and characterization technologies, the site has been termed the 'Turtle Mountain Field Laboratory.' This report provides a summary of both the results and the lessons learned from the Turtle Mountain monitoring system (TMMS) and from studies undertaken by the Alberta Geological Survey (AGS) and collaborators between January 1 and December 31, 2014.

The TMMS is a near-real-time monitoring system that provides data from a network of eight geotechnical sensors on South Peak of Turtle Mountain (site of the 1903 Frank Slide) in the Crowsnest Pass. As of April 1, 2005, the AGS took ownership of this system and the responsibility for long-term monitoring, interpretation of data, and notification of the Alberta Emergency Management Agency should significant movements occur.

As part of this responsibility, the AGS performs an annual detailed review of the data stream. To help in this interpretation, the AGS initiated specific studies to better understand the structure of the mountain and its relationship to the style and rate of movement seen in recent and historical deformations of South Peak. These studies also better define the unstable volumes of rock from the South Peak and Third Peak areas.

This report comprises four main sections.

The first section contains information about the major changes to the TMMS's network during the 2014 field season. This includes a review of the main repair and maintenance activities, a summary of new installations and abandoned stations, and a summary of system performance and reliability.

The second section provides data analysis for the primary, secondary, and non-operational instruments. These interpretations include slope conditions and displacement behaviour from instrumentation results. Since weather factors have affected some of the sensors, this discussion focuses only on the sensors that have provided reliable annual data. The installation of the new secondary instrumentation, LiSAmobile, is described.

The third section reviews the report by O. Hungr on the runout analysis for two potential landslides originating from North Peak of Turtle Mountain. Hungr's report outlines work carried out for the AGS to supplement recommendations from the 2013 expert panel report.

The fourth section discusses the expert panel report itself. This report was prepared for the AGS to provide recommendations for the current and future Turtle Mountain Field Laboratory program. The report outlines the mountain site characterization and hazard assessment, reviews the early warning monitoring system practices, and makes recommendations for the future of the program.

1 Introduction

In 2005, the Alberta Geological Survey (AGS) assumed responsibility for the long-term monitoring and studying of a large, slowly moving rock slide at Turtle Mountain, the site of the 1903 Frank Slide (Figure 1, Figure 2). The first priority for monitoring and studying Turtle Mountain is to provide an early warning to residents of the Crowsnest Pass in the event of a second catastrophic rock avalanche originating from South Peak. The secondary priority is to provide an opportunity for the research community to test and develop instrumentation and monitoring technologies and to better understand the mechanics of slowly moving rock masses, hence the working name 'Turtle Mountain Field Laboratory' (TMFL). The AGS will make available to the research community all data from the TMFL, which will enable researchers to test and develop new monitoring technologies for the mountain. This ongoing research will aid in understanding the movements of the entire South Peak mass, including the lower slope and more recently North Peak, thereby providing a better model for prediction of future movements.

This annual report provides the public and researchers with a synthesized update on data trends and research on the mountain as a stimulus for further study. This report is a brief overview and refers to other papers and articles that provide additional detail regarding the information discussed.

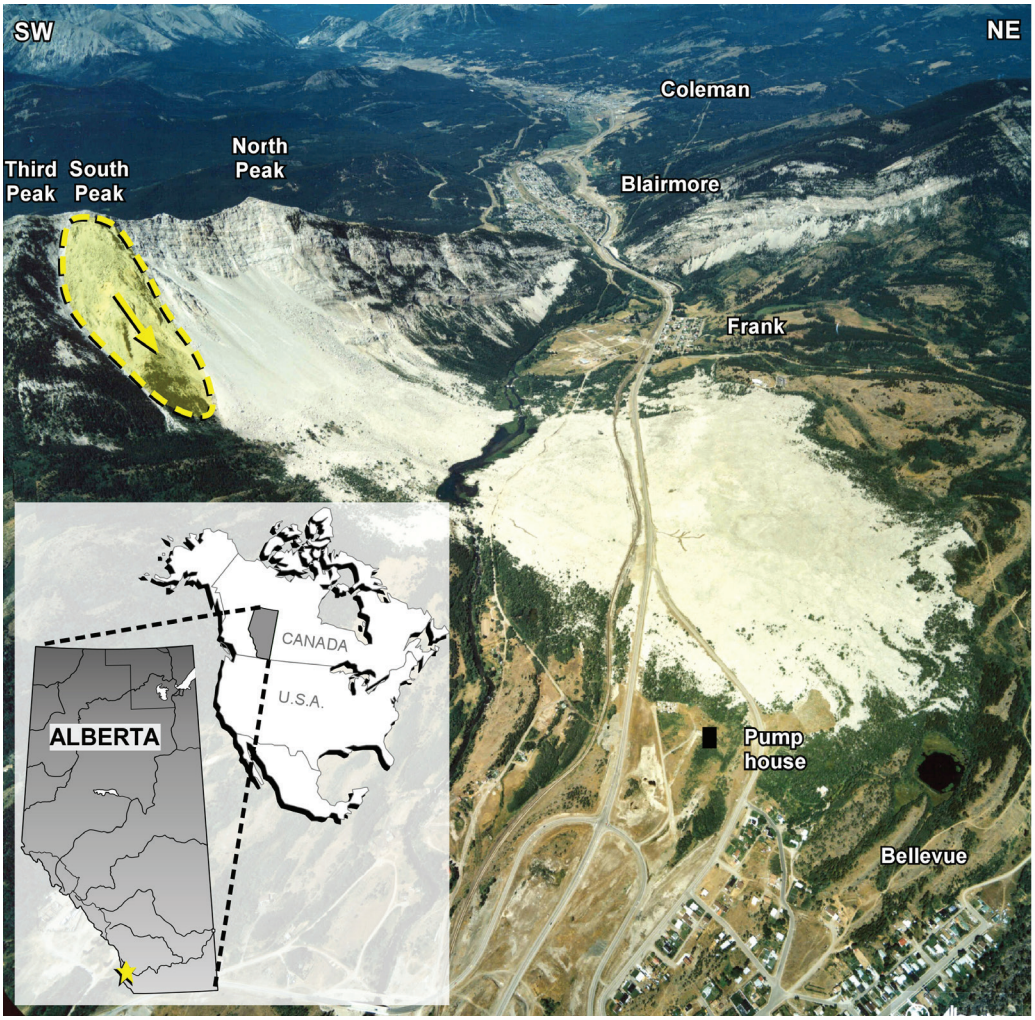

Figure 1. Location of Turtle Mountain in southwestern Alberta and full-extent aerial view of the Frank Slide. The dashed line below South Peak outlines the area identified by Allan (1931, Figure 2) as being most unstable.

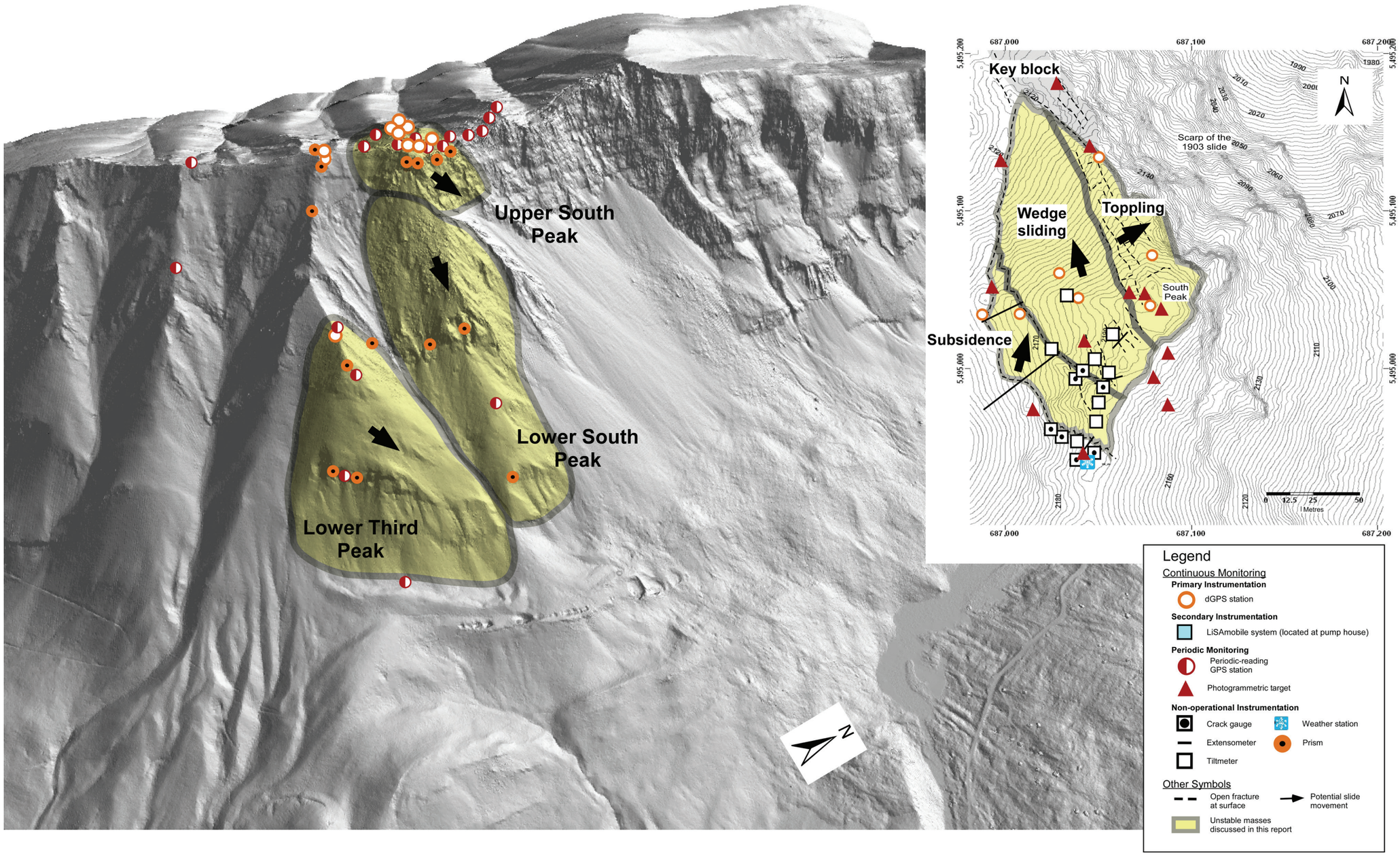

Figure 2. Overview, as of December 2014, of the monitoring network on Turtle Mountain as a whole and South Peak of Turtle Mountain in particular (inset). For readability, primary monitoring instrumentation is shown only on the inset.

2 Sensor Network Activity

This section provides an overview of the major upgrades, repair, maintenance activities, and performance of the sensor network of the monitoring system during 2014. Documentation of the hardware that makes up the various components of the communication stations was provided in Moreno and Froese (2006, 2008a) and is therefore not included in this summary.

The main activities undertaken with respect to the sensor network during 2014 included

- equipment upgrades for the WiFi access points for the dGPS,
- improvements to the Internet service,
- modifications to the continuous and periodic monitoring instrumentation use, and
- installation of the LiSAmobile ground-based interferometric synthetic aperture radar (GB-InSAR) equipment.

Due to the poor quality and reliability of data collection from the primary sensors, AGS discontinued the use of the extensometers, crackmeters, and tiltmeters. Increased weather complications throughout the year have caused the primary sensors to fail often. The replacement and upgrading of the primary sensors are costly and difficult to manage due to the environmental conditions on the mountain. Data will continue to be obtained from the primary sensors on a daily basis; however, only a few sensors are currently operational. A subscription to a third-party monitoring sensor system, Atlas Monitoring, was cancelled in March 2014. This subscription did not provide the program with vital sensor information as most sensors are currently inoperable.

NavStar Geomatics Ltd. (NavStar) dGPS became the primary sensors for the TMMS in 2014 and provide up-to-the-minute status reports via e-mail and the desktop application GeoExplorer. When sensor thresholds are breached, the AGS reviews the data with input from NavStar to determine if the threshold was broken due to sensor malfunction or actual movement.

Ellegi srl. leased a GB-InSAR system known as LiSAmobile to the AGS for a one-year probationary period, giving us time to review the equipment and monitoring system. Over this period, we have received monthly data updates and monitoring reports on a quarterly basis. The quarterly report is reviewed by the TMFL team and then is compared to the dGPS results provided by NavStar. The AGS's lease with Ellegi provides for customer service and technical support in case of emergency or equipment changes.

2.1 Upgrades and Repairs

2.1.1 Turtle Mountain Hardware and Software Upgrades

In 2014, the computer hardware at the Blairmore Provincial Building was replaced to allow for the AER-wide installation of Windows 7. The upgraded hardware included a new Internet gateway (Figure 3) from CheckPoint Software Technologies Ltd. This Internet gateway is more secure and allows us to provide virtual private network (VPN) access to our network to both Ellegi and NavStar.

While it was anticipated that the hardware and operating system upgrades would alleviate system connectivity issues, the system continued to experience problems, requiring manual restarts in some cases.

NavStar conducted minor software upgrades to GeoExplorer throughout 2014, although no major changes were made to the application.

Figure 3. CheckPoint Software Technologies Ltd. Internet gateway, installed at the Blairmore Provincial Building in May 2014.

2.1.2 dGPS Upgrades

In 2014, no dGPS hardware was upgraded or repaired by the AGS or NavStar. On September 6, 2014, we lost contact with the Third Peak B station. The problem is currently being investigated by the AGS and NavStar. NavStar suggests that a possible explanation for the outage may be outdated station firmware. NavStar has made multiple unsuccessful attempts to bring the Third Peak B station online remotely. A possible solution would be to manually update the firmware, which would require a site visit.

The situation is being monitored closely, but any trip to the stations has been postponed until spring 2015 due to early snow fall settling on the mountain top, which is a safety concern.

2.1.3 Non-operational Instruments

After reviewing the 2013 instrument data, we decided that the use of certain instruments would be discontinued in the 2014 season. This was based on different underlying issues with each instrument (described below). The term 'non-operational instrument' includes instruments that are abandoned because they are damaged or produce only poor-quality data. Some non-operational instrumentation may still be collecting sporadic data, but such data will not be used by the TMFL. We will reassess non-operational instruments in 2015 and determine if they can be repaired or otherwise made fully operational, or if the equipment should be decommissioned and removed.

2.1.3.1 Weather Station

Despite previous attempts at replacing instruments on the weather station, the AGS decided not to repair the station during the 2014 field season. The instruments require frequent maintenance and are not considered a critical data source for monitoring.

In March 2014, we lost communication with the weather station. Various attempts to bring the station back online were made remotely from Edmonton. The weather station began recording and sending data sporadically (about once a week), but these data appear to be corrupt and incomplete.

A snow storm in early October 2014 caused the remaining operational instruments to fail. Attempts were made to bring the station back online remotely from Edmonton. The weather station's status is currently under review. This review will decide if the station will be repaired during the 2015 field season or if the equipment will remain non-operational and be decommissioned.

2.1.3.2 Crackmeters

All fifteen crackmeters (CkMt) became non-operational over the course of 2013 and 2014. Due to the lack of accurate data, the crackmeter network was abandoned for the 2014 field season.

2.1.3.3 Tiltmeters

Six out of ten tiltmeters (T) were operational and reporting data from January to March 2014. The non-operational tiltmeters are assumed to have been damaged by weather events in 2012 and 2013. Due to the lack of accurate data, the tiltmeter network was abandoned for the 2014 field season.

2.1.3.4 Extensometers

Extensometers (EX) EX-1, EX-2, EX-3, and EX-4 were damaged by weather events in 2012 and 2013, rendering all extensometers non-operational for 2014. No maintenance or repair was performed on the equipment.

2.2 Performance

Continuous slope monitoring is very difficult in the harsh and highly variable weather conditions on Turtle Mountain. However, the effects of these adverse conditions on the normal operation of the monitoring system are minimized with a series of preventive measures, including frequent inspections, replacement of aging equipment, and system modifications and upgrades. This section provides detailed information on sensor performance in 2014.

The TMMS has been operational for more than ten years. This has enabled us to understand not only the challenges of maintaining a reliable and continuously running system but also to identify the factors that affect the normal operation of the monitoring network. For the primary sensor network (crackmeters, tiltmeters, extensometers), we find that factors such as high humidity in tiltmeters, snow loading on crackmeters, and lightning strikes can severely affect the instruments' ability to operate. To mitigate the effects of these environmental factors, desiccant packs have been put inside tiltmeter enclosures, protective roofs have been installed over each crackmeter array, and lightning protection has been added to all sensors. These measures have yielded mixed results. While desiccant packs have helped improve tiltmeter reliability considerably, the protective roof has been able to protect the crackmeters against snow loading only in a few cases. None of the different measures taken to protect the primary sensor network against electrical surges has worked well, thus making lightning strikes the main cause of sensor damage. On average, two lightning events that are capable of causing sensor damage are recorded each year. Each event can leave up to 50% of the primary system disabled, and the cost of repairing this equipment is high.

For these reasons, despite extended attempts at repairing and protecting the various meters, we have decided that the TMMS primary sensors will no longer be used. Instead, the continuous-reading dGPS stations will now be the TMMS's primary sensor instrumentation, and LiSAmobile will be the new secondary sensor instrumentation.

2.2.1 New Primary Sensor: Continuous-Reading dGPS Monitoring System

The new primary sensor network consists of the continuous-reading dGPS system supported by NavStar. The system is still vulnerable to large amounts of precipitation and can produce inaccurate results. The dGPS system performed reasonably well during the 2014 reporting period with few interruptions in service.

NavStar advised that a dGPS firmware upgrade should be installed to enhance the connectivity in 2015. The firmware upgrade is being planned for the spring maintenance trip in 2015.

2.2.2 New Secondary Sensor: LiSAmobile GB-InSAR

2.2.2.1 Ellegi Contract and Installation

The newly installed LiSAmobile system was leased to AGS for the 2014 season by Ellegi of Milano, Italy. The LiSAmobile system is an advanced ground-based InSAR instrument (GB-InSAR) and is the new secondary sensor. Contact was made with Ellegi in 2013 to gain information on replacing the previous IDS (Ingegneria Dei Systemi) IBIS GB-InSAR system, which did not produce satisfactory results in the 2012 and 2013 field seasons. Ellegi had a preliminary visit to Turtle Mountain to review the parameters of the TMMS in October 2013. A feasibility study was provided to the AGS in November 2013 with recommendations for the LiSAmobile system that would potentially be installed in 2014. The contract between Ellegi and the AGS was signed in May 2014 with the following services outlined:

- 12 months of leasing services of one LiSAmobile system,
- specialized engineer or technician for installation of the system and adjustment of parameters,
- all components and installation tools required for initial installment of equipment,
- one on-site visit per contract year for equipment maintenance,
- remote assistance with maintenance and operation of LiSAmobile equipment and data processing,
- quarterly reports with analysis and displacement maps, and
- 3D georeferenced displacement maps in electronic format.

Installation of the LiSAmobile system was scheduled for June 16–20, 2014. Before the installation, additional upgrades to the TMMS network system and to the physical building location were needed. See Section 2.1.1 for additional network system upgrade information.

2.2.2.2 Upgrades to the Pump House Building

The LiSAmobile system required the installation of a conduit pipe on the northwest side of the building. Installation of a conduit pipe (Figure 4) allowed for the LiSAmobile system's umbilical cord to run from the equipment on the roof to the power source (Figure 5) inside the pump house building. Cox Electric was contracted to install the conduit pipe. Upon assessment, it was determined that zonolite (a type of asbestos) could be present in the concrete wall. Because we could not be certain either way, all the material had to be presumed contaminated. Once the material was removed, foam was sprayed onto the wall, creating a barrier to avoid any future contamination. Next, a 3″ conduit was installed from the roof to the base of the building, where a weather box was connected. A weather head was also installed on the roof to prevent water entering the conduit. The weather box allowed for a break in the pipe system for future inspections of cables without having to remove the system cables entirely. An additional hole was drilled into the bottom of the weather box to allow for moisture or condensation to drain.

2.2.2.3 Fabrication of Materials and Installation of LiSAmobile

Due to the LiSAmobile system being substantially larger than the previous IDS IBIS GB-InSAR system, the layout of the system had to be altered. The newly established Municipality of Crowsnest Pass Council recommended that building permits, schematics, and applications be required for any further work on altering the building. The TMFL team met with the Municipality of Crowsnest Pass building inspector, planning engineer, and chief administrative officer. Ultimately the municipality decided that permits would be waived in 2014 due to the nature of the program and that the integrity of the building would not be altered.

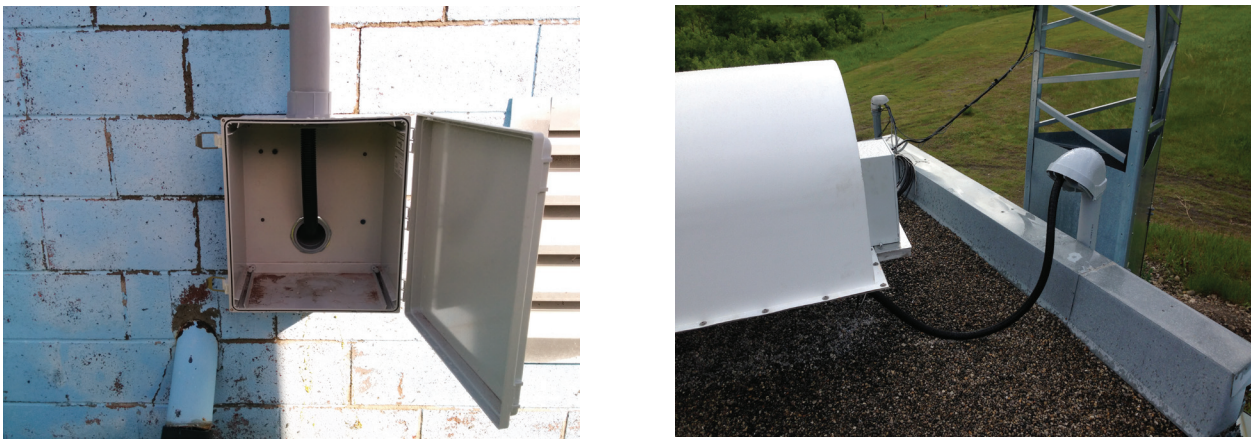

Figure 4. Installed 3″ conduit pipe, weather box (left), and weather head (right) located at Bellevue pump house. Location of the LiSAmobile system.

Figure 5. Power box located inside the pump house building and connected to the LiSAmobile system on the pump house roof.

Randy Rinaldi Welding Ltd. was contracted to fabricate all metal materials required and provide installation services, such as welding and assembly, for the LiSAmobile system. The AGS purchased the following from Randy Rinaldi Welding Ltd.:

- 1 metal base plate,
- 1 aluminum base plate,
- 1 pedestal,
- 2 steel plates,
- 3 bracket extensions, and
- all fasteners required.

Some of the IDS IBIS system infrastructure could be reused. The existing "L" brackets were removed from the building and altered to extend the length of the bracket to incorporate the new pedestal. The "L" brackets were repositioned on the southwest side of the building for the best possible trajectory angle. Next, two steel plates were anchored onto the "L" brackets to provide a larger base for the pedestal. The pedestal was mounted onto the steel plates then levelled (Figure 6). The necessary small adjustments to balance the pedestal were achieved by repositioning the fasteners. Once the pedestal measured at near zero or zero degrees from horizontal, the pedestal's installation position was marked with chalk and the pedestal was removed.

Next, the aluminum base plate was installed for the enclosure (radome) that would protect the system from environmental factors. Two slits were cut into the aluminum base plate to allow for slight adjustments to the system's trajectory angle. Additional holes were drilled into the aluminum base plate for the power and fibre optics umbilical cable. Once the Ellegi engineer was satisfied with the trajectory angle, the pedestal was aligned with the chalked marks and fastened to the steel plates.

The radome consists of two semicircular dome segments made of fibreglass (Figure 7), which allows the radar head to transmit and receive signals while providing protection from the weather. The radome was fastened flush against the aluminum base plate to fully enclose the LiSAmobile system. The radome was fastened with sixty bolts that require a specialized tool to install or remove.

After a year, the performance of the radome will be assessed to determine if it is suited for Alberta's mountain climate or if other materials (e.g., wood and microwave window film) should be used in its construction.

Finally, a heating and air conditioning unit was installed to keep a consistent temperature of approximately 22°C within the radome for optimal working conditions. Within the first four months of testing, the temperature within the radome fluctuated between 15 and 30°C, which, according to Ellegi, is considered an acceptable range. The performance of the temperature regulation unit will be reviewed

Figure 6. Pedestal installation for optimal trajectory angle of LiSAmobile radar head (photos courtesy of Ellegi).

a)

b)

Figure 7. (a) LiSAmobile system without radome and temperature regulation unit; (b) LiSAmobile system completely assembled (photos courtesy of Ellegi).

in 2015 to determine if the heating and cooling of the LiSAmobile system was adequate under extreme temperature conditions in the summer and winter.

2.2.2.4 Initial Start-Up of LiSAmobile System

After some preliminary testing, the Ellegi engineer ran multiple scans (Figure 8) and tests over a 24-hour period that determined that the system was installed correctly. The Ellegi engineer was able to successfully scan the mountain and obtain radar images for processing.

3 Data Analysis

3.1 Deformation Monitoring Data

3.1.1 Crackmeters

The continuously recording crackmeters were installed to determine whether the surface fractures open at constant rates or rapidly in one event. However, as already stated in Section 2.2, these sensors are sensitive to snow and ice loading, which introduces large errors in the readings. The crackmeters were non-operational in 2014 due to lightning damage and have not been replaced. Therefore, no 2014 displacement data was available to analyze. The crackmeter network will remain non-operational until further notice.

The reader may refer to earlier reports (from 2005 to 2012) for historical information and graphs.

3.1.2 Tiltmeters

The tiltmeter network was intended to provide data that would allow for a better understanding of the rotating component of the displacements. This system, consisting of ten sensors, was installed in 2005 by AMEC Earth and Environmental (2005). The sensors are located in two clusters: one at the sliding wedge and the other at the subsiding zone behind the sliding wedge. Spatial coverage is therefore limited, and no sensors are located within the most active part of the rock mass at the northeastern part of South Peak. Six tiltmeters were operational and recording data during January to March 2014.

Some of the sensors show the effects of high humidity inside the instrument enclosure, making the interpretation of small rotations very difficult. In previous years, all sensors showed annual fluctuations (but with no long-term cumulative rotations) and diurnal fluctuations associated with daily air temperature cycles. The 2014 tiltmeter data have not been processed due to inaccuracies and missing data.

The reader may refer to earlier reports (from 2005 to 2013) for historical information and graphs.

3.1.3 Extensometers

Extensometer data were collected during 2014 but are considered nonviable.

The reader may refer to earlier reports (from 2005 to 2013) for historical information and graphs.

3.1.4 Continuous-Reading dGPS Monitoring Network

To detail the history of displacements on active fractures, six single-frequency dGPS stations were installed near prominent fractures in 2008 (Moreno and Froese, 2008a). These Novatel SuperStar II dGPS units have millimetre resolution in the horizontal direction and centimetre resolution in the vertical

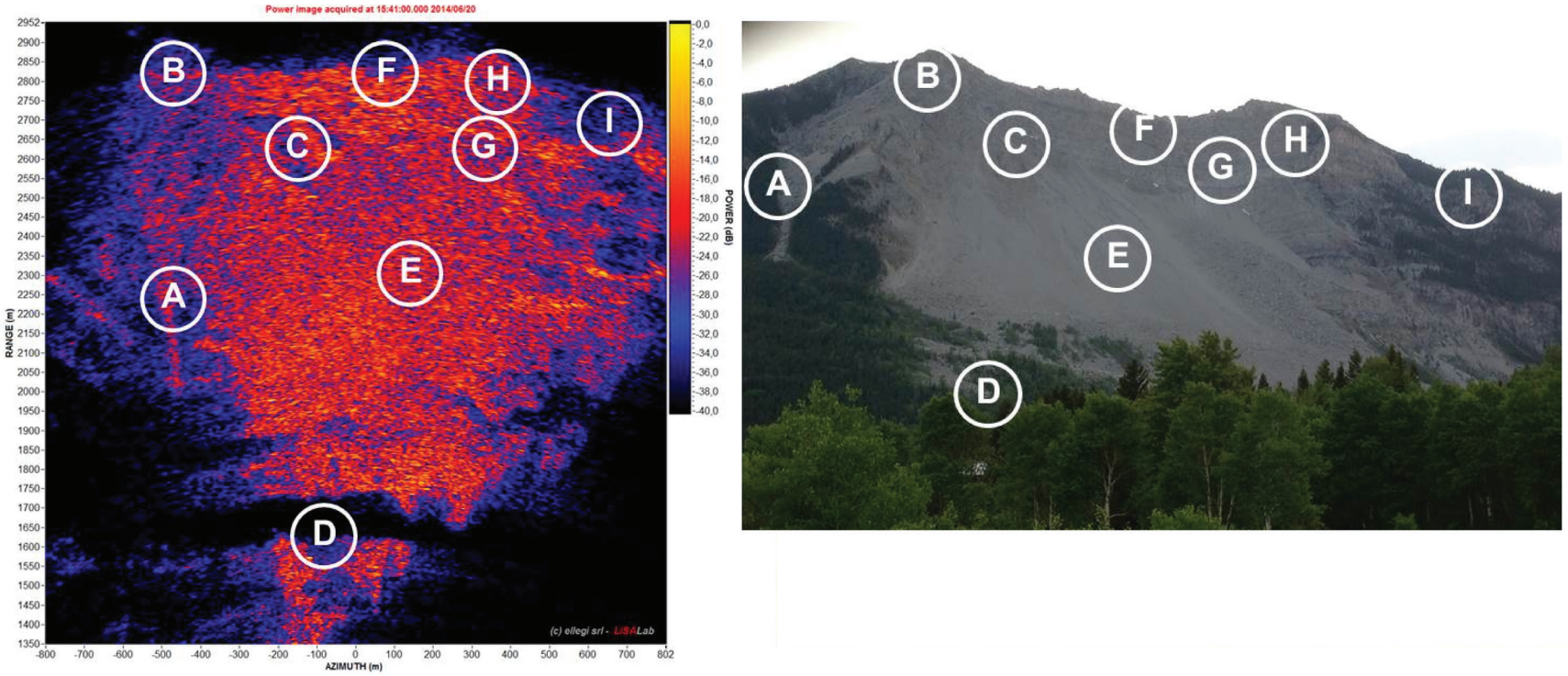

Figure 8. First image produced by the LiSAmobile system over the 24-hour testing period June 19–20, 2014.

direction. Later in 2008, this network was complemented with four dGPS stations: two on South Peak (in areas with the largest potential movements) and two on the middle to lower part of the eastern slope below South Peak (in areas of suspected movement; Figure 2).

The trends in displacement at the dGPS stations during 2014 (Figure 9 and Figure 10) are consistent with monitoring results of past years, which show seasonal variation without significant displacements associated with movement.

3.1.5 LiSAmobile GB-InSAR

In June 2014, a ground-based radar device was installed at the Bellevue pump house station (Figure 11) for monitoring small displacements on the east face of Turtle Mountain. The LiSAmobile GB-InSAR uses the interferometric synthetic aperture radar technique to measure small displacements at each point on the surface of the mountain face.

LiSAmobile consists of two main parts: the radar head and mechanical components. The radar head is an active radar sensor that transmits microwave pulses towards an object and receives in return a backscattered signal. The radar head, which consists of two antennas (transmit and receive), is attached to a linear positioner (cradle) mounted on a horizontal track. The travel distance of the radar head along the track can be adjusted to allow for optimal scanning coverage of the mountain face. The radar head travels back and forth along the 4 metre track once every ~8.5 minutes.

The LiSAmobile system is connected via the Internet through a WiFi connection that allows VPN access. The data is transferred to Ellegi via VPN to be processed. The initial upload connection speed was measured at approximately 50 kbps, which resulted in one image being downloaded every 5–10 minutes. New hardware was installed at the Blairmore Provincial Building to increase the speed of the connection (Section 2.1.1).

The LiSAmobile system obtains raw data from measurements from the radar head. With this raw data, both 2D and 3D assessments can be completed. The displacement maps produce a pixelated image of ground displacements that range from positive to negative values. Positive values indicate movement away from the radar head and the negative values indicate that the movement is towards the radar head. However, positive values can also result from vegetation growth or atmospheric moisture within the line of sight.

3.2 Discussion and Interpretation of Monitoring Data

Since the installation of most of the sensors in 2005 and 2006, new studies have improved our understanding of the complex slope deformations on South Peak. The model proposed by Froese et al. (2009) indicates that South Peak is moving as three different masses (Figure 2, inset): a toppling zone, with blocks moving to the east; a wedge zone that is sliding to the northeast; and a subsidence zone that is moving predominantly downward and to the west. The subsidence zone comprises the heavily fractured area on the west side of South Peak, where the majority of the sensors are located. The new understanding of the kinematics of these three separate masses has enabled a more critical evaluation of the movement trends measured by the sensors. This section is a discussion of the specific sensor trends in relation to the expected deformations.

3.2.1 Crackmeters

The time-series data of crack opening and temperature for the crackmeters deployed at Turtle Mountain have been described in earlier reports from 2005 to 2012. The historic displacement measurements

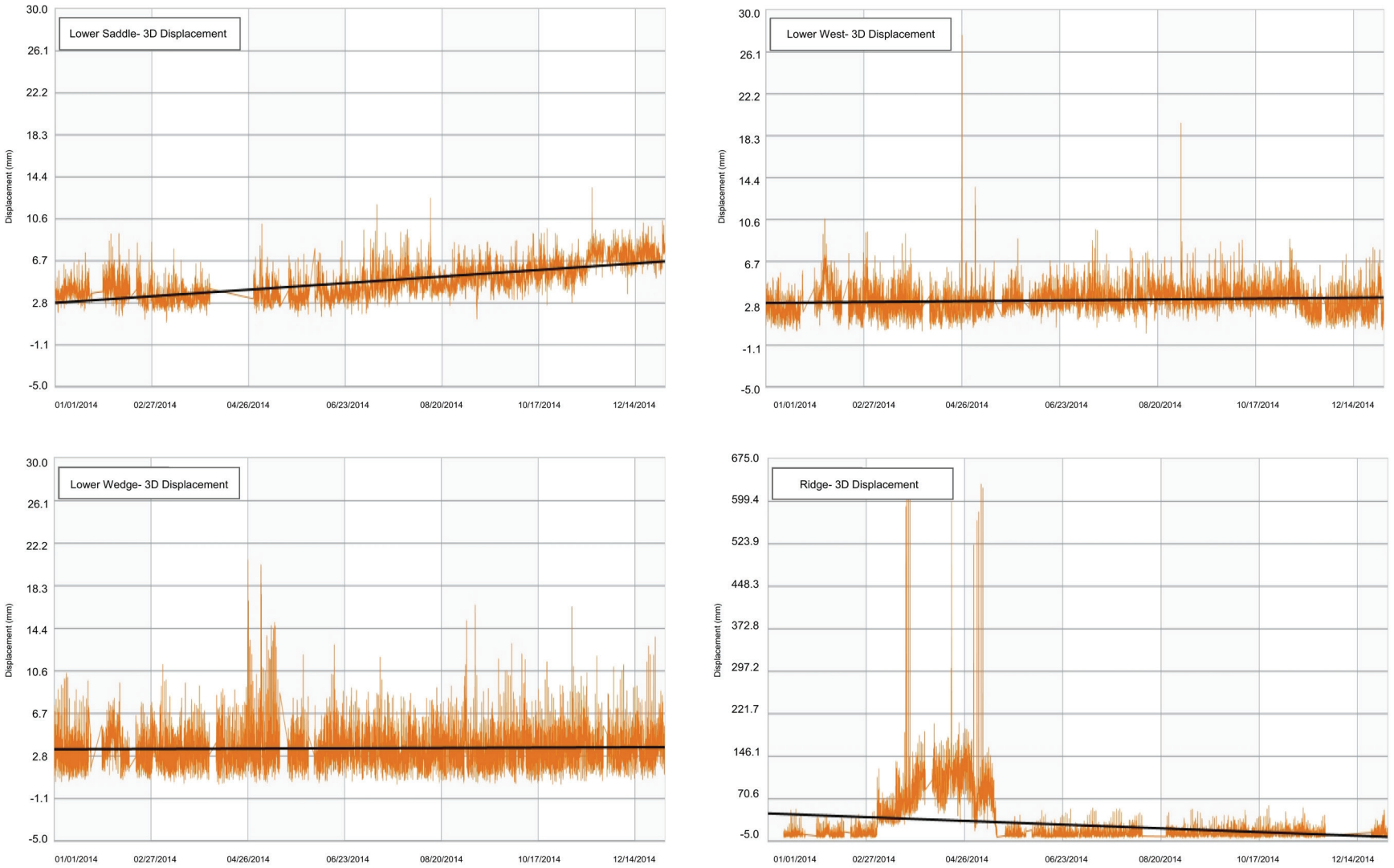

Figure 9. Surface displacements derived from dGPS stations during 2014.

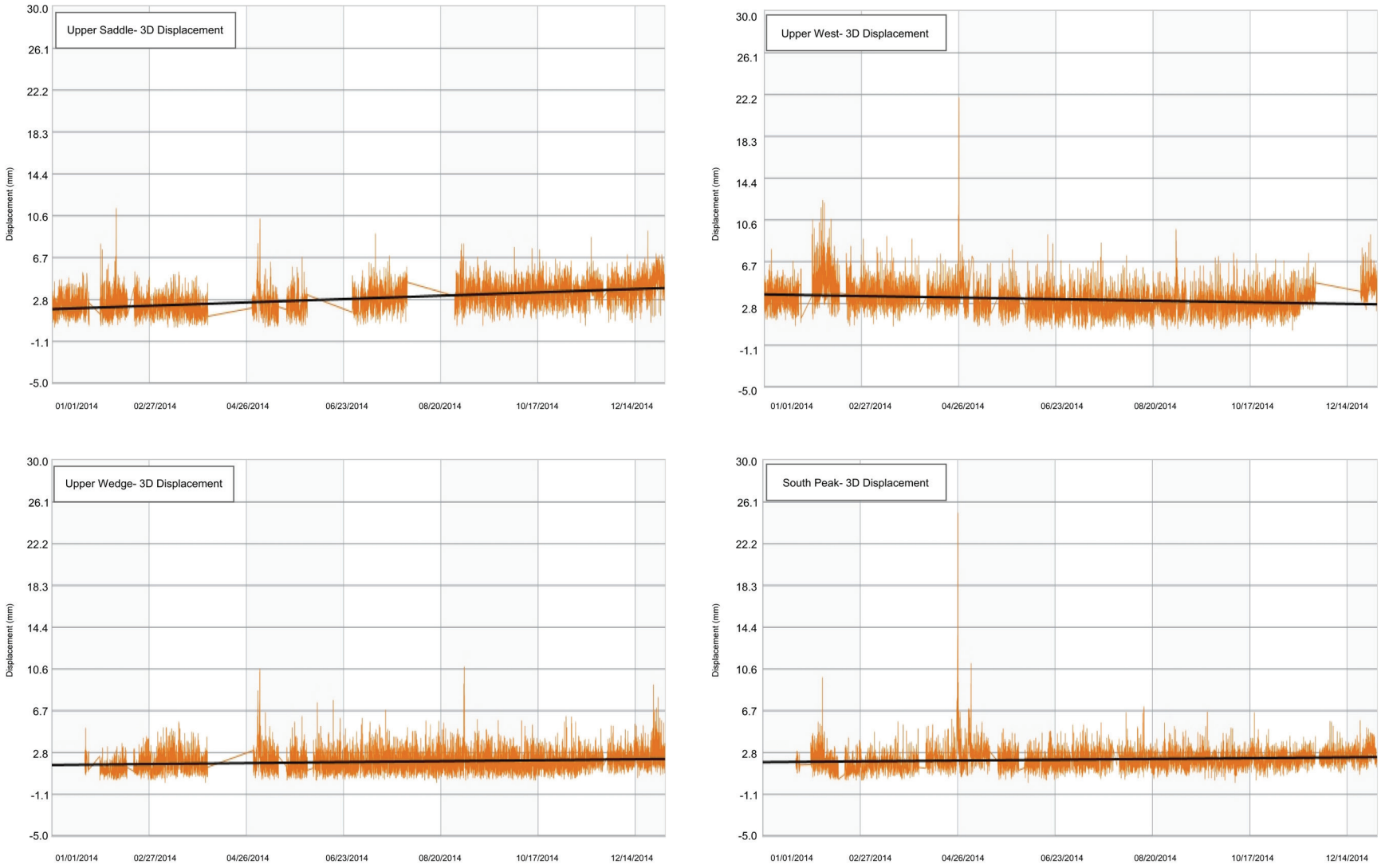

Figure 10. Surface displacements derived from dGPS stations during 2014.

Figure 11. LiSAmobile system at the Bellevue pump house station.

exhibited diurnal and annual cycles, which correlate with temperature cycles and are probably of thermoelastic origin. Because of the difficulties in maintaining this monitoring system (discussed in Section 3.1.1), the crackmeter monitoring system is largely non-operational and there is no plan to repair the system.

3.2.2 Tiltmeters

Most of the tiltmeters are in the subsidence zone. Therefore, we expect these sensors to register small displacements over time. Unfortunately, most of the tiltmeters display different degrees of noise in their readings, which makes the small displacements almost impossible to detect. Because of difficulties in maintaining this monitoring system (discussed in Section 3.1.2), the tiltmeter monitoring system is largely non-operational and there is no plan to repair the system.

3.2.3 Extensometers

The extensometer network does not have the same fine level of resolution as do the crackmeters and tiltmeters, so they are sensitive only to large displacements (many millimetres to centimetres). In addition, the installation of these sensors in the summer of 2004 preceded our new understanding of deformation kinematics on South Peak. These sensors measure only the component of displacement in the line of the sensor, but the movement in some cases is expected to be at oblique angles to the orientation of the extensometer. Therefore, we expect these sensors to identify displacements only during very large movements. Because of difficulties in maintaining this monitoring system, the extensometer monitoring system is largely non-operational and there is no plan to repair the system.

3.2.4 Continuous-Reading dGPS Monitoring Network

In contrast to the previous three sensor types, many of the more recent dGPS stations have been installed based our new understanding of the deformation mechanisms on South Peak and on other portions of the eastern face of Turtle Mountain.

During 2014, the dGPS monitoring network experienced various interruptions throughout the year due to varying weather conditions. Large storms that produced excessive rain and snow disabled the system temporarily at various times. A series of snow storms from March 2 through March 8, 2014, buried the equipment on top of Turtle Mountain as well as the weather station in the immediate vicinity. This resulted in a lack of precipitation data collected in the Crowsnest Pass area. Precipitation data was obtained from the closest operable station in Sparwood, British Columbia, which is approximately 35 km from Turtle Mountain.

On April 3, 2014, the dGPS monitoring network solar panels became covered in snow and were thus unable to recharge their batteries. Due to the risk of avalanche on the mountain top, it was decided that a recovery team would not travel up to remove snow. The TMMS network was closely monitored by the AGS and NavStar during this time. We decided to leave the solar panels covered and let the dGPS stations run on battery power until the batteries were fully discharged.

The Third Peak B battery became depleted on May 5, 2014, with 11.7 V remaining. This remaining voltage in the battery protects the battery from fully depleting and causing potential damage. On May 15, 2014, the Third Peak A battery became depleted with 11.6 V remaining. From May 15 to 20, the dGPS monitoring network was not recording or transmitting data. On May 20, 2014, the snow covering the Third Peak B battery melted, the solar panels began recharging the battery, and the unit began transmitting data. Shortly after, on May 22, 2014, the Third Peak A battery also began working again.

Throughout 2014 the entire dGPS network measured only minimal annual movements. The Lower Saddle station in particular, showed possible increased acceleration of movement with displacement values increasing by a few millimeters throughout 2014. However, considering that this station is positioned in the most unstable location, this is not unexpected. We expect that deformations will continue to be so small that additional years of data will be required to identify clear block movement trends.

3.2.5 LiSAmobile GB-InSAR

The 3D displacement maps displayed in Figures 15–20 depict how the slopes on the east face of the mountain are affected by slow and small movements, measured in the millimetre range. The 3D displacement maps were created through a collection of data from the LiSAmobile system over a 91-day period, in approximately 15-day increments. The 3D displacement maps were produced from data collected from June 20 to September 20, 2014 (first quarter). Due to high rates of displacement in the debris zone (Region G) and vegetation zone (Region F) located in the central and lower area of the mountain face, we cannot accept the displacement data with complete confidence. Additional testing will be completed in Region F to attempt to improve the image and understand the region's behaviour better.

The results from the first quarterly report provided to the AGS from Ellegi in September 2014 are shown in Tables 1–3. LiSAmobile data shows no movement of larger coherent blocks of material (generalized movement) have been identified near North and South Peak throughout 2014.

Displacements at points of interest (P_1–12) from June 20 through September 20, 2014, have been measured and described as follows (Figures 12–14 and Tables 2 and 3).

Table 1. LiSAmobile overall calculated results from June 20 to September 20, 2014, in Regions A to G.

Region	Location Description	Displacement (mm)	Approximate Region Area (m^2)
A	Close to North Peak	−3.0 to −20.0	4600
B	Between North and South Peak	−6.0	600
C	Close to South Peak	−4.0	1200
D	Debris area toe of South Peak rock wall	−25.0	–
E	Debris area toe of North Peak rock wall	−25.0	–
F	Mid to lower vegetative rock wall	–	–
G	Debris zone run out area	−3.6	–

Table 2. LiSAmobile measured results from June 20 to September 20, 2014, in POIs 1 to 12.

Region	Point of Interest (POI)	Displacement (mm)	Displacement Description
A	P_1	−1.6 to −20.5	Continuous movements
	P_2		
	P_3		
	P_4		Accelerated movement after August 2014.
B	P_5	−3.0	Continuous movement
C	P_6	−1.8 to −3.0	Continuous movement
	P_7		
D	P_8	–	Debris zone POI data is omitted
E	P_9	≤−9.3	Displacement primarily in June and July. Decline in displacement during August.
	P_10	−0.7	Range between −0.8 and +1.2 mm, with an average displacement of +0.3 mm.
F	P_11	–	POI data is omitted
G	P_12	−3.6	Lower debris area

Table 3. Points of interest found in regions A to G on Turtle Mountain, displaying UTM (easting and northing) coordinates and elevation (metres above sea level).

POI	X (m)	Y (m)	Z (m asl)	Region
P_1	686862	5495554	2071	A
P_2	686871	5495570	2066	A
P_3	686867	5495591	2069	A
P_4	686851	5495607	2074	A
P_5	686974	5495314	2118	B
P_6	687071	5495062	2190	C
P_7	687079	5495079	2182	C
P_8	687216	5495036	2077	D
P_9	687069	5495634	1819	E
P_10	687247	5495666	1708	E
P_11	687186	5496115	1611	F
P_12	687774	5495445	1543	G

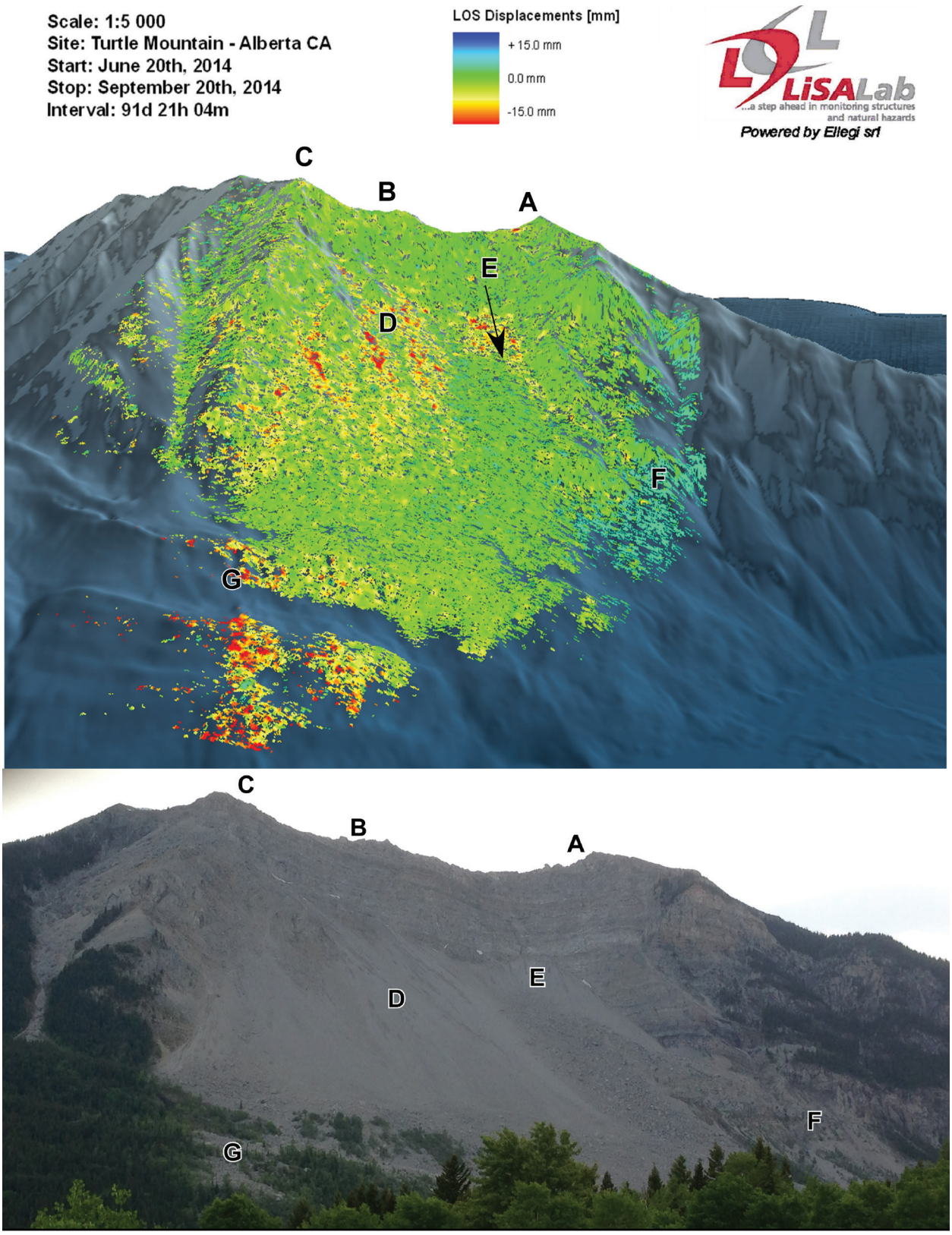

Figure 12. 3D displacement map (top) measured from June 20 through September 20, 2014, and view of the eastern face of Turtle Mountain (bottom). Letters A to G denote locations of regions described in Table 1.

The analyses completed by Ellegi concluded that no generalized block movement was recorded during the first quarter of monitoring from June 20 through September 20, 2014 (Figures 15–20). During the second quarter of monitoring, the points of interest (P_1–12) will continue to be monitored and will be compared to the first quarterly results. Additional points of interest may be added to further quarterly analyses if additional areas of displacement or localized rock falls are identified. Results from the second quarter will be reported in next annual report.

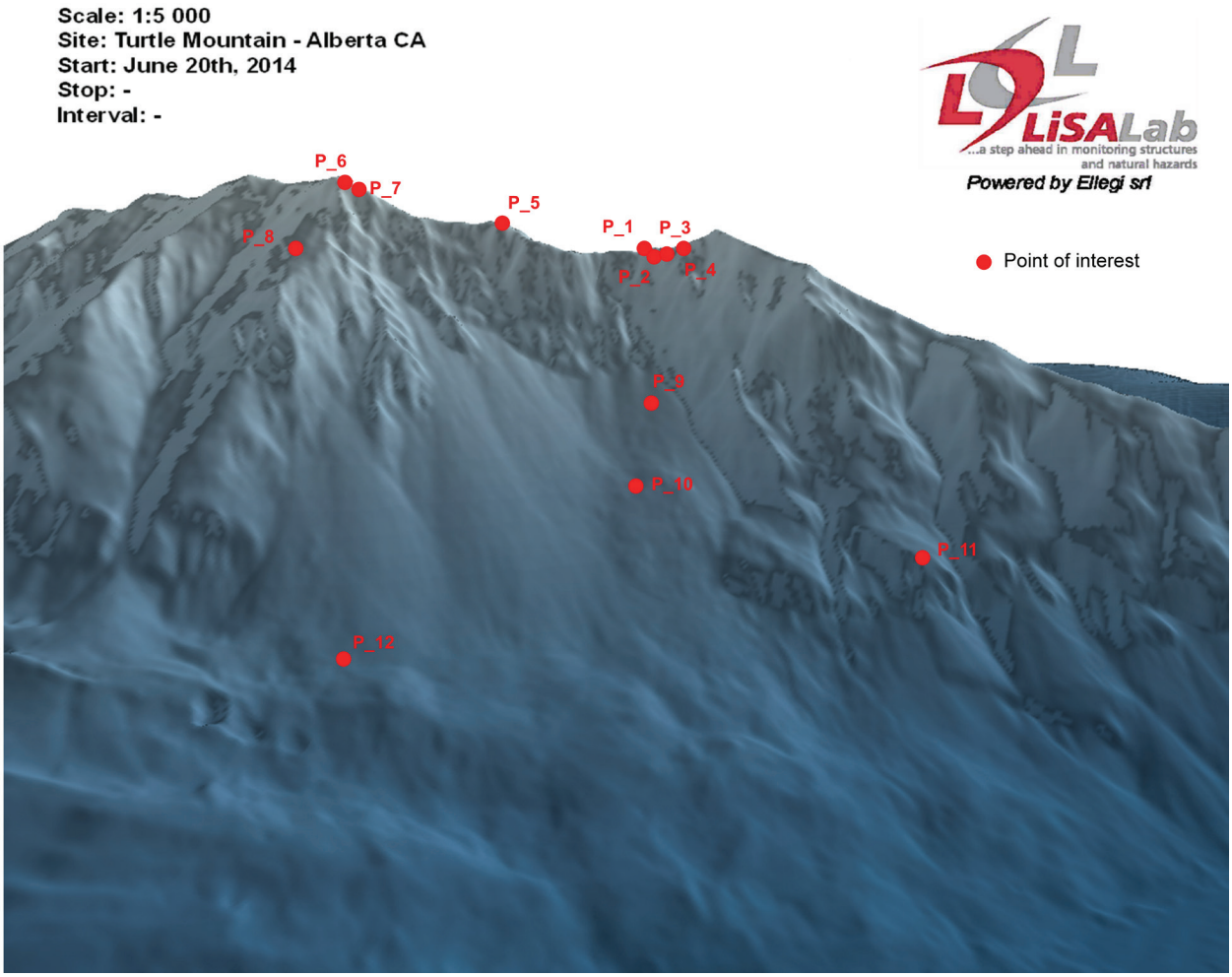

Figure 13. Turtle Mountain points of interest in regions A–G (Figure 12).

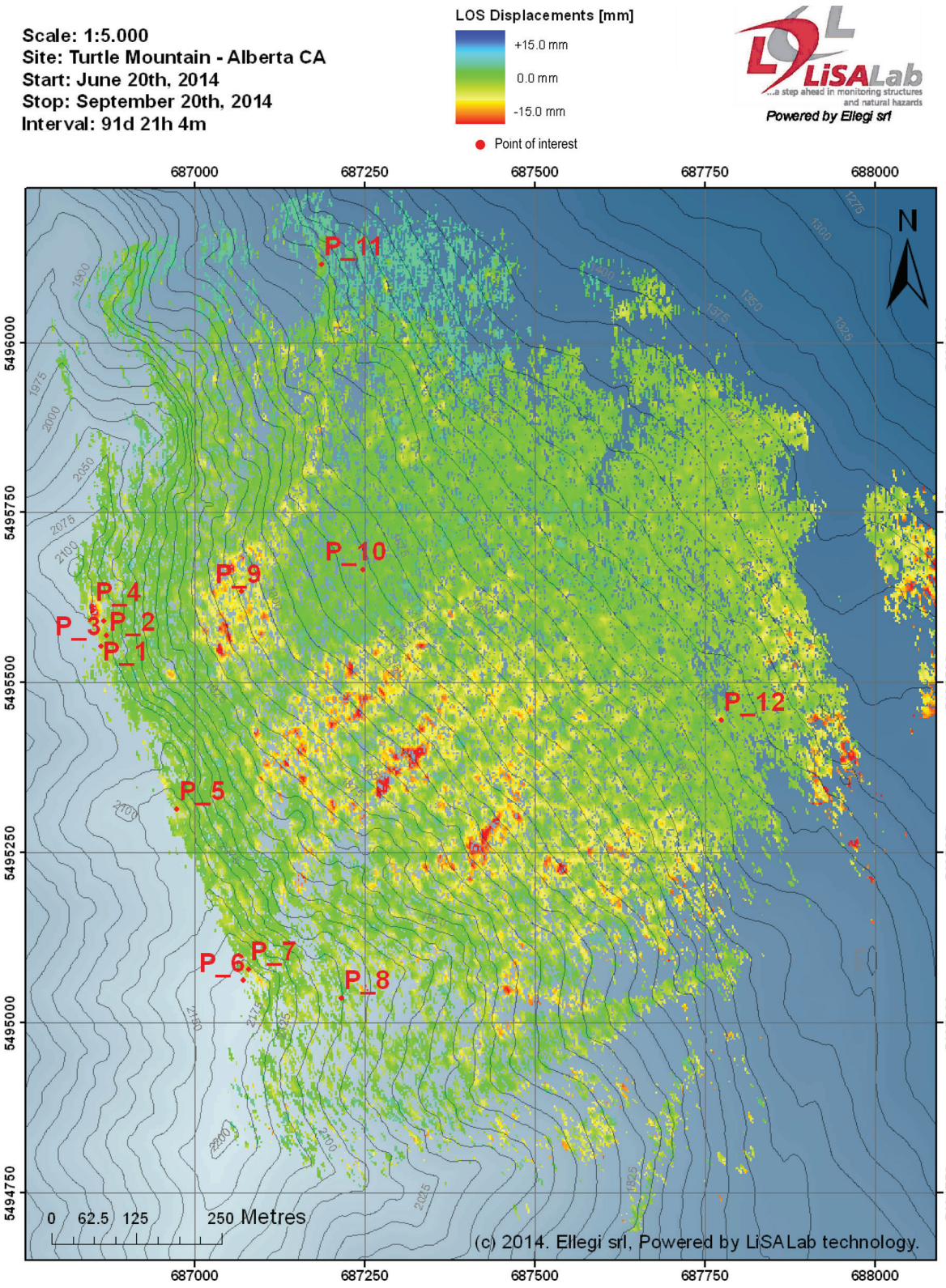

Figure 14. Map of 3D displacement measured from June 20 through September 20, 2014, displaying twelve points of interest found throughout regions A–G (Figure 12).

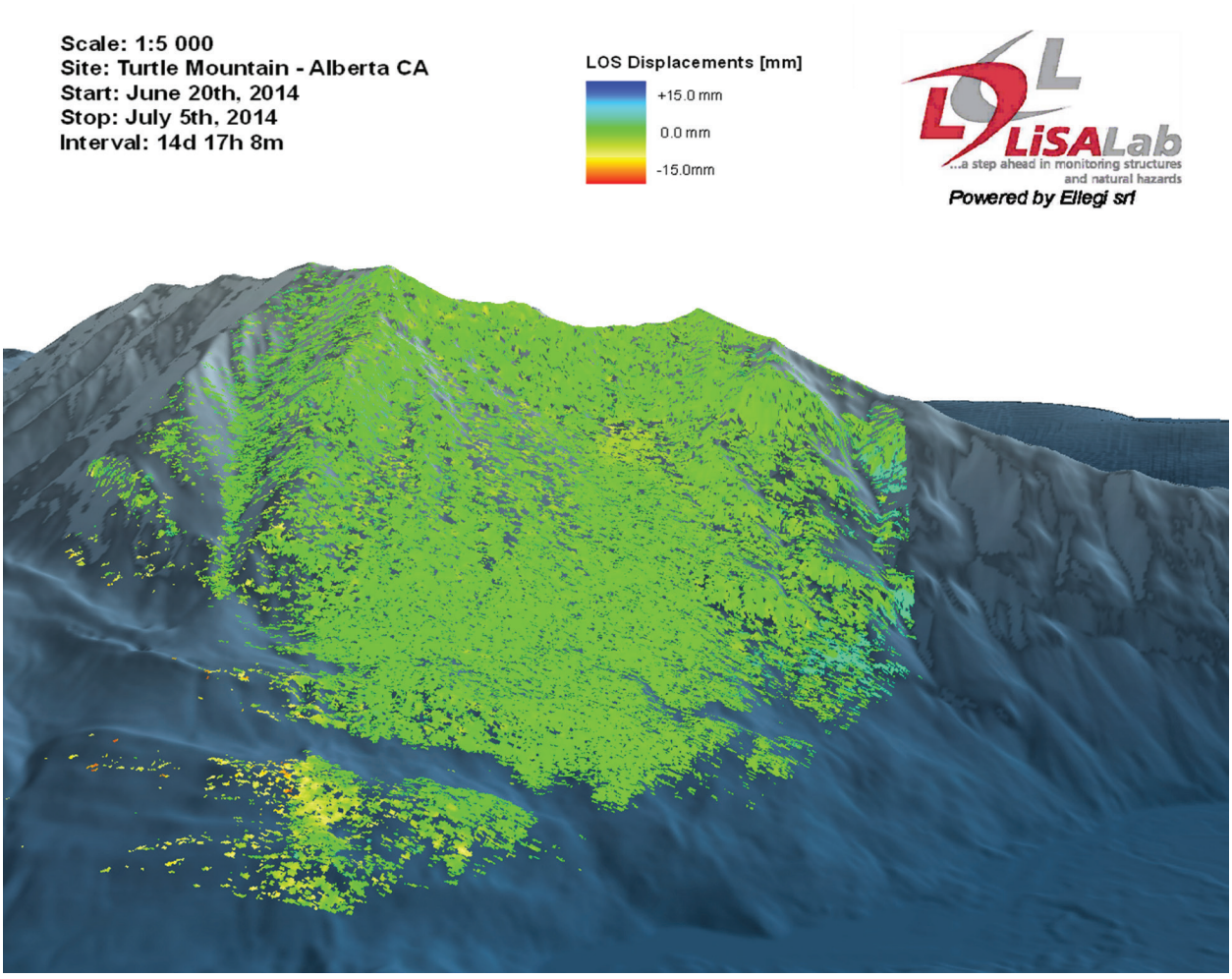

Figure 15. Line of sight 3D displacement map of Turtle Mountain measured during 14-day interval from June 20 through July 5, 2014.

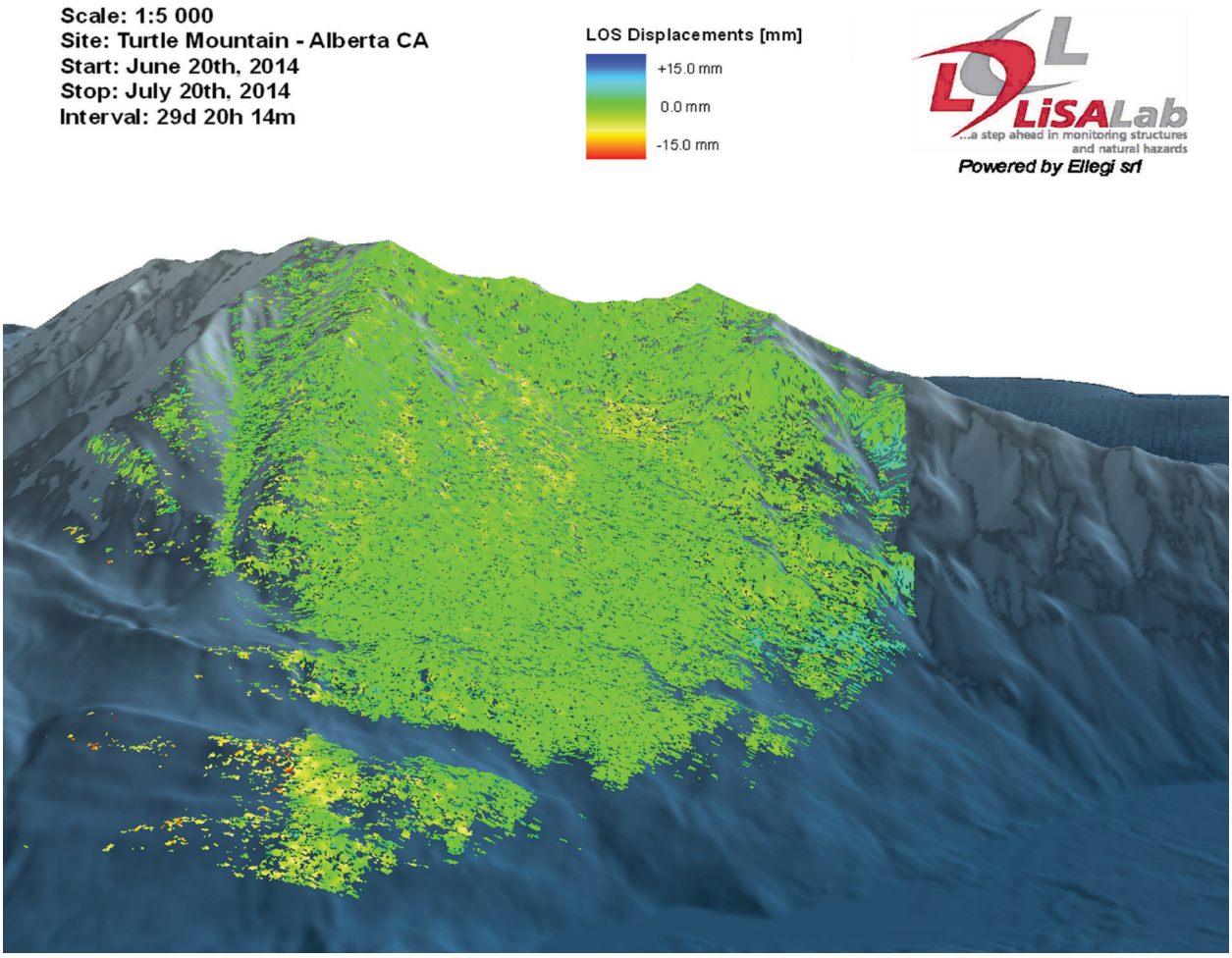

Figure 16. Line of sight 3D displacement map of Turtle Mountain measured during 29-day interval from June 20 through July 20, 2014.

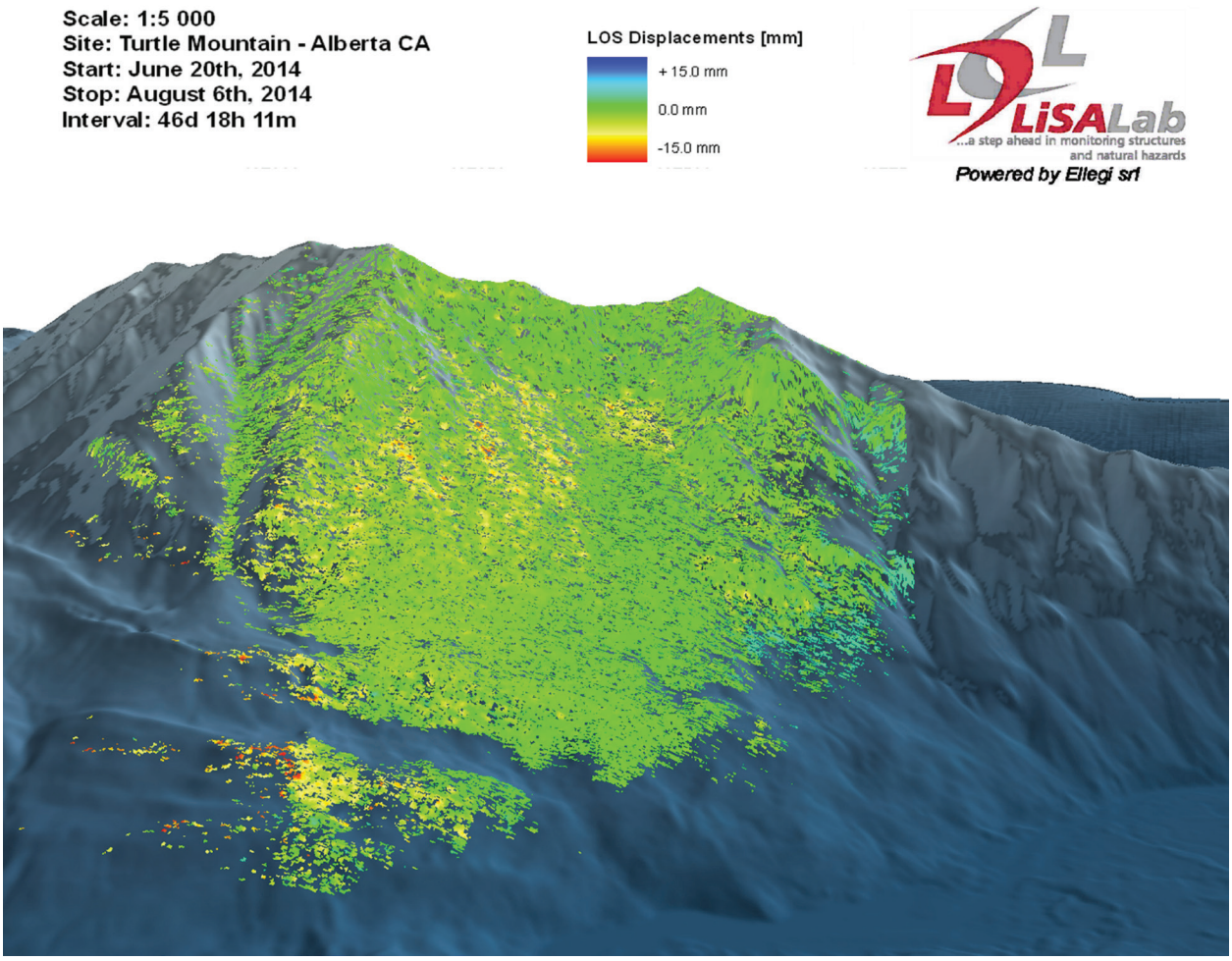

Figure 17. Line of sight 3D displacement map of Turtle Mountain measured during 46-day interval from June 20 through August 6, 2014.

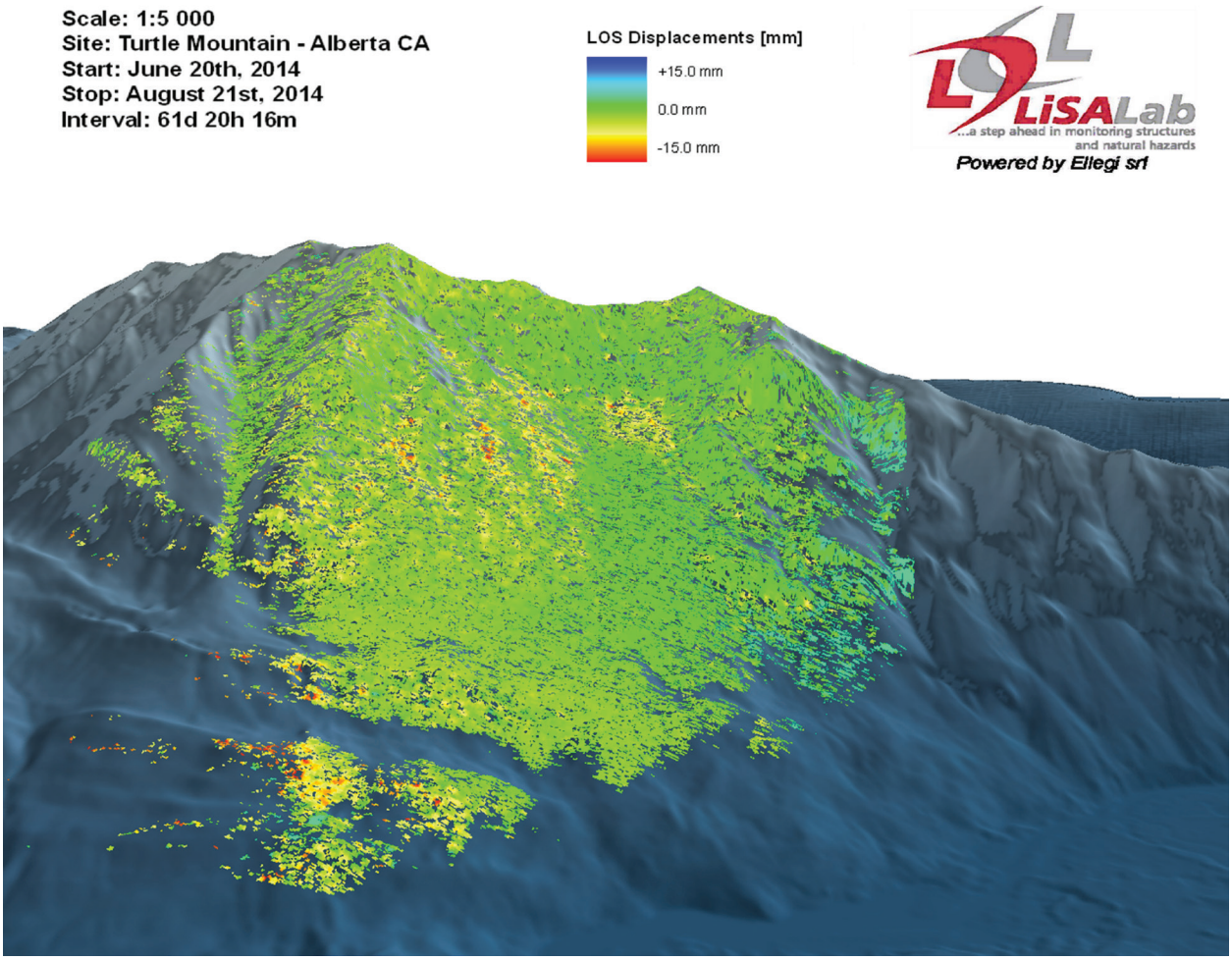

Figure 18. Line of sight 3D displacement map of Turtle Mountain measured during 61-day interval from June 20 through August 21, 2014.

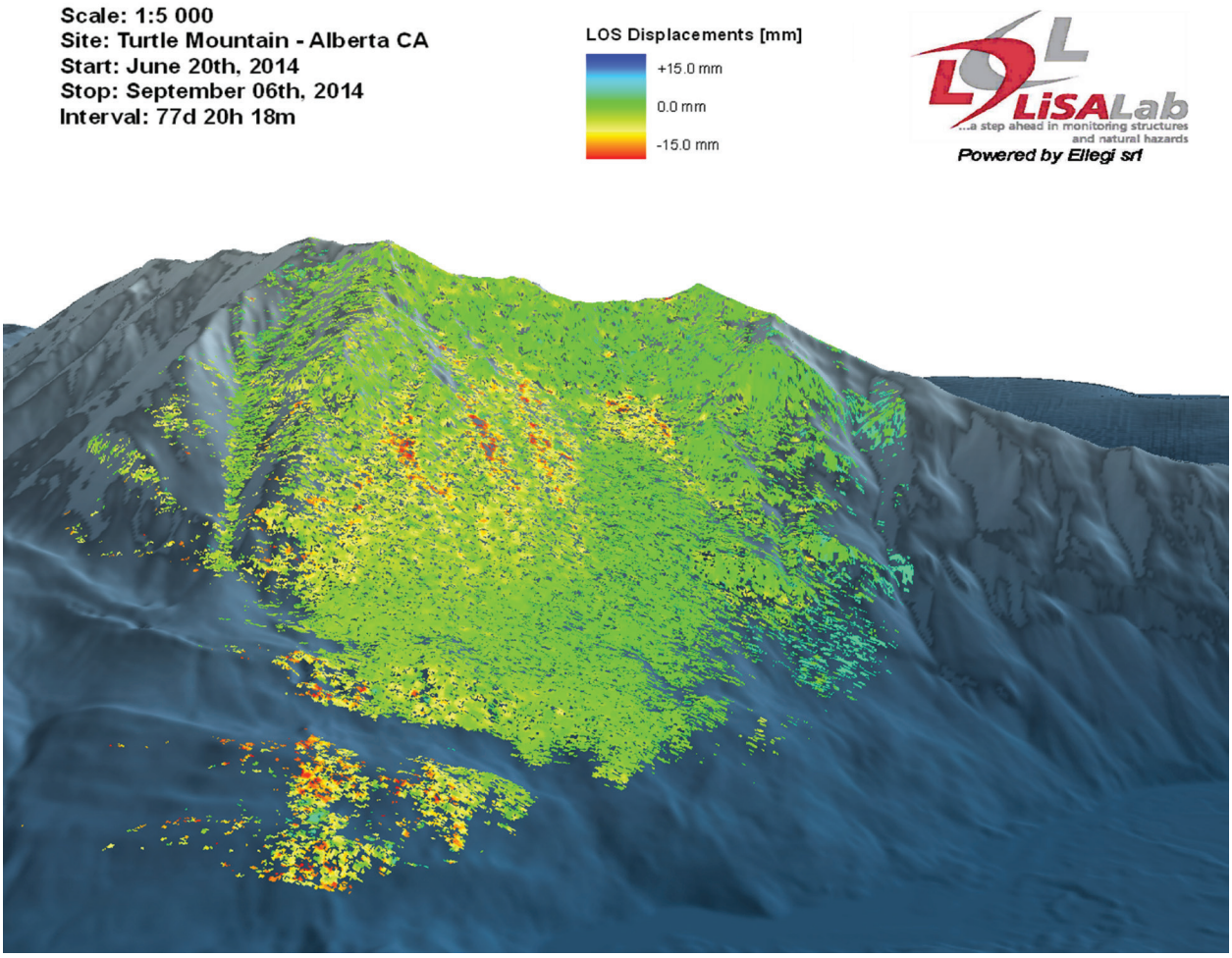

Figure 19. Line of sight 3D displacement map of Turtle Mountain measured during 77-day interval from June 20 through September 6, 2014.

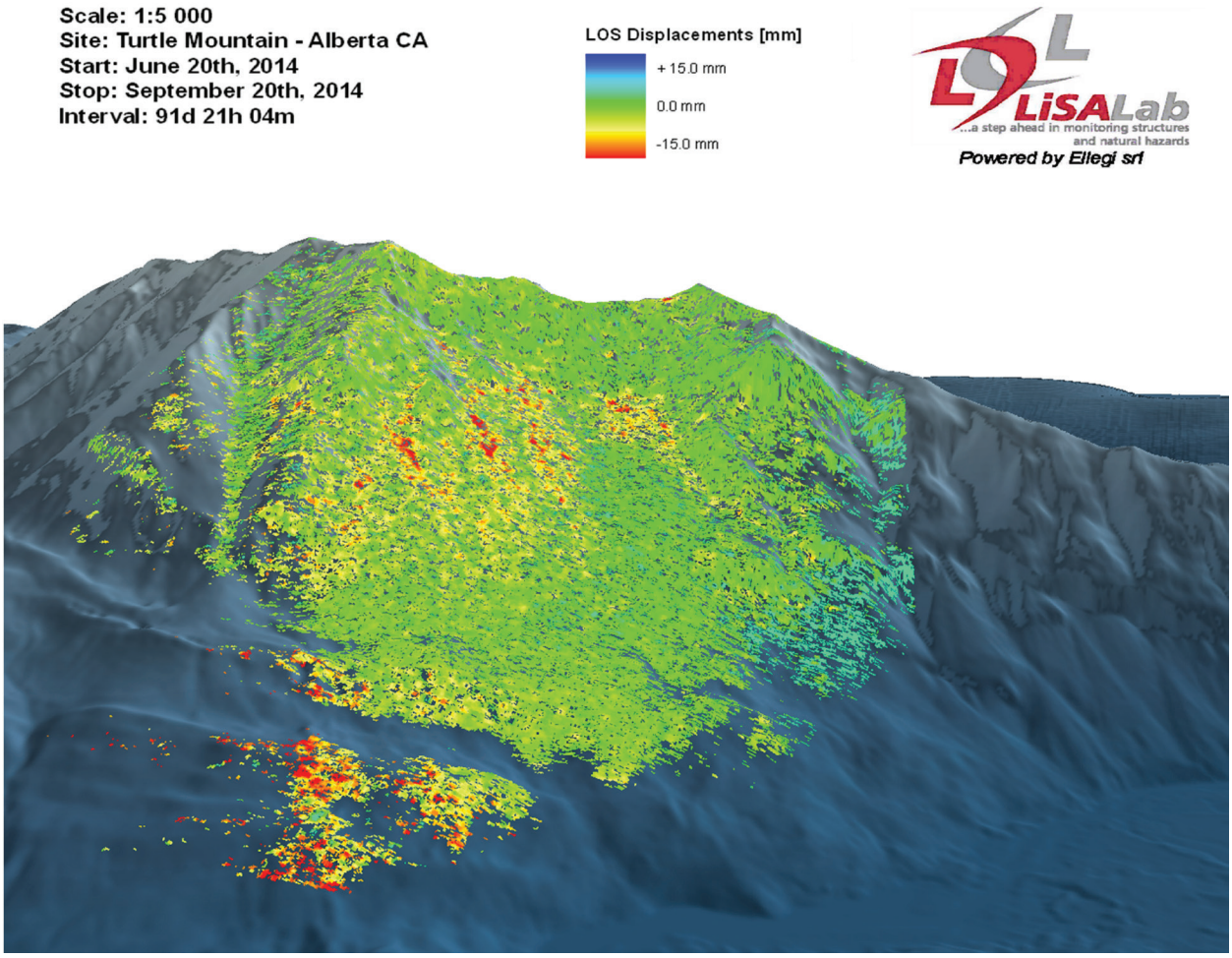

Figure 20. Line of sight 3D displacement map of Turtle Mountain measured during 91-day interval from June 20 through September 20, 2014.

4 Supporting Studies and Research

In 2013, the AGS contracted O. Hungr of Geotechnical Research Inc. to conduct a runout analysis on the North Peak of Turtle Mountain. In March 2014, the report was delivered to the AGS with the analyses and recommendation from the North Peak modelling (Appendix 1). The report analyzed two potential failure scenarios: a shallow- and a deep-rock failure (Hungr, 2014). Structural and stability analysis data of the potential failure scenarios were obtained through the University of Lausanne, Switzerland (Humair and Jaboyedoff, 2013; Appendix 2).

The smaller "shallow" failure scenario was estimated to produce a volume of 240 000 m^3 of rock debris, while the larger "deep" failure scenario was estimated to produce a volume of 3.5 million m^3 of rock debris (Appendix 2). Hungr used 2-dimensional (2D) and 3-dimensional (3D) numerical models to produce six separate runout analyses (Figure 21 and Figure 22) of each the "shallow" and "deep" potential failure scenarios. These twelve analyses samples provide an in-depth assessment of possible North Peak runout scenarios. These scenarios are not imminent, but the analyses allow the AGS to gain a better understanding of possible events that may take place on North Peak. The AGS has reviewed the North Peak runout analyses and intends to use this investigation to update the *ERCB/AGS Roles and Responsibilities Manual for the Turtle Mountain Monitoring Project, Alberta* (Moreno and Froese, 2009b).

Findings from the North Peak runout analyses suggest that debris produced by a "deep" failure will travel a greater distance and cross Highway 3 and the railway, while that produced by a "shallow" failure will stay contained at the base of the mountain (Hungr, 2014).

5 Expert Panel Review Report

In October 2014, the AGS received the final report (Appendix 3) from a panel of experts from Norway, Italy, and Canada, which had been asked to review the design, operation, and performance of the TMMS and provide recommendations for its future. Currently, the AGS is evaluating the expert panel recommendations and will complete a full review of the Turtle Mountain Monitoring Program with consideration of the panel's recommendations by early 2015.

Further details will be provided to the Municipality of the Crowsnest Pass council once the AGS has reviewed the recommendations. A public open house will be planned with the Municipality of Crowsnest Pass to communicate the panel's recommendations in early 2015.

6 Conclusions

Recent application of modern characterization, monitoring, and modelling technologies has greatly increased our understanding of the 1903 Frank Slide and of the existing rock-slope hazard at Turtle Mountain. Based on these findings, monitoring focus was shifted to a wider area on the eastern face of Turtle Mountain below Third Peak and South Peak. Analysis of the data from the near-real-time monitoring system in these areas does not indicate any type of significant movement—that is, any movements, if occurring, are below the detection limit of the sensors (less than a few millimetres per year). The rate of displacement is well below any level of concern and has remained essentially constant for the years of monitoring.

Keeping the previous primary sensor network continuously running has proven to be very difficult and expensive. Therefore, it has been replaced with the continuous-reading dGPS monitoring system. The

new secondary monitoring system (LiSAmobile) will continue to be monitored and reviewed for testing purposes. The AGS will continue to investigate other monitoring systems as part of the TMFL.

Communication of the risks associated with these hazards to the affected population is also ongoing. We publish the most recent results annually (Moreno and Froese, 2009a, 2011, 2012; Moreno et al., 2013; Warren et al., 2014, 2016) and present them in public meetings with the municipal officials and residents in the affected zones. Updates are also available on the "Turtle Mountain Monitoring Program & Field Laboratory" page of the Alberta Geological Survey website (http://www.ags.gov.ab.ca/geohazards/turtle_mountain/turtle_mountain.html).

Based on a review of the sensor thresholds, a system of four alert levels (green, yellow, orange, and red) was developed by AMEC (2005) and subsequently incorporated into the Alberta Emergency Management Agency's emergency response protocol for Turtle Mountain. This protocol establishes that the AER, through the AGS, is responsible for determining the appropriate alert level for a potential emergency at Turtle Mountain. Thus, to ensure that this role is fulfilled, the AER maintains its own internal emergency response protocol (based on Moreno and Froese, 2009b). The emergency response protocol is revised as often as is required to ensure that its current version reflects best practice and is fit for its purpose. At a minimum, one review is done every year. The next review will be completed in early 2015 to ensure that all changes made to the system in 2014 are considered. The protocol will be updated based on the AGS's evaluation and recommendations from the expert panel review.

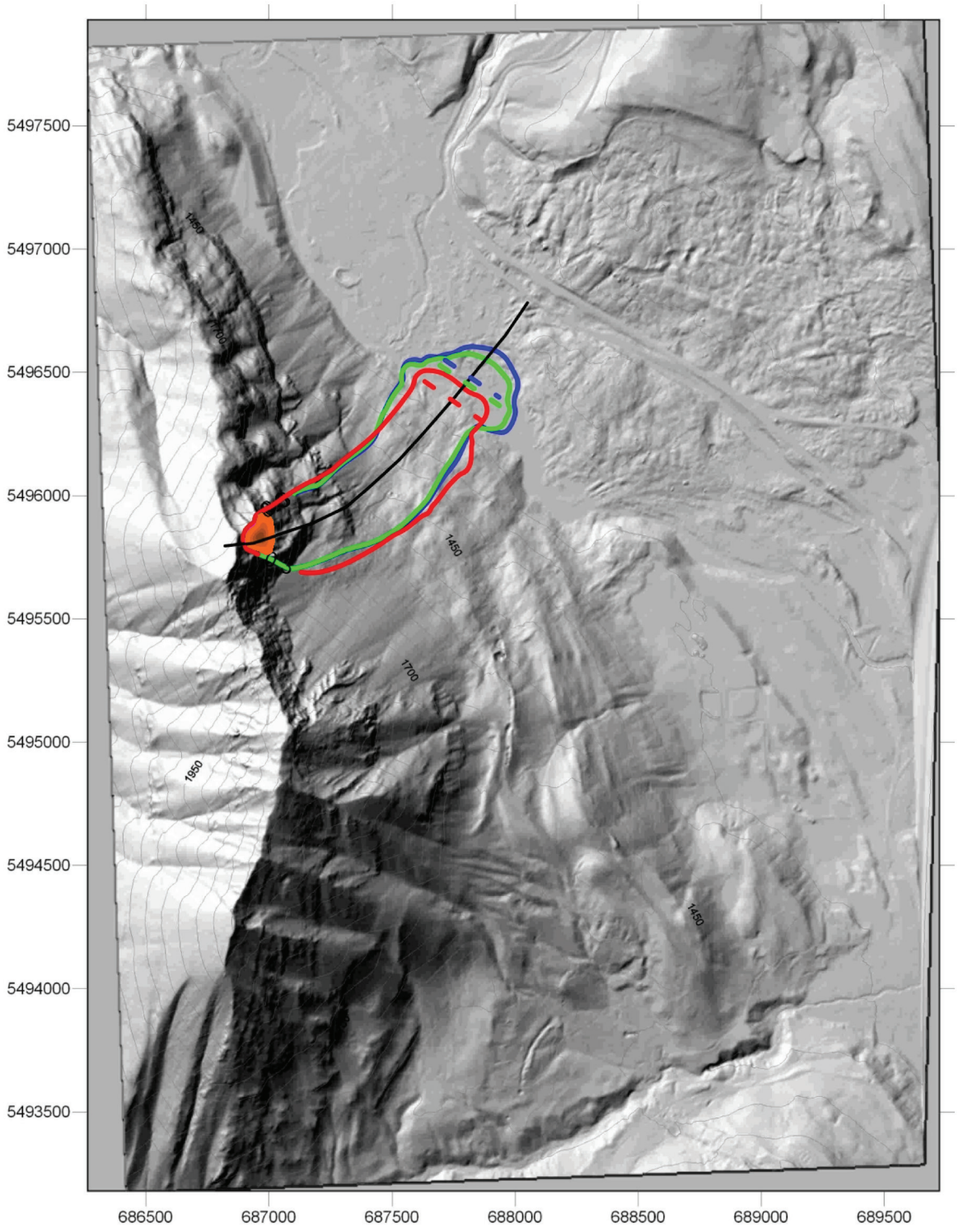

Figure 21. Runout-modelling results for "shallow" rock failure at North Peak (modified from Hungr, 2014, Figure 6; Appendix 1). Solid lines depict outline of runout based on 3D model analyses and dashed lines depict outline of runout based on 2D analyses. Orange area delineates area of failure.

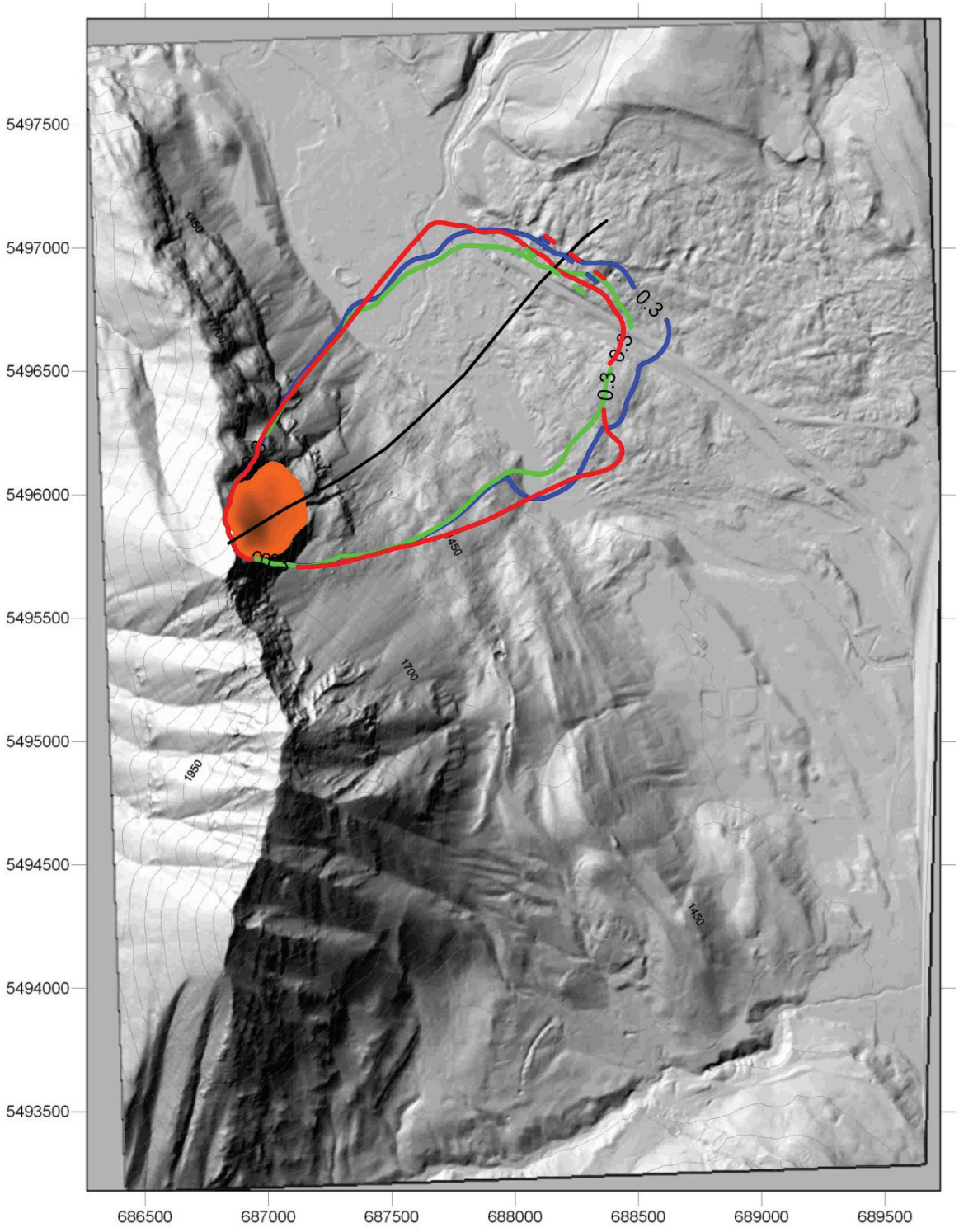

Figure 22. Runout-modelling results for "deep" rock failure at North Peak. Solid lines depict outline of runout based on 3D model analyses and dashed lines depict outline of runout based on 2D analyses. Orange area delineates area of failure (Hungr, 2014, Figure 7; Appendix 1).

7 References

Allan, J.A. (1931): Report on stability of Turtle Mountain, Crowsnest District, Alberta; Alberta Department of Public Works, Alberta Provincial Archives, 14 p.

AMEC Earth and Environmental (2005): Turtle Mountain monitoring project, summary report—WP11.03 and 12.03, subsurface geotechnical and microseismic monitoring system; unpublished report prepared by AMEC Earth and Environmental for Alberta Municipal Affairs, 17 p.

Froese, C.R., Moreno, F., Jaboyedoff, M. and Cruden, D.M. (2009): 25 years of movement monitoring on the South Peak of Turtle Mountain: understanding the hazard; Canadian Geotechnical Journal, v. 46, p. 256–269.

Humair, F. and Jaboyedoff, M. (2013): North Peak area stability analysis (Turtle Mountain): description and mechanisms of the unstable volumes; unpublished report, Faculty of Geosciences and Environment, University of Lausanne, Switzerland, 24 p. [Included in this report as Appendix 2.]

Hungr, O. (2014): North Peak of Turtle Mountain, Frank, Alberta: runout analysis of two potential landslides; Geotechnical Research Inc., 19 p. [Included in this report as Appendix 1.]

Moreno, F. and Froese, C.R. (2006): Turtle Mountain Field Laboratory monitoring and research summary report, 2005; Alberta Energy and Utilities Board, EUB/AGS Earth Sciences Report 2006-07, 94 p., URL <http://www.ags.gov.ab.ca/publications/abstracts/ESR_2006_07.html> [September 2014].

Moreno, F. and Froese, C.R. (2008a): Turtle Mountain Field Laboratory: 2006 data and activity summary; Energy Resources Conservation Board, ERCB/AGS Open File Report 2008-1, 29 p., URL <http://www.ags.gov.ab.ca/publications/abstracts/OFR_2008_01.html> [September 2014].

Moreno, F. and Froese, C.R. (2008b): Turtle Mountain Field Laboratory: 2007 data and activity summary; Energy Resources Conservation Board, ERCB/AGS Open File Report 2008-7, 40 p., URL <http://www.ags.gov.ab.ca/publications/abstracts/OFR_2008_07.html> [September 2014].

Moreno, F. and Froese, C.R. (2009a): Turtle Mountain Field Laboratory: 2008 data and activity summary; Energy Resources Conservation Board, ERCB/AGS Open File Report 2009-15, 22 p., URL <http://www.ags.gov.ab.ca/publications/abstracts/OFR_2009_15.html> [September 2014].

Moreno, F. and Froese, C.R. (2009b): ERCB/AGS roles and responsibilities manual for the Turtle Mountain Monitoring Project, Alberta, ERCB/AGS Open File Report 2009-06, 35 p., URL <http://www.ags.gov.ab.ca/publications/abstracts/OFR_2009_06.html> [September 2014].

Moreno, F. and Froese, C.R. (2011): Turtle Mountain Field Laboratory: 2009 data and activity summary; Energy Resources Conservation Board, ERCB/AGS Open File Report 2011-05, 22 p., URL <http://www.ags.gov.ab.ca/publications/abstracts/OFR_2011_05.html> [September 2014].

Moreno, F. and Froese, C.R. (2012): Turtle Mountain Field Laboratory: 2010 data and activity summary; Energy Resources Conservation Board, ERCB/AGS Open File Report 2012-03, 22 p., URL <http://www.ags.gov.ab.ca/publications/abstracts/OFR_2012_03.html> [September 2014].

Moreno, F., Pearse, J. and Froese, C.R. (2013): Turtle Mountain Field Laboratory, Alberta (NTS 82G): 2011 data and activity summary; Alberta Energy Regulator, AER/AGS Open File Report 2013-18, 23 p. URL <http://www.ags.gov.ab.ca/publications/abstracts/OFR_2012_03.html> [September 2014]

Warren, J.E., Morgan, A.J., Chao, D.K., Froese, C.R. and Wood, D.E. (2014): Turtle Mountain Field Laboratory, Alberta (NTS 82G): 2012 data and activity summary; Alberta Energy Regulator, AER/AGS Open File Report 2014-09, 16 p. URL <http://www.ags.gov.ab.ca/publications/abstracts/OFR_2012_03.html> [September 2014]

Warren, J.E., Wood, D.E., Chao, D.K. and Shipman, T.C. (2016): Turtle Mountain Field Laboratory, Alberta (NTS 82G): 2013 data and activity summary; Alberta Energy Regulator, AER/AGS Open File Report 2015-09, 43 p. URL <http://www.ags.gov.ab.ca/publications/abstracts/OFR_2015_09.html> [February 2016].

Appendix 1 – Runout Analysis

NORTH PEAK OF TURTLE MOUNTAIN, FRANK, ALBERTA
RUNOUT ANALYSES OF TWO POTENTIAL LANDSLIDES

Report to:
AER-Alberta Geological Survey
4th Floor, Twin Atria Building
4999 - 98 Avenue, Edmonton, Alberta, T6B 2X3

by:
O.Hungr Geotechnical Research, Inc.
4195 Almondel Rd., West Vancouver, B.C., V7V 3L6

March 12, 2014

List of Figures

1. Introduction

This report describes work carried out under Purchase Order [redacted], dated October 3, 2013. Its purpose is to carry out analysis of runout of two potential rock avalanches from the North Peak of Turtle Mountain, southern Alberta, adjacent to the source of the 1903 Frank Slide. A similar analysis of several potential landslides from the South Peak were completed in 2008 (OHGR, 2008a and 2008b). The present study is considered to be an extension of the previous work, following the same methodology.

2. Site Description

The general location of the Turtle Mountain was briefly described in the previous reports and in many publications, some of which are listed among the References. The specific slope area of the North Peak was recently subject to a structural study by a research group of the University of Lausanne, Switzerland (Humair and Jaboyedoff, 2013). The study outlined two alternative rock masses on the slope, which could be considered as scenarios of possible instability. The first, smaller mass would be a "shallow" failure of the frontal part of the spur below the peak, with an original source volume of 240,000 m^3 and is shown in a photo in Figure 1. The second, "deep" mass of 3.5 M m^3 is shown in Figure 2. The probability of failure of either volume is unknown, but it is considered that the "shallow" failure is more likely than the "deep" one.

After carrying out structural and stability analyses using several methods, the Lausanne group constructed topographic maps of the rupture surfaces that would likely be involved in the two potential failures. These are shown in Figures 3 and 4. These maps were provided to us in the form of Digital Elevation Models (DEM) and were utilized as input into runout simulations. The original ground surface was represented by a Lidar-derived DEM with 1m vertical resolution.

3. The Dynamic Models.

The runout analyses were carried out using two numerical models, described in the previous reports and in Hungr (1995) and Hungr and McDougall (2008). The first, DAN-W, is a "pseudo-three-dimensional" model defined by a path profile and requiring that the path width be determined by the user as an input function. The second model, DAN3D, is configured in three dimensions and requires only a DEM of the slope as input. The DEM of the slope was also provided to us by the Lausanne group and path cross-sections were derived from it.

The path files provided were grid files with a 1m grid spacing. Following recent experience with the model, a sensitivity analysis was performed as part of this study, in order to determine the effect that grid spacing and grid smoothing would have on the runout results. It was found that the runout results were relatively insensitive to the choice of spacing and smoothing for this slope. This was based on simulations with spacings of 2m, 5m and 10m and Gaussian smoothing of 0, 1 and 3 passes. The runout

predictions were performed on a grid with 10m spacing and 3 passes of Gaussian smoothing in order to remain consistent with previous analyses.

The failure source volumes were obtained by subtracting the rupture surface maps in Figures 3 and 4 from the DEM of the existing slope. Further, the source volumes were increased by 20%, to account for bulking during failure and movement of the rock mass.

The calibration conclusions from the previous reports, OHGR (2008a and 2008b) were adopted for the North Peak potential landslides. However, our research regarding calibration of the two programs is continuing and, as a result, some new results have been used.

We have obtained new data concerning the geometry of the Jonas North slide. As a result, the Jonas Creek North case is now considered as an example of a rock avalanche with high mobility. It is a poorly preserved prehistoric slide and the reasons for its high mobility are not clear. For that reason, it was removed from the plot of apparent friction coefficient versus slide volume, reproduced in Figure 5. The adjacent Jonas-South event is much less mobile. Figure 5 is now considered to represent the bulk friction resistance of rock avalanches that moved over relatively dry mountain slopes, without being able to entrain large amounts of saturated material. The frictional analyses that have been carried out for forward prediction are based on this figure and are considered as representing the lower-bound estimates of rock avalanche runout.

On the other hand, the highest potential mobility is assumed to be represented by using the Voellmy parameters that provided best fit for the much larger 1903 Frank slide, f=0.1 and ξ=500 m/s^2. Parameters suitable for events of moderate mobility were taken as f=0.15 and ξ=500 m/s^2. For smaller rock avalanches such as those considered in the present study, the degree of mobility may depend on the climatic conditions accompanying the failure. It is likely that events taking place during periods with high ground moisture, especially with snow on the ground, may exhibit higher mobility.

4. Forward Predictions, Potential North Peak Failures.

Six separate analyses have been carried out for each of the two alternative failure scenarios. Three-dimensional DAN3D analyses were completed using the frictional rheology ("low mobility") parameters based on Figure 5 and the two sets of Voellmy parameters mentioned in the previous paragraph. The same analyses were then repeated using the two-dimensional model DAN-W. The reason for using DAN-W was to confirm that the wide lateral spreading of the flow, as commonly predicted by DAN 3D, does not lead to under-estimation of runout.

The comparative results of the six analyses for the shallow failure are summarized in Figure 6 and for the deep failure in Figure 7. Figures 8 to 15 give detailed results of the analyses for the "low mobility" (frictional) and high mobility (Voellmy, f=0.1 and ξ=500 m/s^2) assumptions.

6. Conclusions

The resulting extents of predicted hazard zones for the shallow and deep failure scenario respectively are shown in Figures 6 and 7. It may be seen that the results are relatively insensitive to the assumption regarding the resistance parameters. An important outcome from this analysis is that the "shallow" landslide of 240,000 m^3 is contained within a few hundred metres of the toe of the Turtle Mountain slope, while the "deep" failure over-runs the Crowsnest Highway and the railway track. This conclusion is true for the whole range of resistance parameters tried.

References:

Couture, R. 1998. Contributions aux aspect physiques et méchanique des écroulements rocheux. Ph.D. thesis, University of Laval. (in French).

Humair, F. and Jaboyedoff, M., 2013. North Peak area stability analysis (Turtle Mountain), Description and mechanisms of the unstable volumes. A report by the Faculty of Geosciences and Environment, University of Lausanne, Switzerland, (undated, 24 pp.).

Hungr, O., 1995. A model for the runout analysis of rapid flow slides, debris flows and avalanches. Canadian Geotechnical Journal, 32(4):610-623.

Hungr, O. and McDougall, S., 2008 Two numerical models for landslide dynamic analysis. Computers & Geosciences (In press).

O.Hungr Geotechnical Research, Inc., 2008. South Peak of Turtle Mountain, Frank, Alberta. Runout analyses of potential landslides. Report to the Environmental Geology Section, Alberta Geological Survey/Energy and Utilities Board. April 18, 2008.

O.Hungr Geotechnical Research, Inc., 2008. Turtle Mountain, Frank, Alberta, Runout Analyses Of Potential Landslides on South and Third Peaks. Report to the Environmental Geology Section, Alberta Geological Survey/Energy and Utilities Board. November 15, 2008.

FIGURES

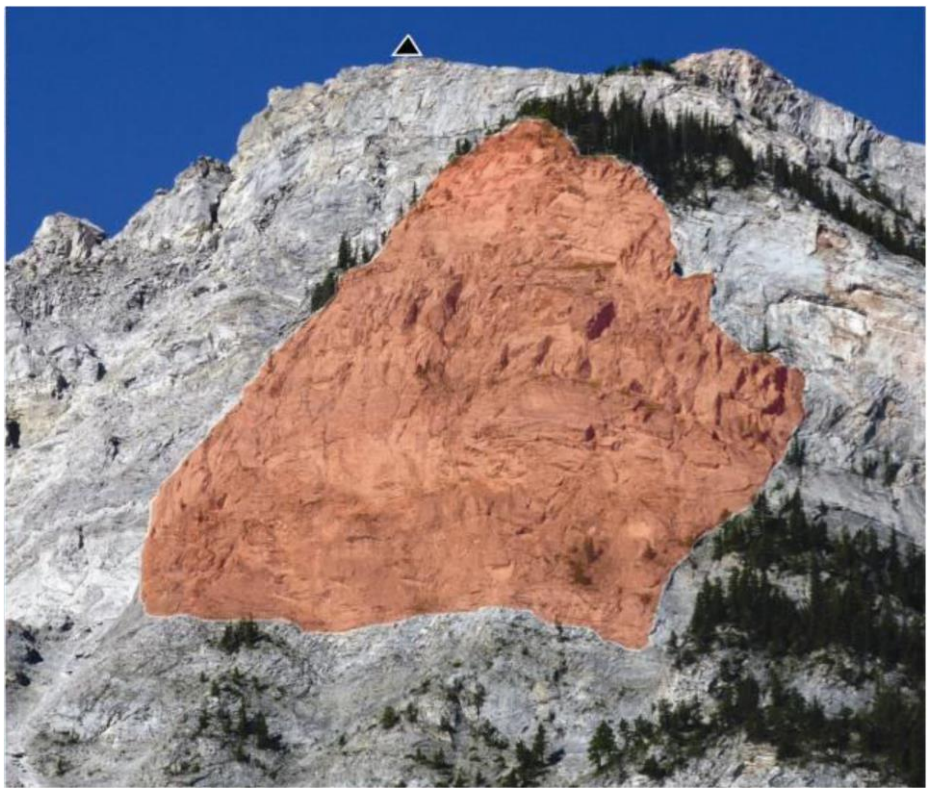

Figure 1
The "shallow" potential failure from the North Peak (Humair and Jaboyedoff, 2013).

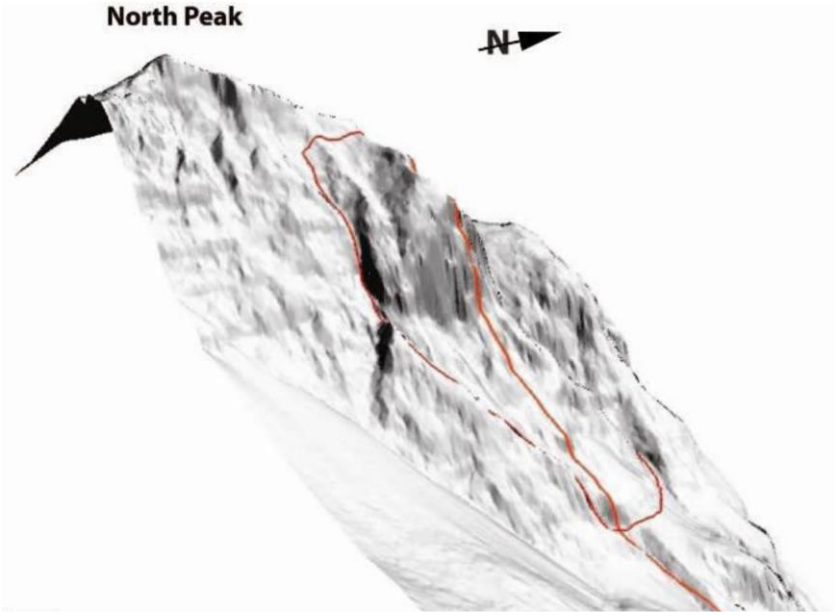

Figure 2
The "deep" potential failure from the North Peak (Humair and Jaboyedoff, 2013).

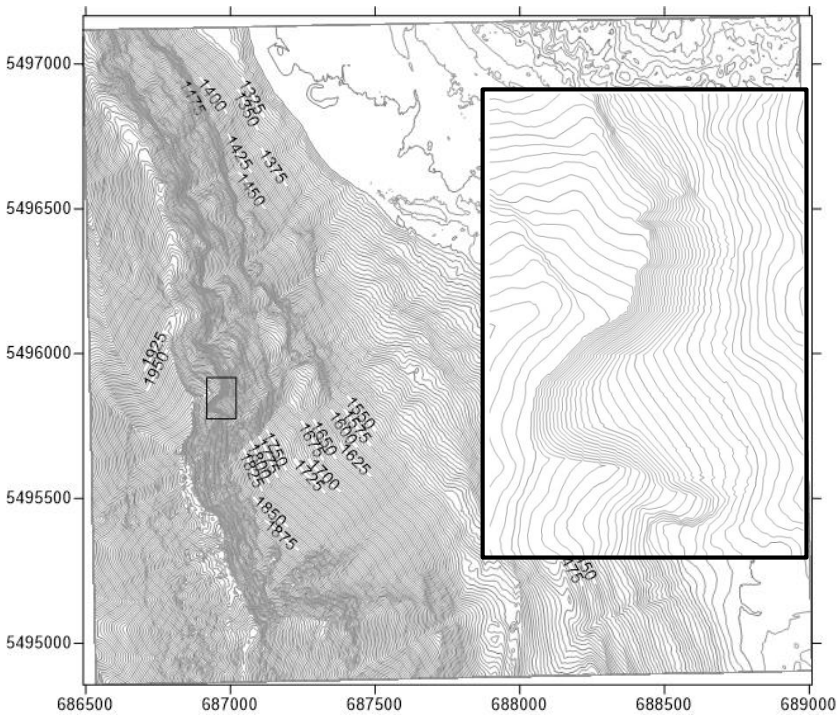

Figure 3

Contours of the "shallow" potential source volume of 240,000 m^3. (Based on data provided by the University of Lausanne research group).

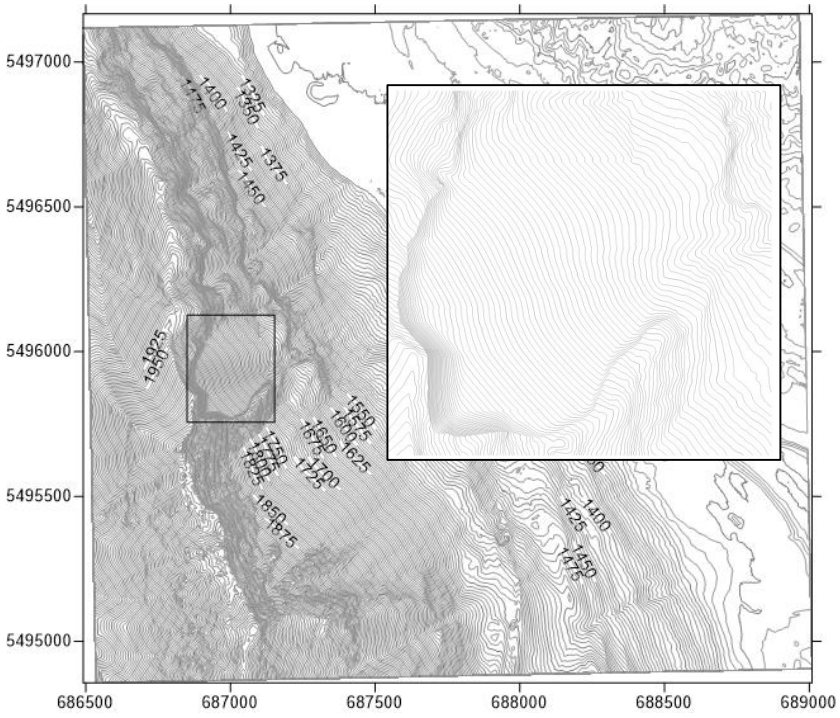

Figure 4

Contours of the "deep" potential source volume of 3.5 M m^3. (Based on data provided by the University of Lausanne research group).

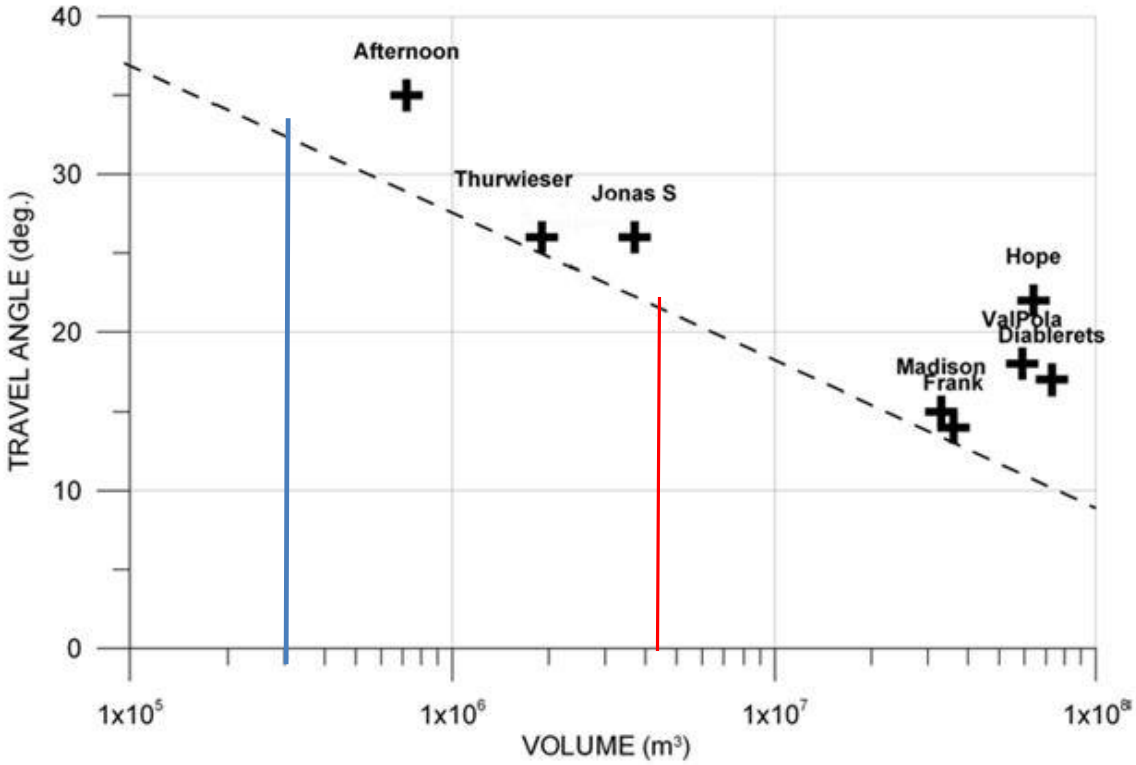

Figure 5: Lower bound plot of bulk basal friction angles that are the best fit for rock avalanches that moved primarily over "dry:" slopes. The blue line represents the bulked volume of the shallow failure and the red the bulked volume of the deep failure. (Copied from November 2008 runout report, with modification).

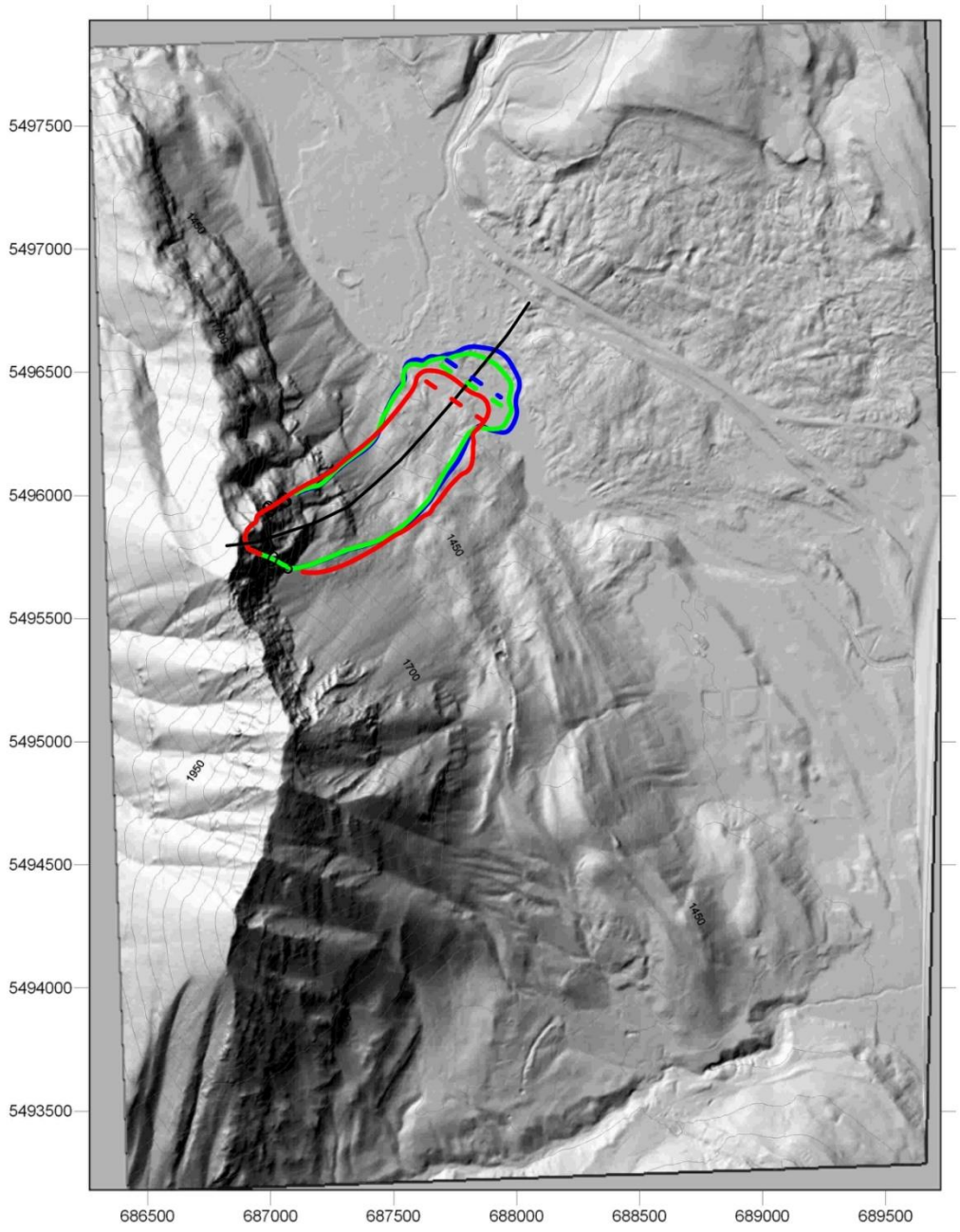

Figure 6
Comparison of DanW and Dan3D results for the shallow failure. The full lines represent the Dan3D results and the dashed lines the DanW results. Red- frictional (friction angle = 31°), Green- Voellmy f=0.15,ξ=500, Blue- Voellmy f=0.1,ξ=500.

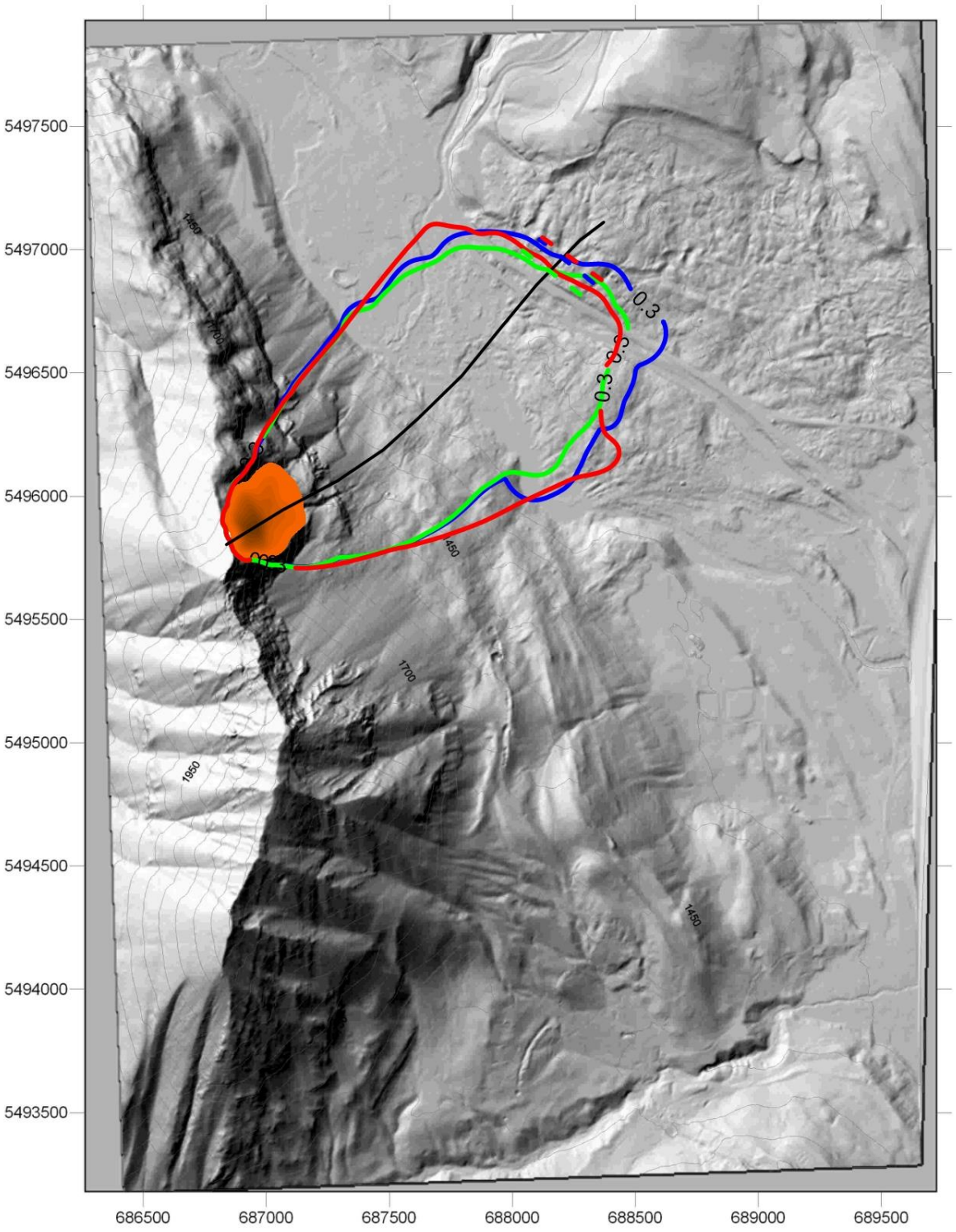

Figure 7
Comparison of DanW and Dan3D results for the deep failure surface. The straight lines represent the Dan3D results and the dashed lines the DanW results. Red- frictional (friction angle = 20º), Green- Voellmy $f = 0.15, \xi = 500$, Blue- $f = 0.1, \xi = 500$.

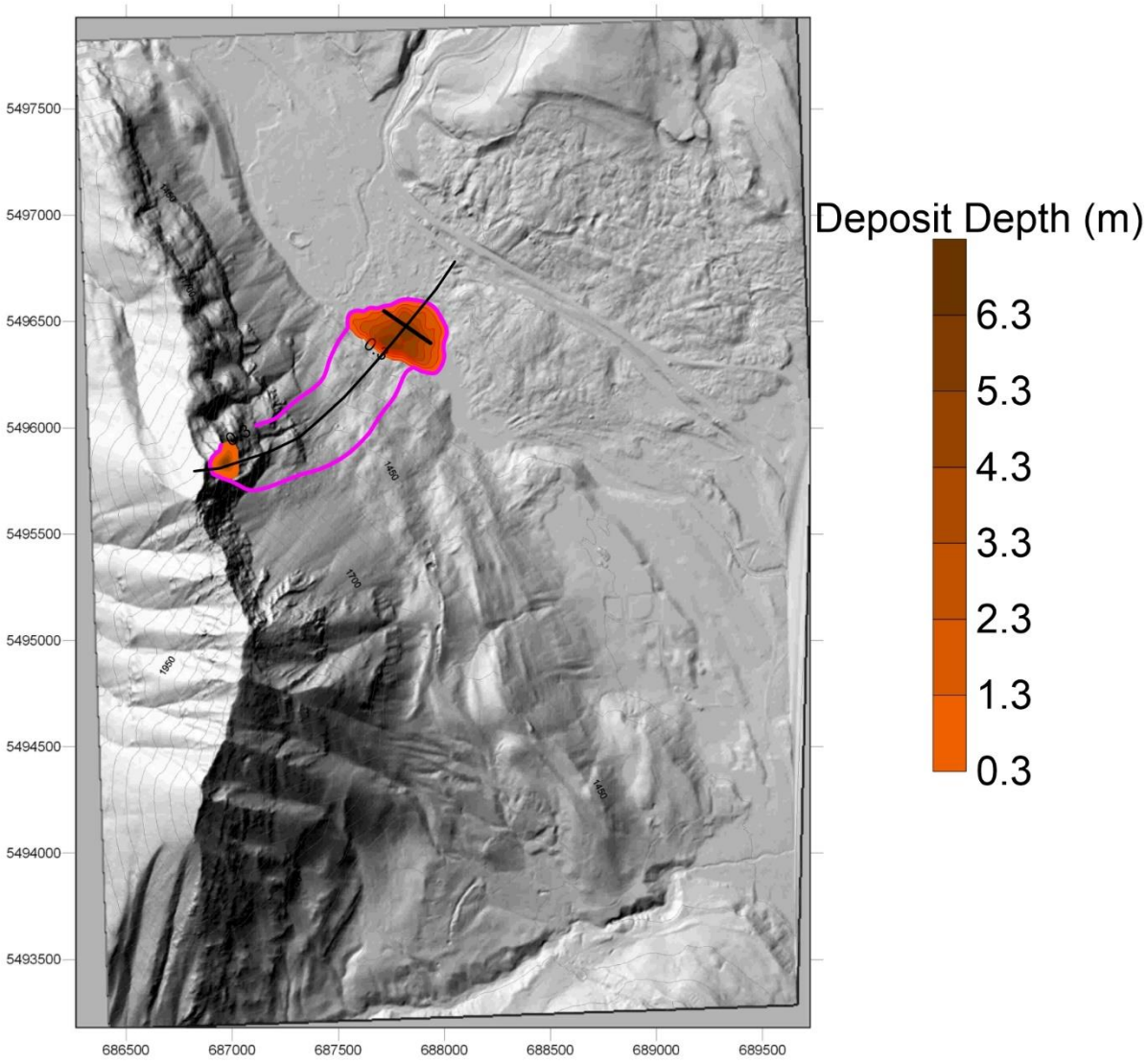

Figure 8
Shallow failure. Predicted final deposit for Voellmy parameters $f = 0.1, \xi = 500$. Color scale corresponds to the deposit depth.

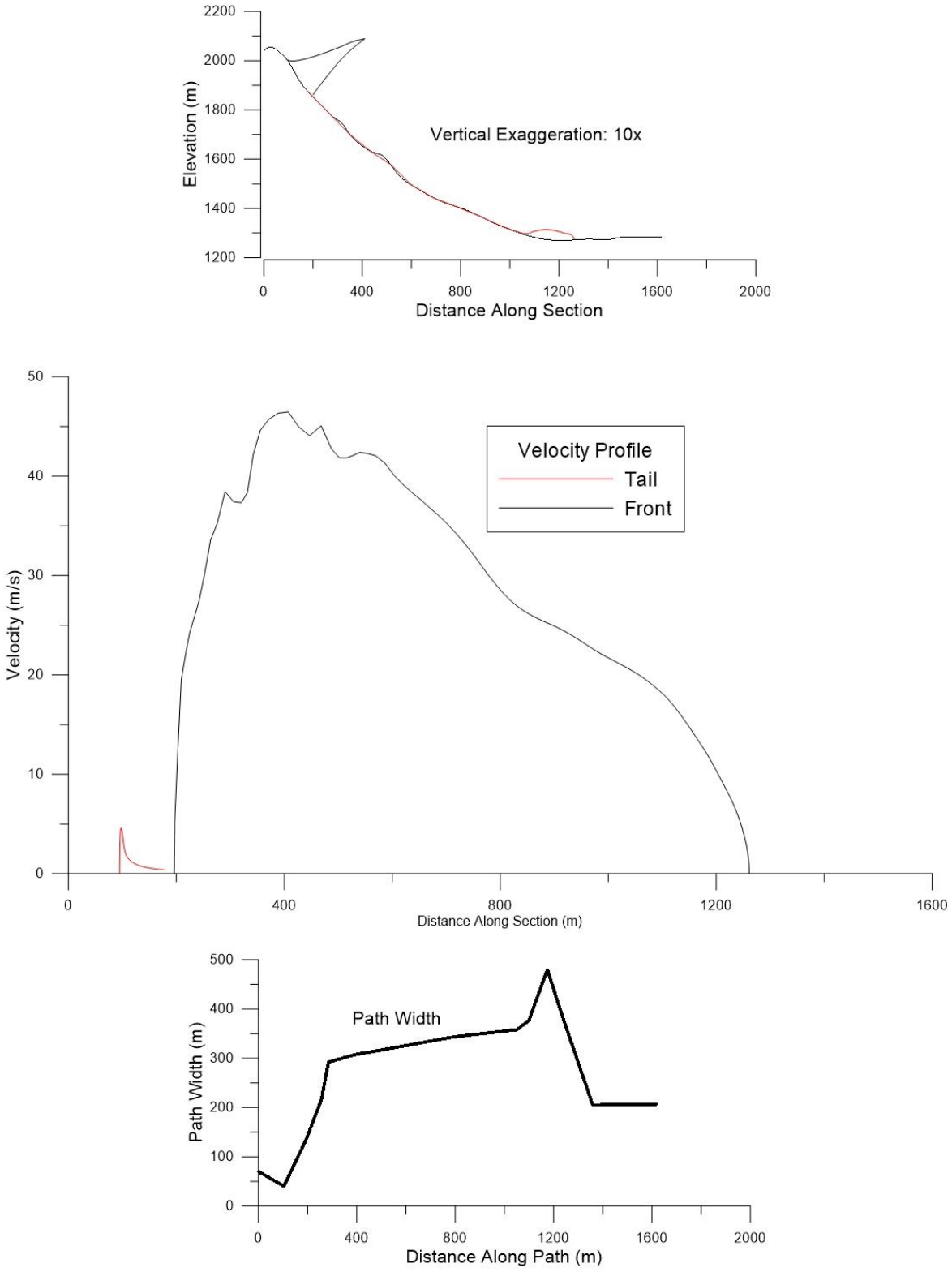

Figure 9
Shallow failure. Dan-W results for Voellmy parameters of $f = 0.1, \xi = 500$.

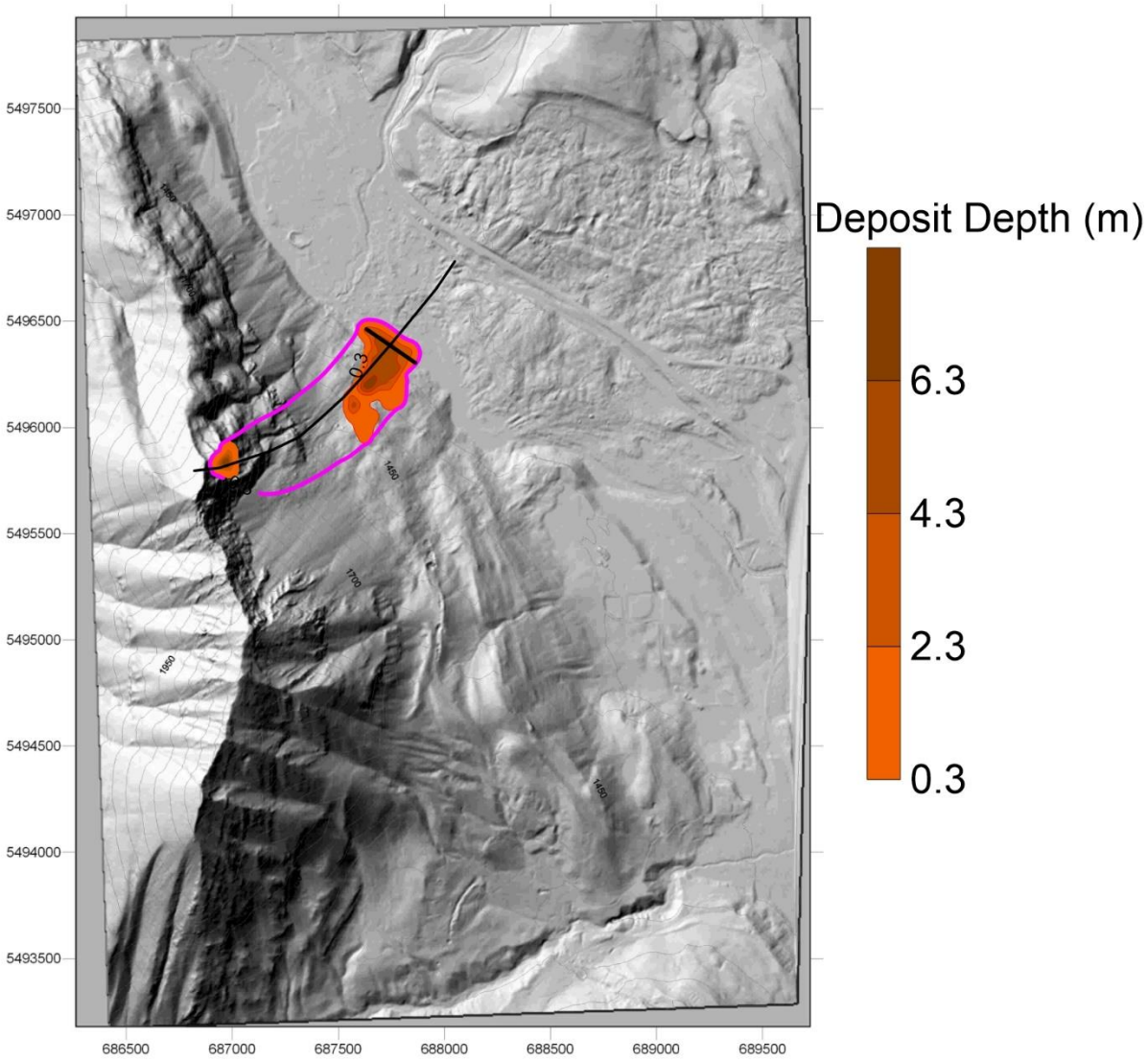

Figure 10
Predicted final deposit for the frictional case (friction angle = 31°).

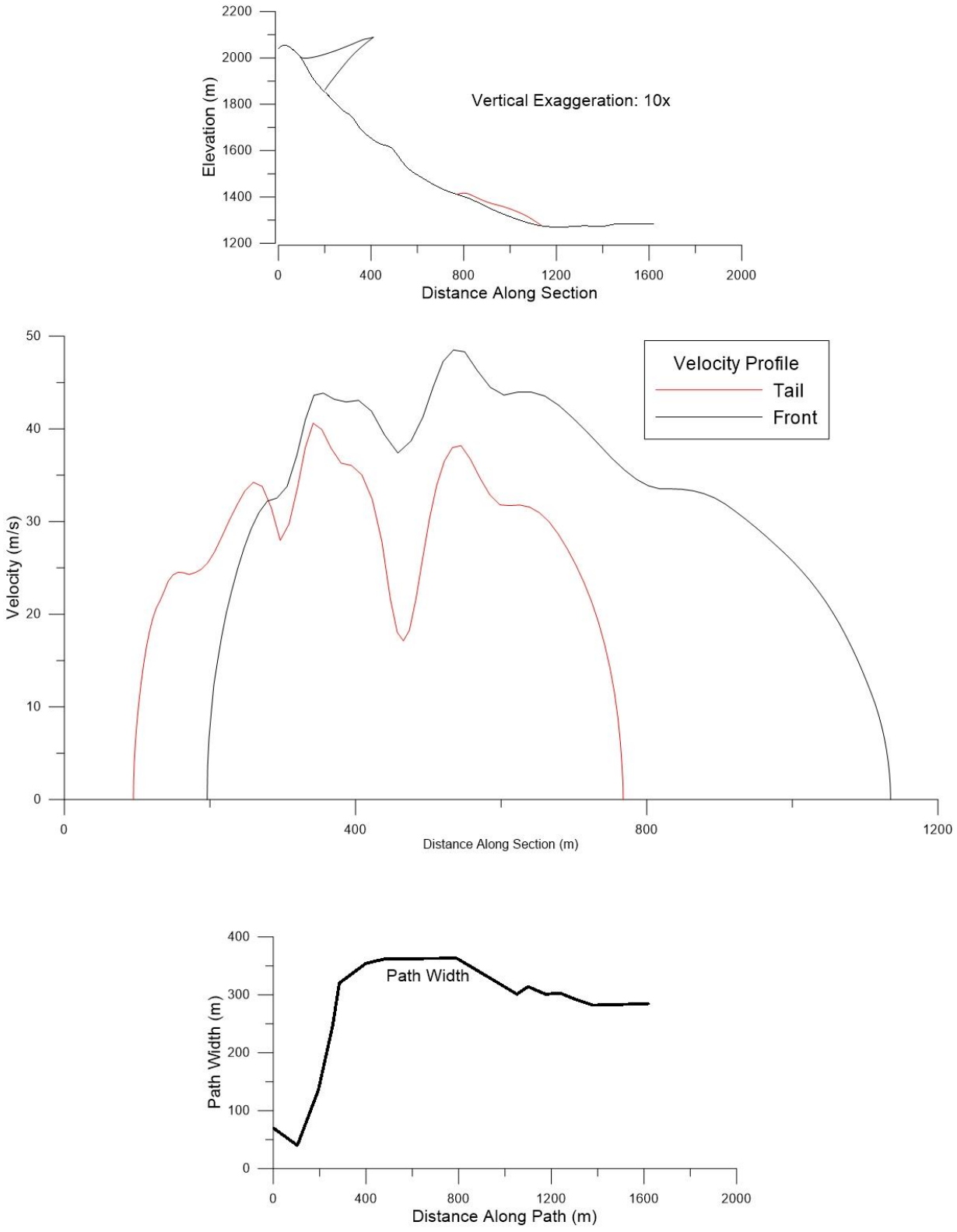

Figure 11
Shallow failure. Dan - W results for frictional simulation with a friction angle of 31º.

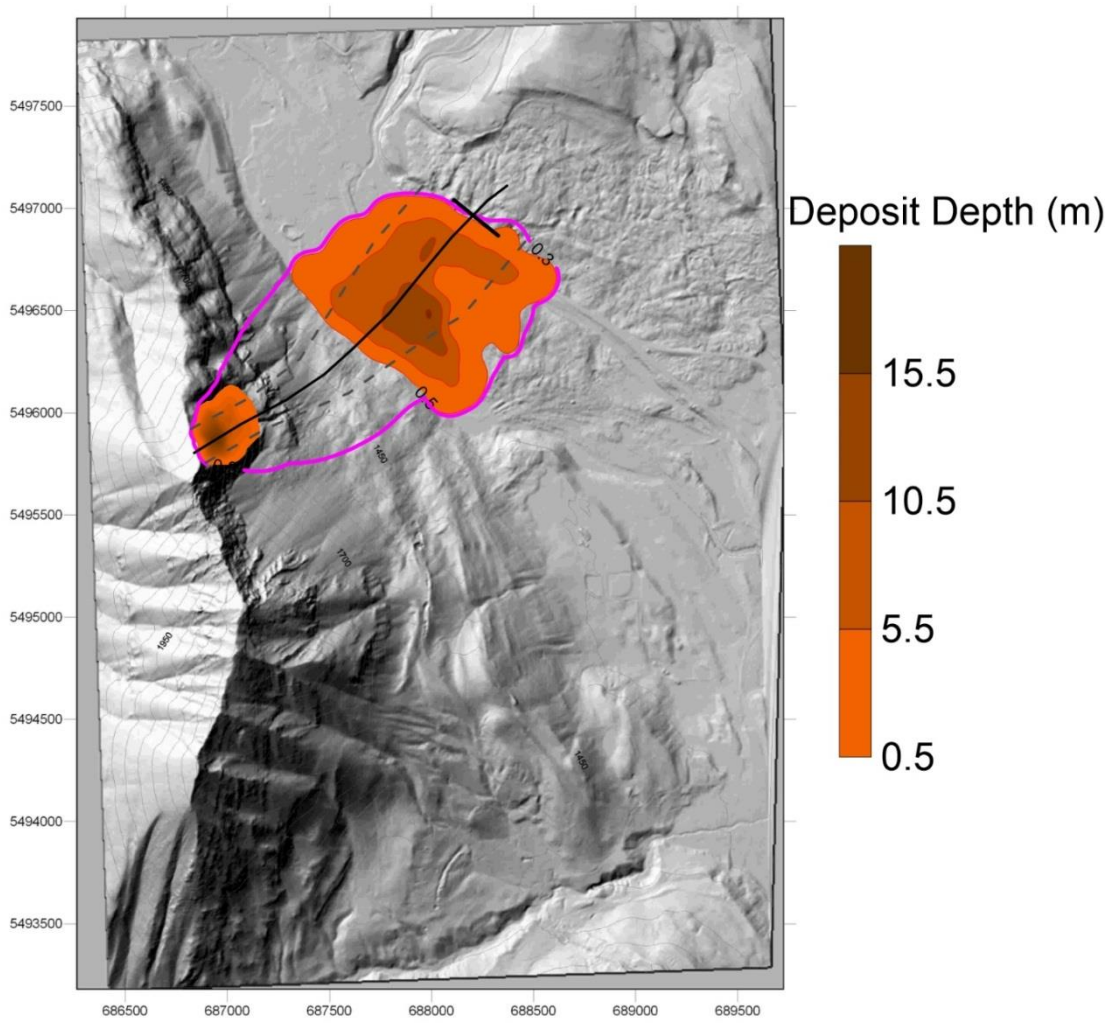

Figure 12
Deep failure. Predicted final deposit for Voellmy parameters $f = 0.1, \xi = 500$.
The dashed grey outline shows the width profile used in Dan-W.

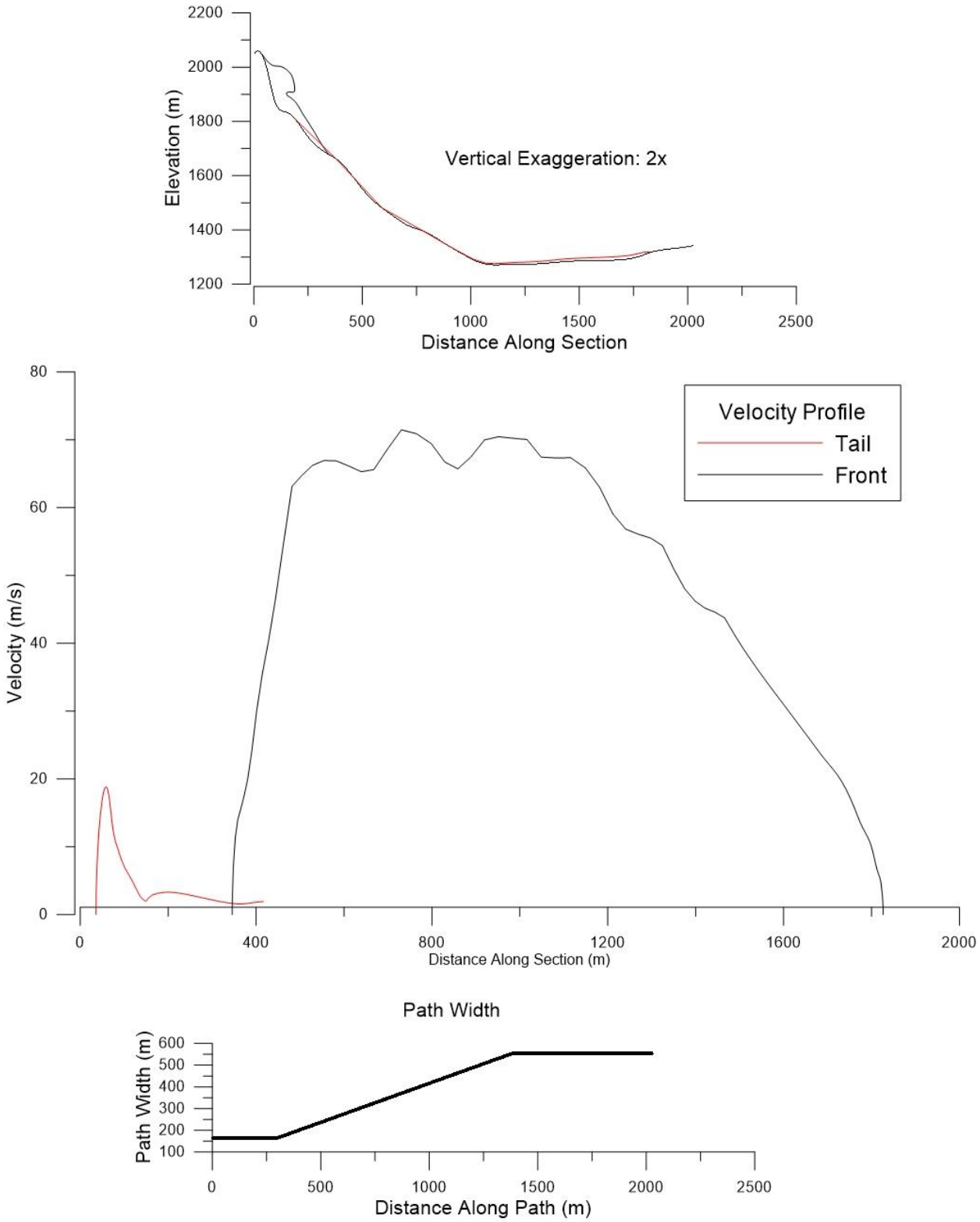

Figure 13
Dan-W prediction for Voellmy parameters $f = 0.1, \xi = 500$.

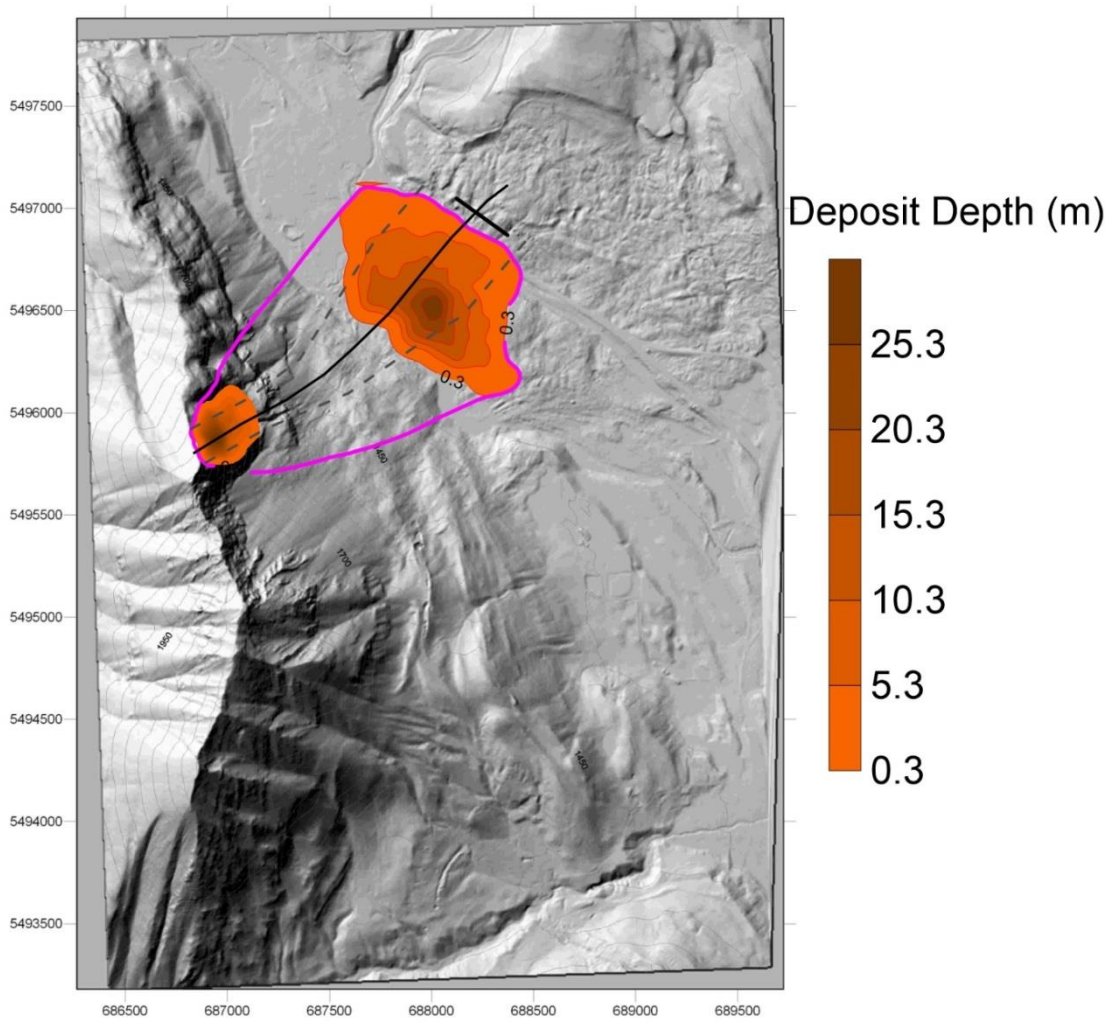

Figure 14
Deep failure. Predicted final deposit for frictional case (friction angle = 20^{o}).
The dashed grey outline shows the width profile used in Dan-W.

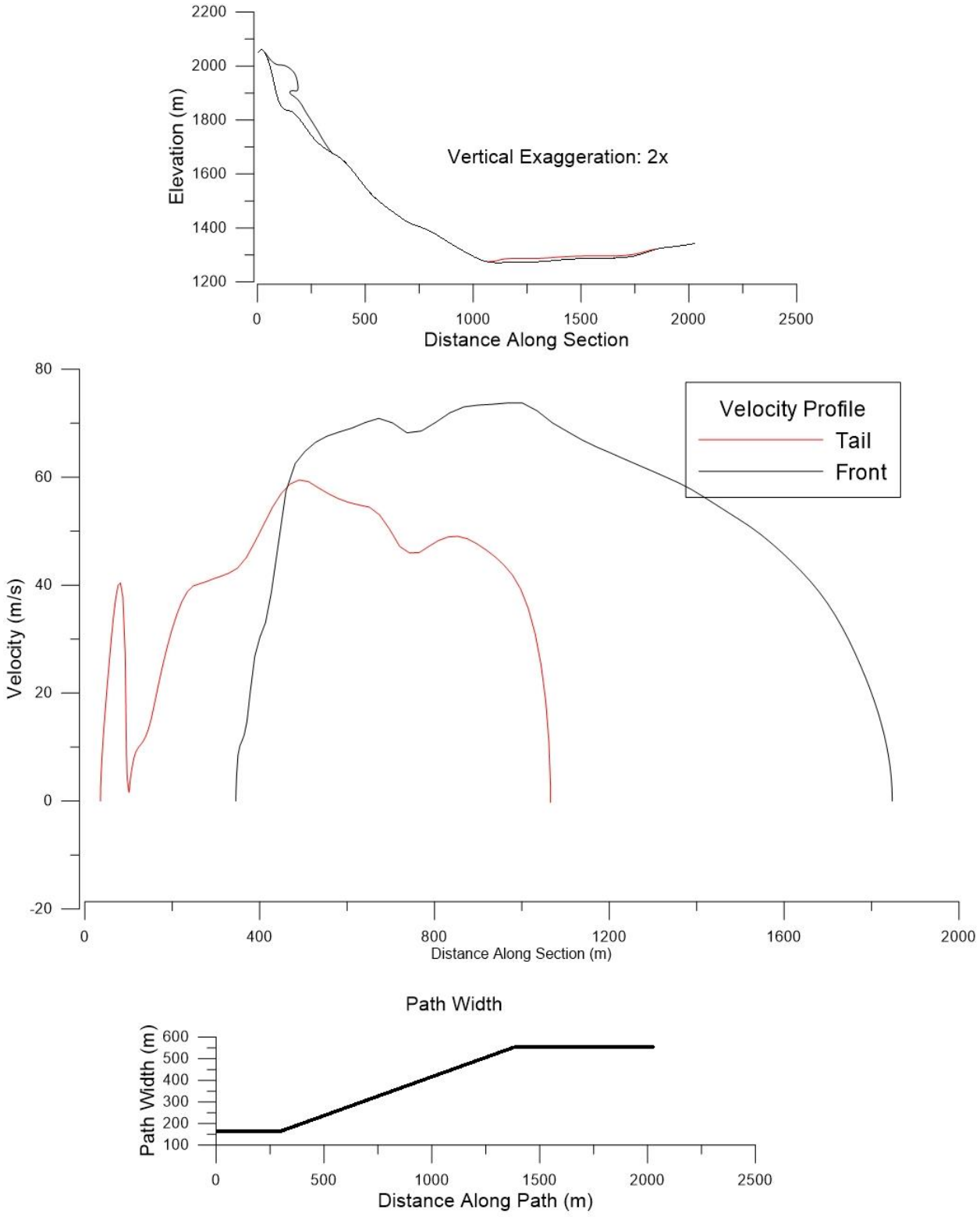

Figure 12
Dan-W prediction for the frictional rheology with a friction angle of 20º.

Appendix 2 – North Peak Area Stability Analysis

UNIL | University of Lausanne
Faculty of Geosciences and Environment
Geopolis
CH-1015 Lausanne

North Peak area stability analysis (Turtle Mountain)

Description and mechanisms of the unstable volumes*

* This report is largely inspired by Chapter 12 of MSc thesis of Florian Humair (*Turtle Mountain anticline (Alberta, Canada): Rock slope stability related fracturing).*

Humair Florian, PhD student

Jaboyedoff Michel, Professor

24 pages

UNIL | University of Lausanne
Faculty of Geosciences and Environment
Geopolis
CH-1015 Lausanne

Contents

UNIL | University of Lausanne
Faculty of Geosciences and Environment
Geopolis
CH-1015 Lausanne

1 Introduction

14 potential instabilities have been recently detected and characterized in Turtle Mountain area (Fig. 1) (Froese et al., 2009, 2012; Humair et al., 2012, 2013; Pedrazzini et al., 2011, 2012). Among them, two are located in North Peak area (NP-1, NP-2) which is the subject of the present report.

The later provides a slope stability analysis of the rocky spur located at the NE of North Peak, in Turtle Mountain (Figs. 1 and 2). In particular it aims at 1) understanding the rock mass structure and the kinematic behaviours and 2) to highlight the volume of a potential rock failure event and its failure mechanism.

This sector un-monitored by in-situ devices has been noticed as potentially unstable and investigated more in details during summer 2011 field survey (Florian Humair, Michel Jaboyedoff and Andrea Pedrazzini). Recent Ground-Based InSAR acquisition performed by the AGS demonstrated signs of activity at the base of this zone (Jamie Warren and Jill Pearse from the AGS).

This report is presented in the following way: 1) *Structural features*, 2) *Kinematic analysis* highlighting the potential structurally controlled failure modes, 3) *2D Numerical simulation* using Distinct Element Code modelling (UDEC^{TM}, Itasca, 2004) to investigate the influence of the discontinuity sets orientation on the slope stability, 4) Estimation of the unstable volumes performed using the Sloping Local Base Level method and 5) Summary.

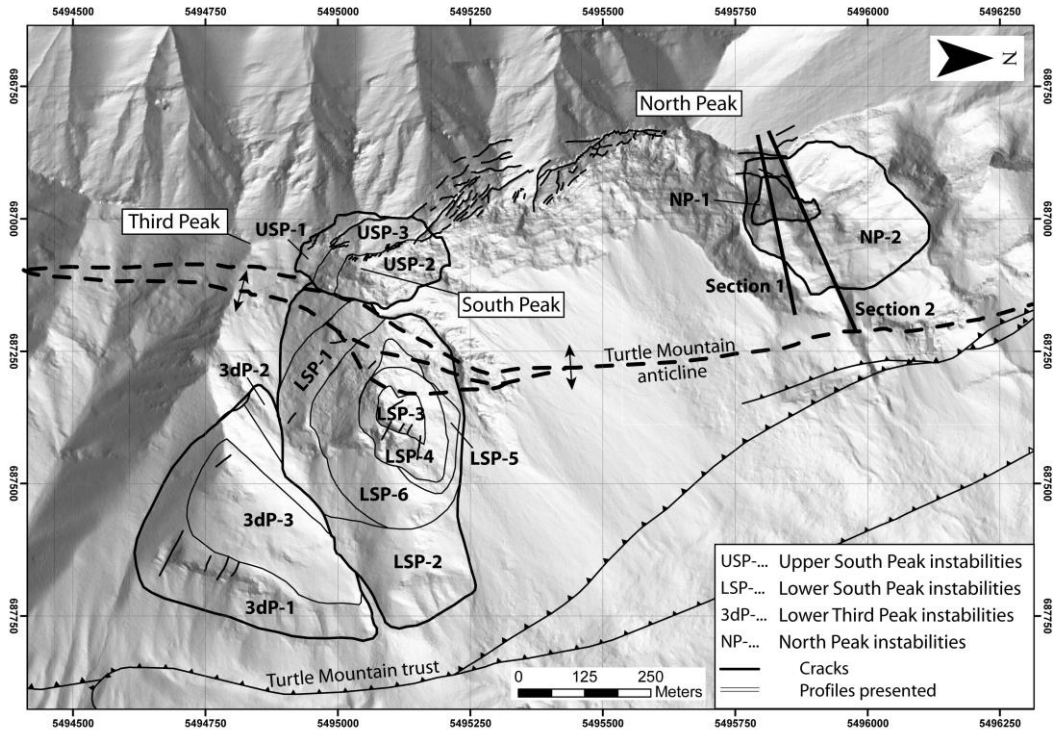

Figure 1: Outline of the fourteen unstable zones, cross-sections 1 and 2 are shown. Modified after Froese et al., 2012.

UNIL | University of Lausanne
Faculty of Geosciences and Environment
Geopolis
CH-1015 Lausanne

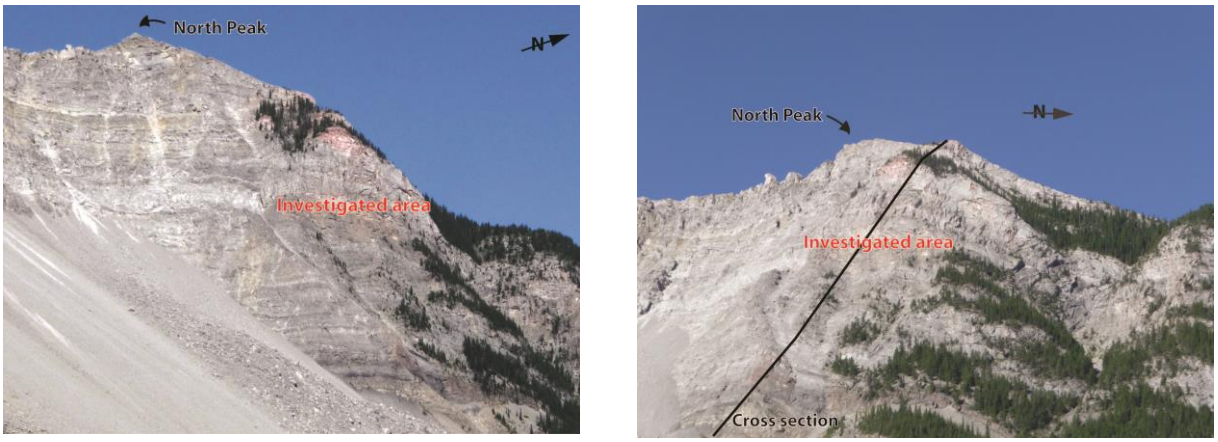

Figure 2: Views of the investigated zone and Section 1.

UNIL | University of Lausanne
Faculty of Geosciences and Environment
Geopolis
CH-1015 Lausanne

2 Structural features

2.1 Fracturing

Table 1: Characteristics of the discontinuity sets detected in North Peak area. Persistence and spacing categories from ISRM (1978).

Name (colour)	Dip direction	Dip	1 σ [°]	2 σ [°]	Persistence	Spacing
BP (black)	276	45	8	14	Very high	Moderate to Wide
J2 (red)	048	60	18	29	High	Moderate to Wide
J3' (blue) and J3' (orange)	098	52	17	28	High	Moderate to Wide
J4 (dark blue)	160	56	19	32	Low to medium	Moderate to Wide
J8 (green)	019	90	12	21	High to very high	Wide to very wide
"crack J3"	100	62	-	-	Very high	Extremely wide

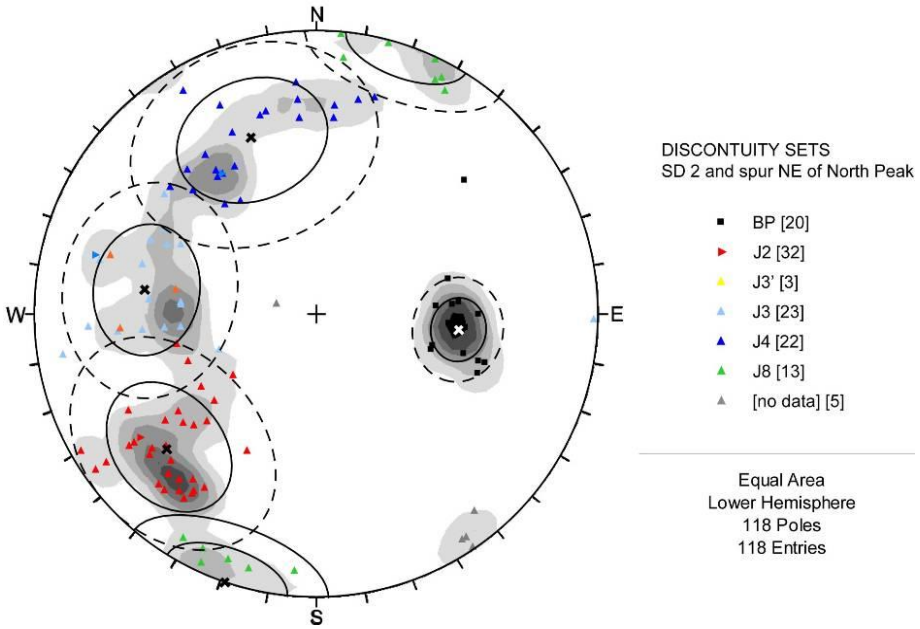

Figure 3: Pole representation of the discontinuities in North Peak area in equal area, lower hemisphere. The variability one sigma (full black ellipses) and two sigma (dashed black ellipses) are displayed.

Five main sets of discontinuity are revealed in North Peak area (Fig. 3 and Table 1): Bedding (BP), J2, J3/J3', J4 and J8 (Pedrazzini et al., 2011; Humair et al., 2013).

In addition, locally, an open (2 cm +/-1) and highly persistent (>20 m) fracture set is revealed (steep sub parallel to J3/J3' fracture [100/62°]). This fracture (named "crack J3") (Fig. 4) is attributed to J3/J3' in the kinematic analyses but is considered as a single set in the UDEC models.

UNIL | University of Lausanne
Faculty of Geosciences and Environment
Geopolis
CH-1015 Lausanne

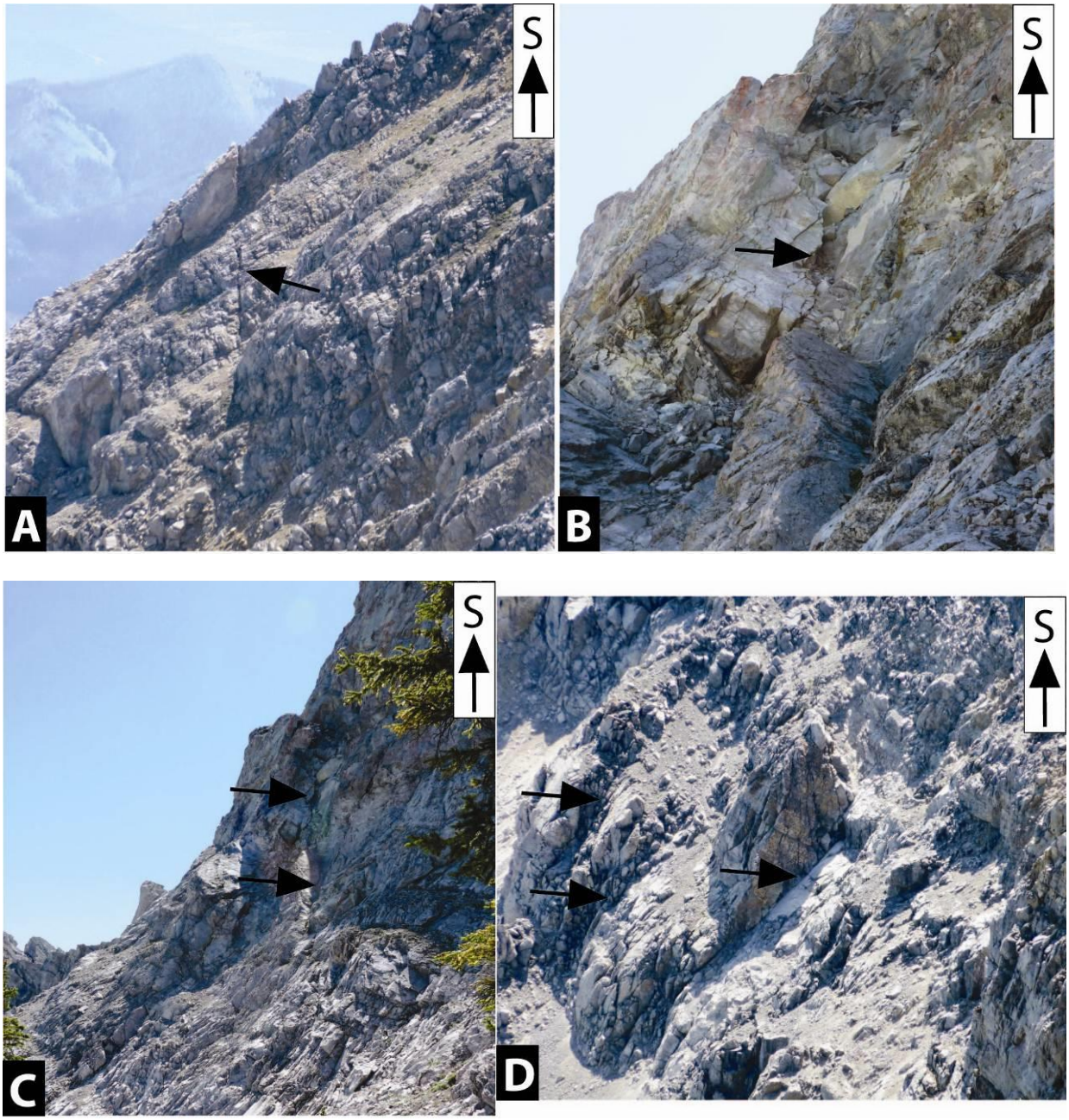

Figure 4: Field examples of persistent fractures "crack J3". A) Southern prolongation of a fracture. B) and C) Persistent fracture located at the top of the spur. D) Persistent fractures southward of the spur in the cliff of the Frank Slide scar.

UNIL | University of Lausanne
Faculty of Geosciences and Environment
Geopolis
CH-1015 Lausanne

2.2 Fracturing projection on cross section

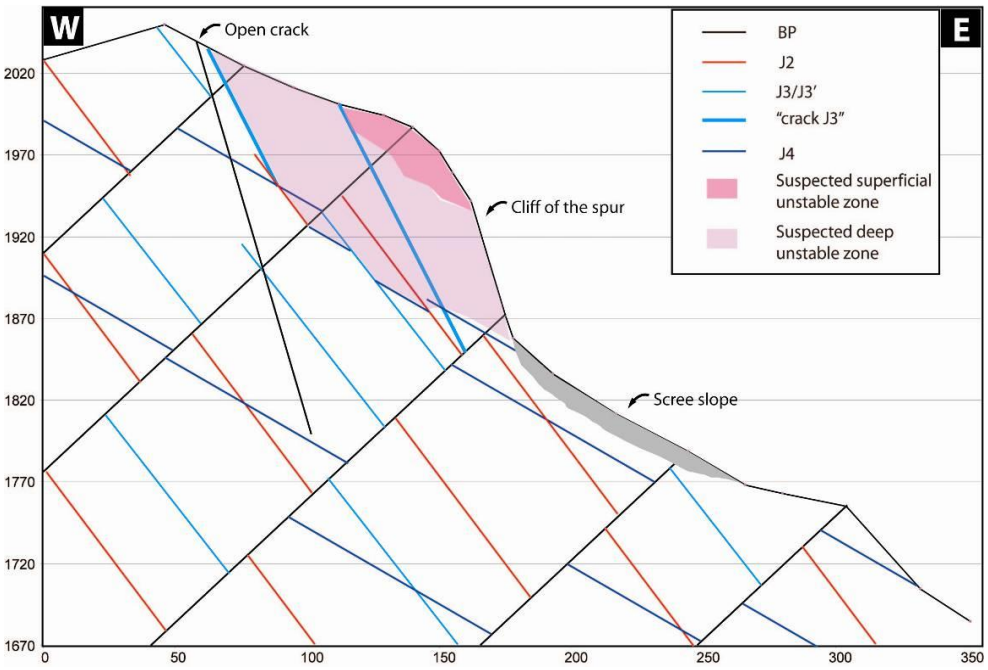

Figure 5: Conceptual model of the profile used for UDEC modelling (un-scaled). The traces of the discontinuities are shown as well as the suspected unstable areas (deduced from field observations). As J8 is parallel to the profile, it is not represented in the profile. This set has no kinematic relevance in 2D and is considered as lateral release surface.

3 Kinematic analysis

Based on Markland's test, kinematic analyses are performed for simple structurally controlled failure mechanisms (planar sliding, wedge sliding and toppling). The friction angle along the discontinuities is fixed at 30° (Benko and Stead, 1998). This is conducted for two topographies, respectively 080/70 and 100/70 in order to take into account the variation of the face's orientation.

- Planar sliding along J2, J3/J3' and J4 are possible (Fig. 6A).
- Wedge sliding is possible along intersection lines J2^J3, J2^J4 and J3^J4 (Fig. 6B). Theoretically, wedge sliding can also occur between J2^J8, J3^J8 and J4^J8. However, due to the steepness of J8, the failure would more likely correspond to a planar sliding on either J2, J3/J3' or J4, laterally constrained by J8. J8 is thus considered as a lateral limit that allows the lateral delimitation of the sliding blocks.
- Block toppling across BP cannot be excluded especially when regarding the high persistence and close spacing of this discontinuity set.
- Overhanging failure mechanism along BP is also likely to mobilize small volumes (not demonstrated using stereographic technique).

UNIL | University of Lausanne
Faculty of Geosciences and Environment
Geopolis
CH-1015 Lausanne

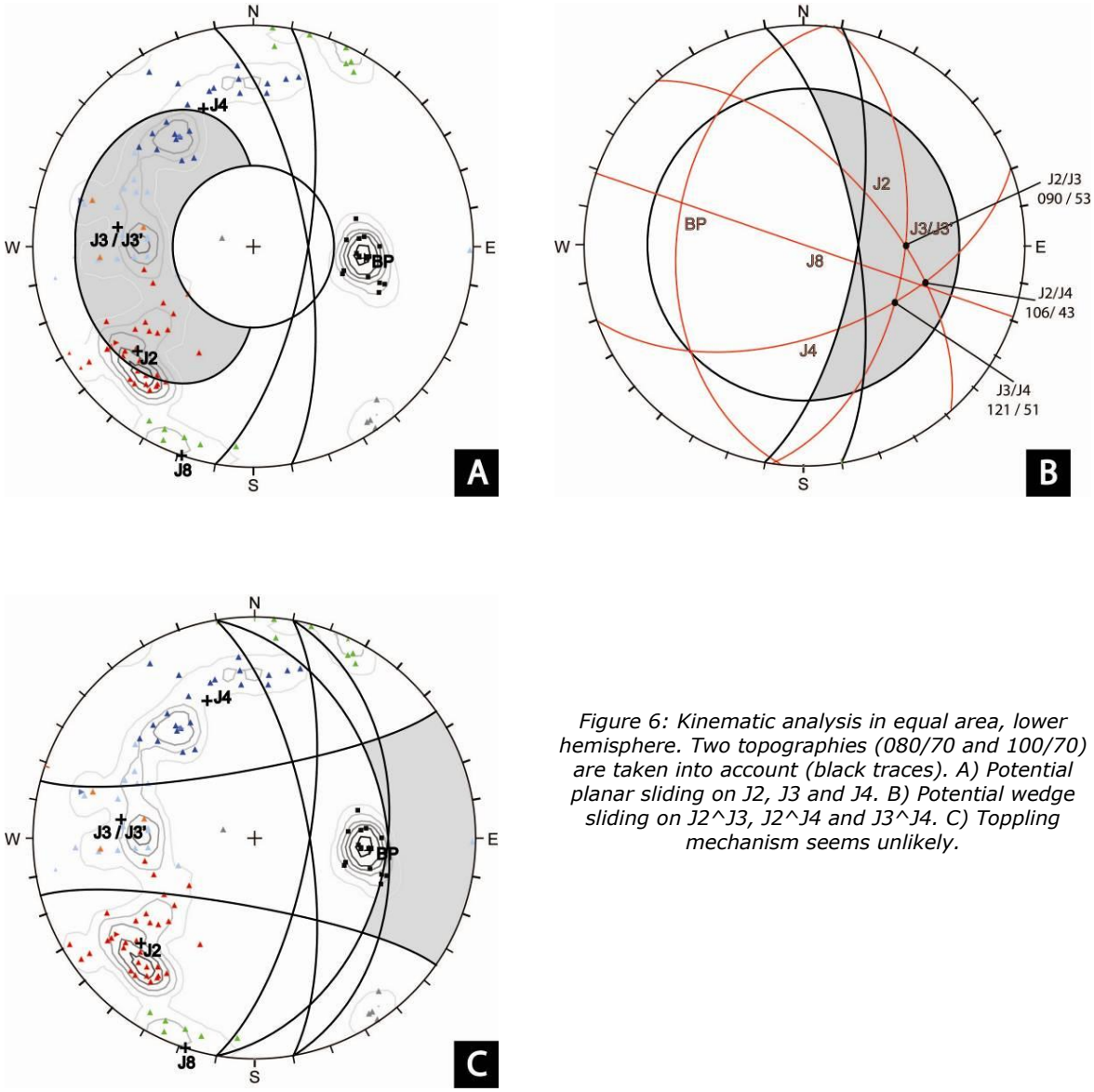

Figure 6: Kinematic analysis in equal area, lower hemisphere. Two topographies (080/70 and 100/70) are taken into account (black traces). A) Potential planar sliding on J2, J3 and J4. B) Potential wedge sliding on J2^J3, J2^J4 and J3^J4. C) Toppling mechanism seems unlikely.

UNIL | University of Lausanne
Faculty of Geosciences and Environment
Geopolis
CH-1015 Lausanne

4 Numerical modelling - UDEC™

4.1 Introduction

A two-dimensional distinct element code is performed (UDEC™ Itasca, 2004) to investigate the failure mechanism and the volumes involved in the potential rock slope failure as well as to assess the role of each set of discontinuity in the slope stability.

Different *calibration models* are run in order to point out different parameters' influence on North Peak slope stability and to propose models that are coherent with field observation (not presented in the present report; see Humair MSc, 2011 for more details). The different tested parameters are: discontinuity sets number, persistence, spacing, friction angle and joint stiffness.

4.2 Modelling parameters and procedure

The location of the cross section is presented in table 2 and figures 1 and 2.

Table 2: Modelled cross section information (cross section1).

Cross section	
Length [m]	351
Strike [deg]	265 - 085
Point 1 [meters]	686824/5495835
Point 2 [meters]	687175/5495866

Based on 1) field mapping, 2) calibration models and 3) 3DEC (Itasca, 2008) simulations conducted on South Peak by Brideau et al. 2011, six models are performed, each of them displaying slight variations of the discontinuity sets properties (Table 3). They are conducted with a friction angle of 30° and 35° which are thought to be the most adapted angles in this study case according to field observation and previous comparable simulations (Brideau et al., 2010; Benko and Stead, 1998). The other varying parameter is the persistence of set J4. As this set is less persistent than the others (field surveys), a shorter persistence is introduced in order to perform more constrained modelling.

The rock material properties are invariant for all presented models as only the Livingstone formation affects the cross section (Table 4). The determination of their respective values is based on Benko and Stead (1998) and Brideau et al. (2011).

All simulations are executed with 25000 calculation steps and assume rigid blocks and a linear elastic constitutive criterion is adopted to represent deformation of the intact blocks.

The limits of the considered surface as unstable is arbitrarily defined in UDEC as the surface affected by displacement longer that 1 meter (Brideau et al., 2011). The calculation of the unstable volume detected in UDEC is performed according to the following: georeferencing of the unstable surface in a GIS environment and calculation of its area which is then multiplied by the suspected lateral extension of the unstable zone (constrained by geomorphic features).

Table 3: Discontinuity sets parameters for the six UDEC models. The default persistence used for "crack J3" is 100m.

Model	Number of sets	Persistence J2, J3/J3' [m]	Persistence J4 [m]	Spacing [m]	Friction angle [°]	Normal/Shear stiffness [GPa]
FM1_J4_p12_jfr_30.sav	5	50	12	10	30	4/1
FM2_J4_p12_jfr_35.sav	5	50	12	10	35	4/1
FM3_J4_p25_jfr_30.sav	5	50	25	10	30	4/1
FM4_J4_p25_jfr_35.sav	5	50	25	10	35	4/1
FM5_J4_p50_jfr_30.sav	5	50	50	10	30	4/1
FM6_J4_p50_jfr_35.sav	5	50	50	10	35	4/1

Table 4: Material properties used in the UDEC numerical models.

Material properties	
Density [kg/m3]	2700
Bulk modulus [GPa]	7
Shear modulus [GPa]	4
Cohesion [MPa]	3
Tensile strength [Mpa]	0
Friction angle [deg]	50

4.3 Results: Volumes estimation

The obtained volumes range between **0.102 Mm^3 and 0.247 mm^3**.

The six models approximately display the same geometry of the failure surface, which **only involves the superficial portion of the rock spur's cliff of the rock spur (Figure 7, 8 and 9 and table 5)**. The differences between the six models lie in the depth of this failure surface. The introduction of a smaller persistence for J4 than for the other sets permits to obtain more realistic models. Indeed, when all sets are fully persistent, the modelling involves a too large potential unstable area, i.e. including the whole spur.

Table 5: Summary of the results of UDEC simulations.

Model	Max displacement [m]	Max velocity [m/s]	Volume [Mm^3]
FM1_J4_p12_jfr_30.sav	23.1	5.9	0.19
FM2_J4_p12_jfr_35.sav	19.25	5.25	0.10
FM3_J4_p25_jfr_30.sav	19.03	5.07	0.20
FM4_J4_p25_jfr_35.sav	17.6	4.88	0.14
FM5_J4_p50_jfr_30.sav	19.5	5.18	0.24
FM6_J4_p50_jfr_35.sav	18.9	5.19	0.16

The potential failure surface and displacement deduced from respectively the most optimistic and the most conservative models are shown in figures 7 and 8 (i.e. *FM2_J4_p12_jfr_35.sav and FM5_J4_p50_jfr_30.sav*).

UNIL | University of Lausanne
Faculty of Geosciences and Environment
Geopolis
CH-1015 Lausanne

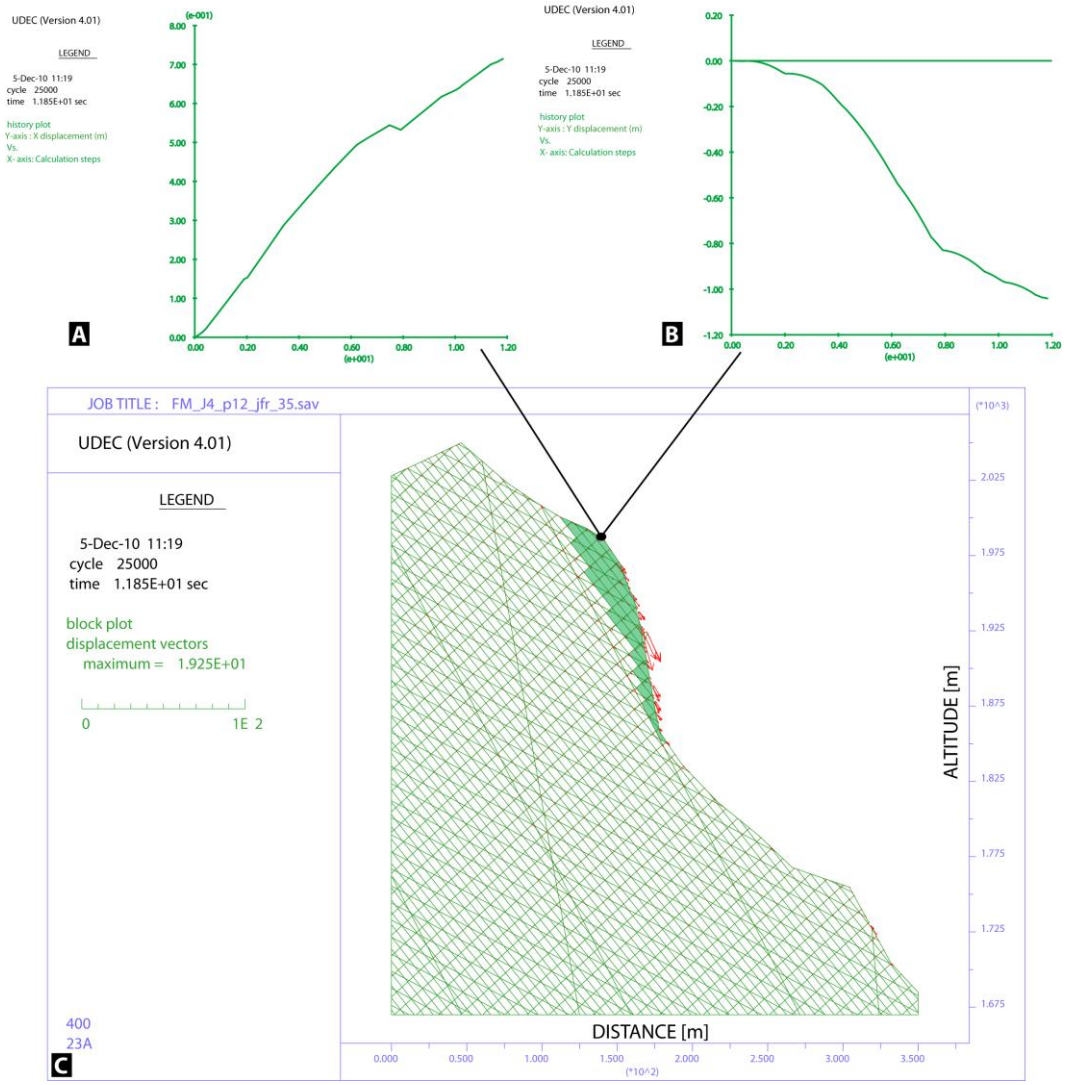

Figure 7: UDEC window for model FM2_J4_p12_jfr_35.sav. A) and B) displacements along X and Y axis at 140m/1985m on the profile. C) Calculated displacements (red arrows) and expected failure surface (green). Step-path sliding along J2, J3/J3' is highlighted by the displacement vectors as well as toppling failure mechanism across BP (Section 3).

UNIL | University of Lausanne
Faculty of Geosciences and Environment
Geopolis
CH-1015 Lausanne

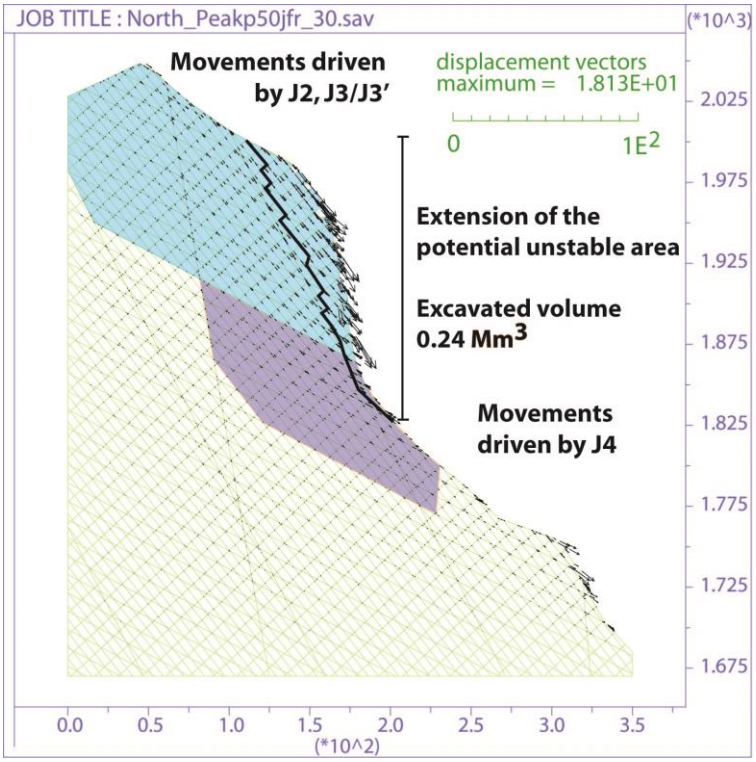

Figure 8: UDEC window for model FM5_J4_p50_jfr_30.sav showing the calculated displacements (black arrows), the expected failure surface (black line) and the control on movements. Movements driven by step-path sliding - subsidence along joint sets J2 and J3/J3' at the top of the cliff and by set J4 at the base of the cliff. Modified after Froese et al. 2012.

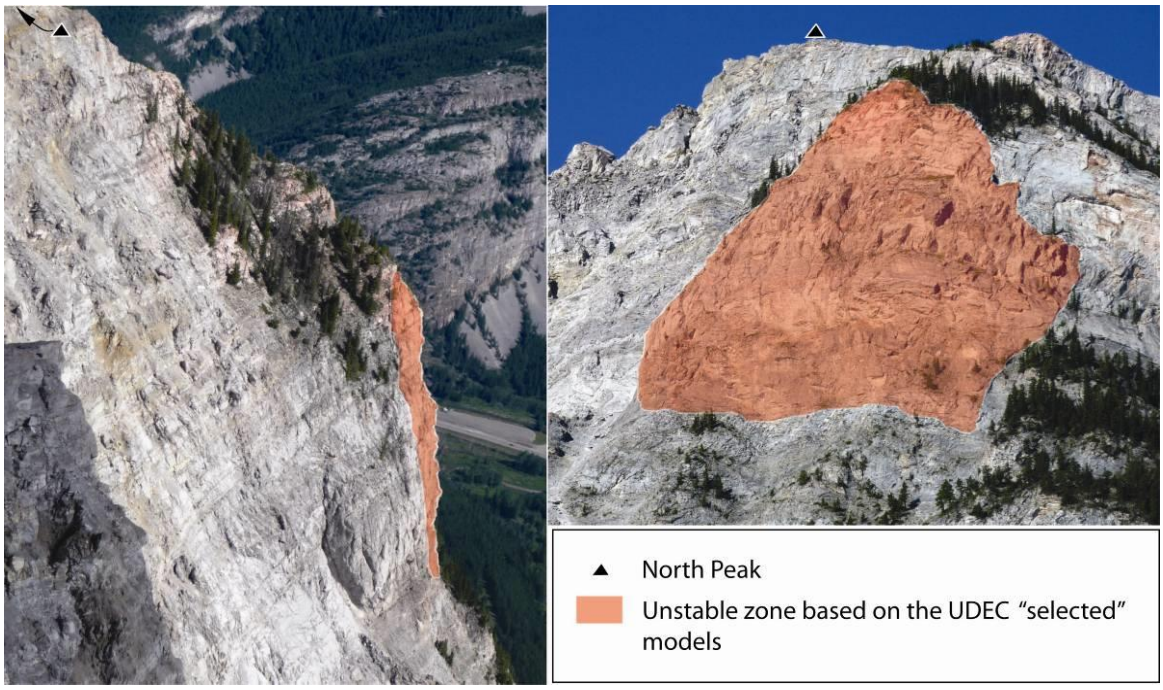

Figure 9: Outline of the present day unstable zone deduced from UDEC modelling. Only the superficial portion of the cliff is involved.

UNIL | University of Lausanne
Faculty of Geosciences and Environment
Geopolis
CH-1015 Lausanne

4.4 Results: Failure mechanism

The failure mechanism deduced from kinematic analysis (Chapter 3) is in good agreement with the numerical analysis. Indeed, when all discontinuity sets are included in the model, the potential **failure mechanism** can be described as a **bi-planar sliding** (Figure 8, 10 and 11) (Brideau and Stead, 2012; Fisher, 2009; Fisher and Eberhardt, 2012; Hoek, 2000):

- The unstable mass is likely to subside (step-path) following J2 and J3/J3' in the upper part of the unstable zone. The influence of "crack J3" is quite similar to J2 and J3/J3' but it leads to an increase of the displacement vectors.
- At the base of the unstable zone, displacement vectors mainly follow J4 discontinuity set. Even if less persistent that other discontinuities, the basal failure surface is expected to propagate by rock bridge breakage between J4 discontinuity set (Figure 11) and allows the unstable compartment to slide "out of the topography".
- As a consequence, sets J2, J3/J3' and "crack J3" have more influence on the upper part of the cliff, whereas the influence of J4 concerns mostly the lower part of the cliff (Figs 7, 8, 10 and 11). BP plays the role of the release surface of the blocks whereas J8 laterally delimit the extent of these latter.

Toppling failure mechanism across BP has also been highlighted by models (Figure 7). According to the models, this mechanism appears to be limited to some blocks only and does not involve the whole unstable zone. Hence, this failure mechanism cannot be totally excluded.

Overhanging failure mechanism is also pointed out, but it is likely to involve only rockfalls of the rockface (Figures 7 and 12).

The kinematic analysis also pointed out potential wedge sliding mechanism. Wedge sliding can hardly be assessed using 2D modelling. However, this failure mechanisms seems unlikely as all open fractures observed at the top of the cliff are formed by either J2 or J3/J3' while J4 is quite less persistent there. Inversely, downward in the cliff, J2 and J3/J3' are not systematically observed whereas J4 is clearly highlighted. It implies that no wedge intersection line is susceptible to strike out of the topography in this area.

As a consequence, the bi-planar sliding seems to be the most appropriate mechanism contributing to the destabilization of the spur along with potential toppling in a minor extent.

UNIL | University of Lausanne
Faculty of Geosciences and Environment
Geopolis
CH-1015 Lausanne

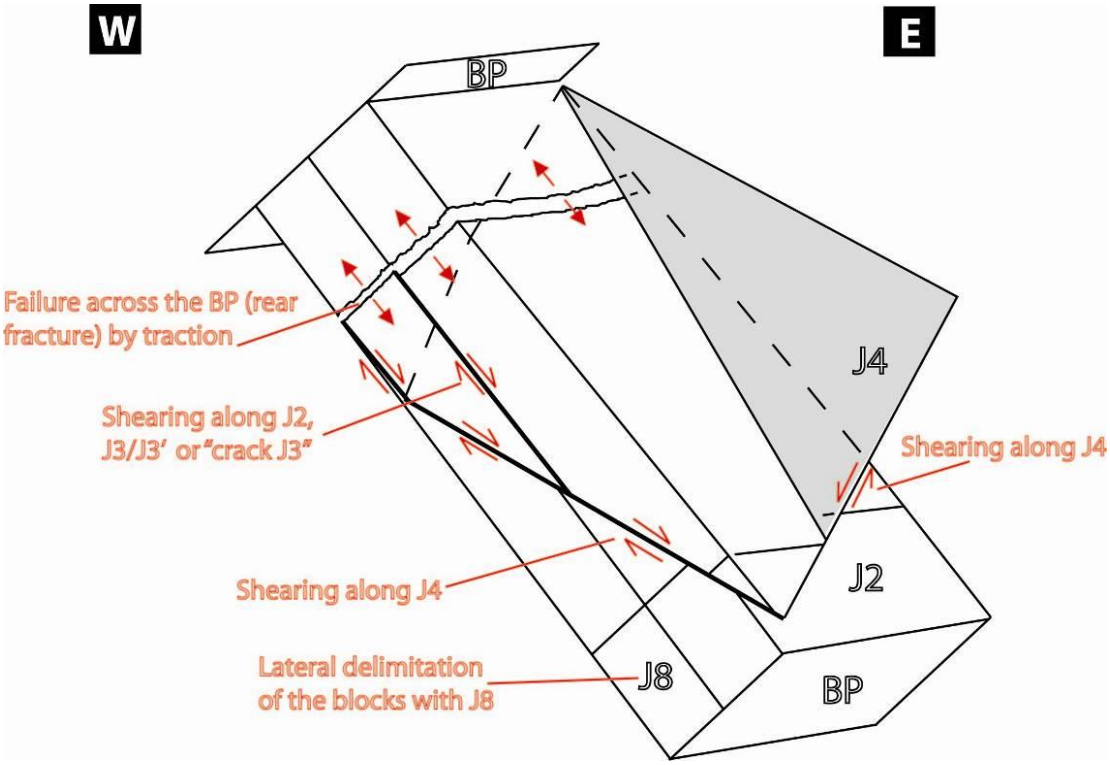

Figure 10: Schematic representation of the suspected failure mechanism with bi planar failure on J2 (or J3/J3' or "crack J3") and J4. The rear release is permit by opening across the BP and the blocks are laterally delimitated by J8.

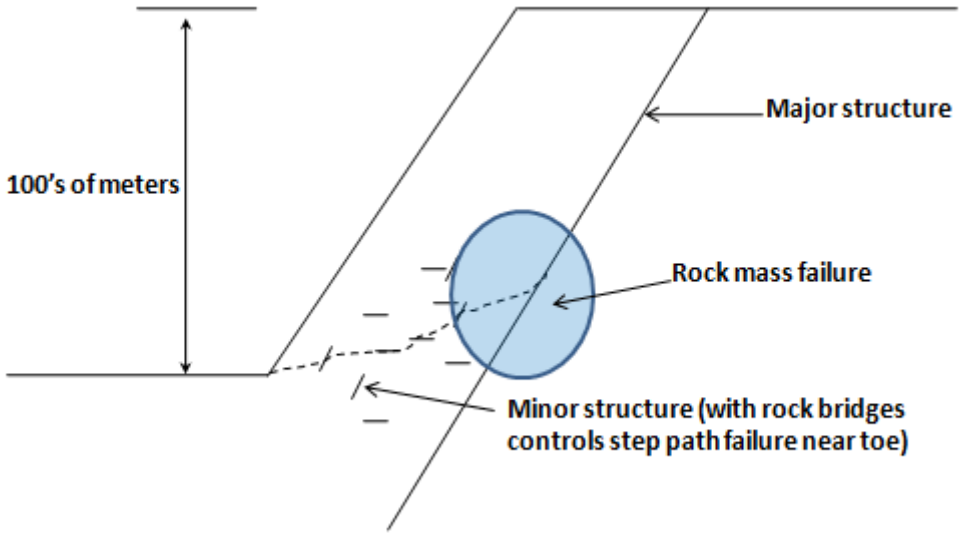

Figure 11: Illustration of a complex slope failure described as a bi-planar failure (After Hoek, 2000 in Fisher, 2009). The active portion of the slide (bounded by a major structure) moves down leading to a rock mass damage zone. The presence of minor non persistent structure allow step-path failure at the toe of the slide.

UNIL | University of Lausanne
Faculty of Geosciences and Environment
Geopolis
CH-1015 Lausanne

Figure 12: View towards the West of the main cliff showing fresh outcrops suggesting evidences of recent shallow block fall.

UNIL | University of Lausanne
Faculty of Geosciences and Environment
Geopolis
CH-1015 Lausanne

5 Volume estimation and failure surface geometry – SLBL method*[1]

5.1 Introduction

In order to compare the volumes of the potential failure surfaces modelled using UDEC, a Sloping Local Base Level (SLBL) analysis is performed (Jaboyedoff et al., 2009). It allows to highlight a 3D failure surface geometry based on a DEM and to define the unstable volume.

Two types of modelling are performed:

- An analysis of the **shallow portion of the spur**, which permits to directly compare the results with the UDEC analysis.
- A modelling of the volume that would be involved in **the case of the whole spur collapse (deep failure)**. Despite the fact that such a large catastrophic event is not likely to occur, this is done in order to point out the maximal volume that could be mobilized in this zone.

5.2 Modelling procedure

The approach consists of defining on a Digital Elevation Model, the extent of the zone that corresponds to the limits of failure. This zone comprised the mobile points (pixels) in opposition to the fixed pixels (out of the unstable zone). Therefore, the extents of the unstable zones (shallow and deep analysis) are defined based on geomorphic criterions.

As no subsurface information in this area exists, the depth of the failure surface was not constrained in the models beforehand. However, some of the presented models use the "slope limit factor" parameter (Tables 6 and 7), which constrains the modelled surface based on the angle of the basal delimiting surface. This factor aims at avoiding an over-deepening of the calculation and allows taking into account the dip of the main discontinuity sets involved in the failure. The modelling is performed using a 1-m grid DEM.

5.3 « Shallow » models

The moving area extent is laterally constrained by boarders of the spur: at the top by the presence of open fractures and at the bottom by the change in the slope angle of the mountain side.

The results give volumes comprised in a range **between 0.183 and 0.249 Mm^3** and the maximal vertical depth of the failure surface reached 70 to 88.1 m (Table 6).The three selected models display a steep concave surface failure in the rear of the spur, with a progressive flattening when approaching the basal boundary of the mobile zone.

Figures 13 and 14 respectively display cross section (of all three models) and visualisation of the SLBL calculation with a post-failure morphology (*model SNP_shall_11*).

[1] * 3 GRD files are provided in appendix (See section 7 *Provided data* in page 23).

UNIL | University of Lausanne
Faculty of Geosciences and Environment
Geopolis
CH-1015 Lausanne

Table 6: Parameters and related results using SLBL method for the shallow potential failure. The curvature is negative in order to obtain a circular like surface.

Parameters				Results		
Model	Curvature - tolerance	Slope limit factor [°]	Max depth	Maximal depth [m]	Mean depth [m]	SLBL volume [Mm^3]
SNP_shall_10	-0.06	50	-	88.1	36.8	0.24
SNP_shall_11	-0.06	60	-	73.1	27.24	0.18
SNP_shall_12	-0.06	60	70	70	27.1	0.18

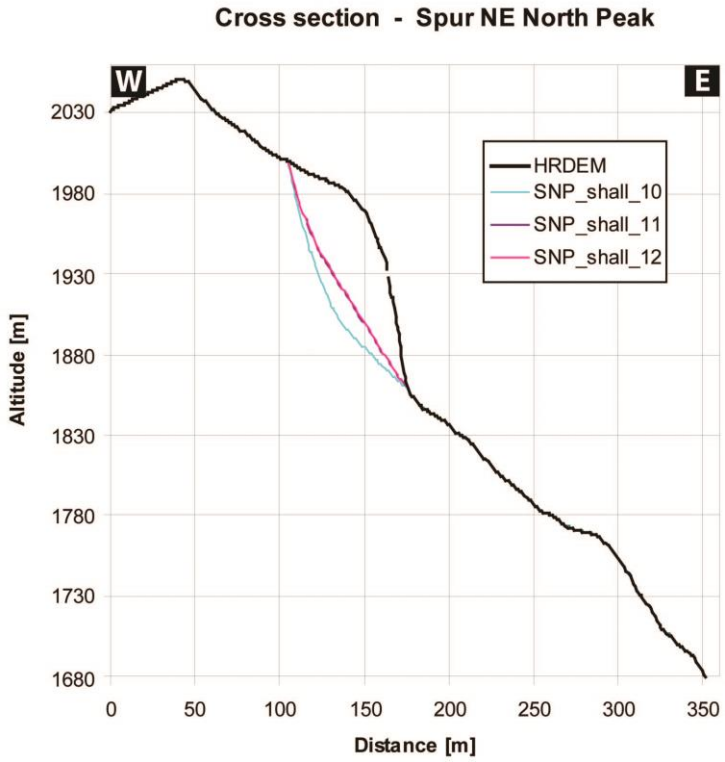

Figure 13: Cross section of the spur showing the shape in 2D of the failure surfaces for the shallow instability calculated using the SLBL method.

UNIL | University of Lausanne
Faculty of Geosciences and Environment
Geopolis
CH-1015 Lausanne

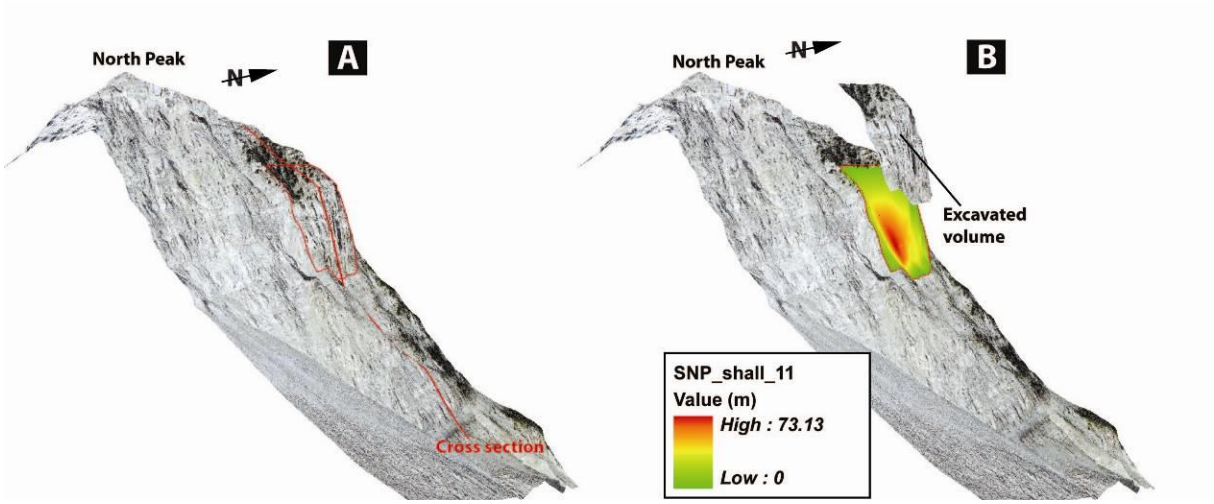

Figure 14: A) View looking the investigated area where the cross section and the extent of the unstable zone are shown in red. B) Representation of the result of the SLBL calculation for the model SNP_shall_11 outlining the depth of the failure surface.

5.4 « Deep » models

The delimitation of this zone is based on the presence of highly persistent fractures at lateral boarders. These fractures can be associated to discontinuity set J1 (023/41 and 019/47). This discontinuity set is not revealed by field surveys in the spur area but is clearly highlighted as a major morpho-structures using COLTOP 3D software. The summit of the potentially moving zone corresponds to a persistent open crack. The basal boundary is fixed at the end of the western limb of the fold, due to the presence of the hinge area. The choice to fix the boundaries of the moving area's basal extent near the hinge area is based on two considerations: 1) the hinge area constitutes a destabilizing zone due to its high density of fracturing, 2) the eastern fold limb displays a different fracturing pattern, i.e. the failure mechanism is also different there.

The results of the deep seated failure modelling range between 126.1 and 186.7 meters for the vertical maximal depth and between **2.68 and 4.4 Mm^3** for the volume (Table 7).

Figure 16 presents the visualisation of the SLBL calculation for models *SNP_deep_21 and 33* and display a post-failure morphology which is quite satisfying, when compared with the topography of the saddle area cliff (between North Peak and South Peak).

UNIL | University of Lausanne
Faculty of Geosciences and Environment
Geopolis
CH-1015 Lausanne

Table 7: Parameters and related results using SLBL method for the deep potential failure. The curvature is negative to obtain a circular like surface.

	Parameters			**Results**		
Model	Curvature-tolerance	Slope limit factor [°]	Max depth [m]	Maximal depth [m]	Mean depth [m]	SLBL volume [Mm^3]
SNP_deep_21	-0.08	50	-	126.6	38	2.68
SNP_deep_33	-0.08	45	-	156.4	50.2	3.54
SNP_deep_40	-0.07	40	-	187.1	62.4	4.40

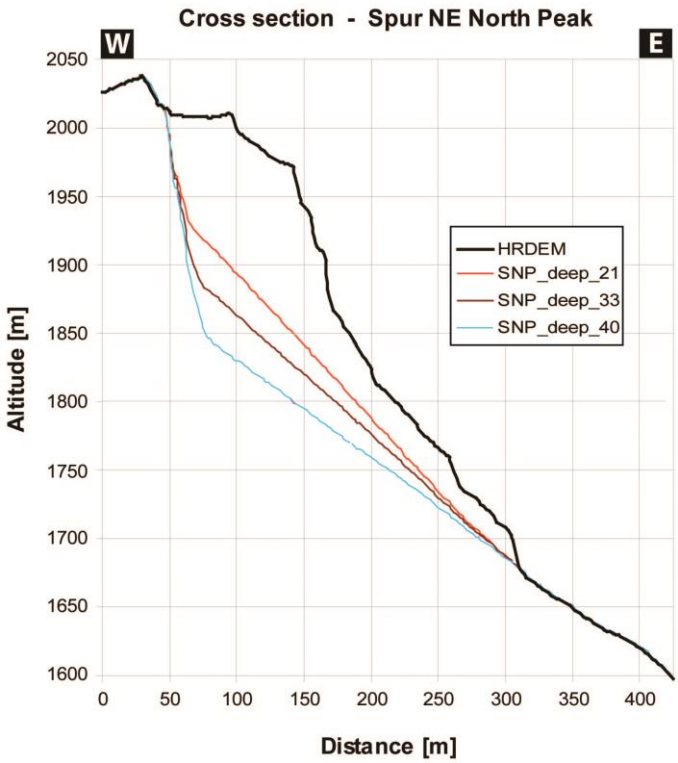

Figure 15: Cross section of the spur showing the shape in 2D of the failure surfaces for the deep instability calculated using the SLBL method.

UNIL | University of Lausanne
Faculty of Geosciences and Environment
Geopolis
CH-1015 Lausanne

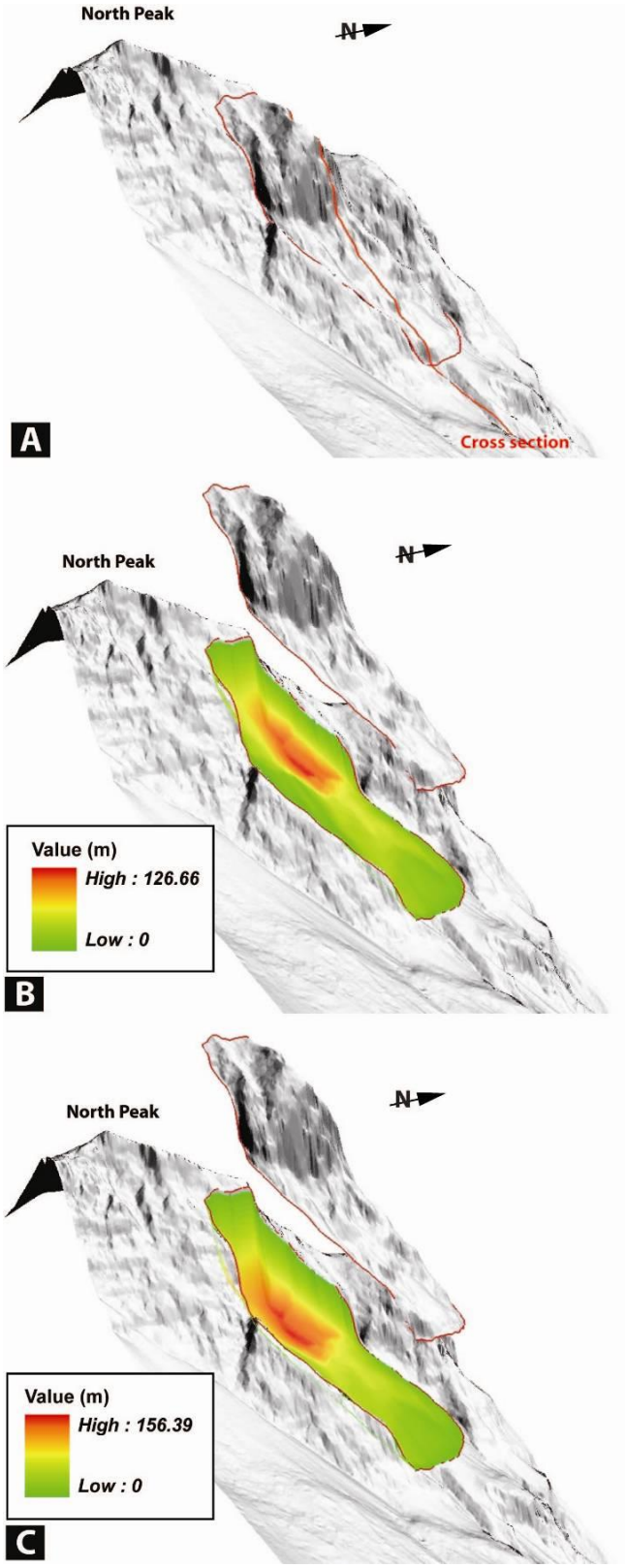

Figure 16: A) View looking the investigated area where the cross section and the extent of the unstable zone are shown in red. B) and C) Representation of the result of the SLBL calculation for the model SNP_deep_21 (B) and SNP_deep_33 (C) outlining the depth of the failure surface.

UNIL | University of Lausanne
Faculty of Geosciences and Environment
Geopolis
CH-1015 Lausanne

5.5 Discussion and summary of the SLBL analysis

Two types of models are performed. The "shallow" models allow a direct comparison with the volumes extracted from the UDEC™ analysis showing a good accordance between both methods (between 0.18 and 0.24 Mm^3). The "deep" models allow volume estimation (between 2.7 and 4.4 Mm^3) of an unlikely catastrophic event involving the collapse of most of the spur NE of North Peak.

Based on the fact that the failure is assumed to be structurally controlled, a slope limit factor corresponding to the detected discontinuity sets has been chosen.

Referring to the hypothesis of the 1903 event failure mechanism (Jaboyedoff et al., 2009), it is obvious that the upper portion of the failed mass was structurally controlled. However, besides resulting of dip slope along bedding plane, the central portion failure (around the hinge area) could be explained by a decrease of the rock mass strength due to the high density of the fracturing. Thus, the control of the potential "deep" failure could result of the diminution of the strength of the rock mass in the central part of the mountain instead of the fracturing orientation only. The decrease of the strength conditions in this zone has been demonstrated using the Geological Strength Index (GSI) by Pedrazzini et al. (2011) and Humair et al. (2010). As a consequence it is not expected that the failure surface of the central portion of the eastern side of the mountain follows specific sets, but rather depends on an irregular geometry controlled by several close spaced joints.

The collapse of the whole spur is an imaginable scenario based on morphological evidences (cracks, slope change…) but required a radical modification of the rock mass properties. This is therefore an unlikely scenario since it implies an important decrease of the parameters governing the stability: diminution of the friction angle of the discontinuities (up to 15°) as well as fully persistent joints sets (both based on UDEC simulations). This implies a dramatic decrease of the joint surface condition and the breakage of all rock bridges. Such a catastrophic scenario could eventually occur after a long period of fatigue (progressive fail of the rock bridges) coupled with an unlikely succession of unfavourable events such as abundant water (radical increase of the seepage and augmentation of the water pore pressure in the joints).

UNIL | University of Lausanne
Faculty of Geosciences and Environment
Geopolis
CH-1015 Lausanne

6 Summary

This report provides a slope stability analysis of the rocky spur located at the NE of North Peak, in Turtle Mountain (Fig. 1). In particular it aims at 1) understanding the rock mass structure and the kinematic behaviours and 2) highlighting the volume of a potential rock failure event and its failure mechanism.

It presents 1) a detailed structural analysis, 2) a kinematic analysis allowing the determination of the failure mechanisms, 3) a distinct element modelling of the potential failure and 4) a complementary estimation of the unstable volumes using the SLBL method.

Six discontinuity sets are outlined by the structural analysis. The kinematic analysis revealed that both planar sliding and wedge sliding mechanisms are likely to occur. Even if not kinematically pointed out, toppling failure mechanism also has to be considered.

Two scenario of potential failure with related volumes estimation are proposed:

1) Failure on the frontal part of the spur (**shallow failure**), corresponding to a volume of **0.24 Mm^3**. Both UDEC^{TM} modelling and SLBL method reach similar volume estimation. The failure mechanism is described as **a bi-planar sliding** involving joint sets J2, J3/J3' and J4, which is in good accordance with the kinematic analysis. Toppling of the unstable zone across bedding is also highlighted.

   ➔ This first scenario shows **the maximal volume** that can be involved in case of failure based on the present-day situation parameters (fracturing, rock mass). It has to be considered if significant signs of increasing activity (deformations, rockfalls) occur in the concerned area.

2) A second scenario is proposed (**deep scenario**) reaching a volume of **3.5 Mm^3**. The volume estimation is based on the SLBL calculation only. This scenario is quite highly unlikely and has to be taken into account only in case of movements' detection (remote monitoring) affecting the whole spur. Indeed, it implies a radical and abrupt decrease of both joint and rock mass quality. Especially a decrease of the friction angle and an increase of the persistence of all joint sets (fully persistent) are required. Based on the present-day parameter, this scenario is therefore considered as highly unlikely without an important decrease of the rock mass.

UNIL | University of Lausanne
Faculty of Geosciences and Environment
Geopolis
CH-1015 Lausanne

7 Provided data

3 files are provides in appendix of this report in different file format: GRD, GRID, TIFF, ASCII:

- **Present day topography** (1m cell size).

- Topography after the SLBL calculation for the "**shallow instability**" with an unstable volume of **0.24 Mm^3** (model *SNP_shall_10*). Note that the volume estimation for the different simulations (UDEC and SLBL) range between 0.1 and 0.24 Mm^3. For runout analysis purpose, the most conservative volume is suggested to be taken into account.

- Topography after the SLBL calculation for the "**deep instability**" with an unstable volume of **3.54 Mm^3** (model *SNP_deep_33*). Note that the volume estimation for the different simulations (SLBL only) range between 2.8 and 4.4 Mm^3. For runout analysis purpose, an average volume of 3.54 Mm^3 is suggested to be taken into account.

The *ArcGis* project (.mxd) is also provided.

UNIL | University of Lausanne
Faculty of Geosciences and Environment
Geopolis
CH-1015 Lausanne

8 References

Benko, B., Stead, D., 1998. The Frank Slide: a reexamination of the failure mechanism. Canadian Geotechnical Journal 35 (2), 299 – 311.

Brideau, M., Pedrazzini, A., Stead, D., Jaboyedoff, M., Froese, C.R., Van Zeyl, D., 2011. Three-dimensional slope stability analysis of South Peak, Alberta, Canada. Landslides 8(2),139–158.

Brideau, M.-A. and Stead, D., 2012 Evaluating kinematic controls on planar translational slope failure mechanisms using three-dimensional distinct element modeling. Geotech. Geol. Eng, 30, 991-1011.

Fisher, B.R., 2009. Improved characterization and analysis of bi-planar dip slope failures to limit model and parameter uncertaintly in the determination of setback distances. PhD thesis, University of British Columbia, 256p.

Fisher, B. and Eberhardt, E., 2012. Assessment of Parameter Uncertainty Associated with Dip Slope Stability Analyses as a Means to Improve Site Investigations. J. Geotech. Geoenviron. Eng., 138(2), 166–173.

Froese, C.R., Moreno, F., Jaboyedoff, M., Cruden, D.M., 2009. 25 years of movement monitoring on South Peak, Turtle Mountain: understanding the hazard. Canadian Geotechnical Journal 46, 256 – 269.

Froese, C.R., Charrière, M., Humair, F., Jaboyedoff, M., Pedrazzini, A., 2012. Characterization and management of rockslide hazard at Turtle Mountain, Alberta, Canada. In: Clague, J.J., Stead, D. (Eds.), Landslides Types, Mechanisms and Modelling. Cambridge University Press, New-York, pp. 310–322.

Hoek, E., 2000. Rock Engineering Course Notes by Evert Hoek (2000 edition)." North Vancouver, B.C., p 313.

Humair, F., 2011. Turtle Mountain anticline (Alberta, Canada): rock slope stability related fracturing - folding, fracturing, rock mass condition, slope stability investigations and geological modeling. (Unpublished Master Thesis) Institute of Geomatics and Risks Analysis and Institute of Geology and Paleontology, University of Lausanne, Switzerland.

Humair, F., Charrière, M., Pedrazzini, A., Güell I Pons, M., Volpi, M., Foresti, L., Jaboyedoff, M., Epard, J.-L., Froese, C.R., 2010. The Frank Slide (Alberta, Canada): from the contributing factors to the processes of propagation. Proceedings of the 63rd International Canadian Geotechnical Conference & 6th Canadian Permafrost Conference (Calgary)

Humair F, Pedrazzini A, Epard J.-L., Froese C, Jaboyedoff M., 2013. Structural characterization of Turtle Mountain anticline (Alberta, Canada) and impact on rock slope failure. Tectonophysics, 605 (2013) 133-148. doi:10.1016/j.tecto.2013.04.029.

International Society for Rock Mechanics (ISRM), 1978. Suggested methods for the quantitative description of discontinuities in rock masses. International Journal of Rock Mechanics and Mining Sciences and Geomechanics Abstracts 15, 319 – 368

Jaboyedoff, M., Couture, R., Locat, P. 2009. Structural analysis of Turtle Mountain (Alberta) using digital elevation model: Toward a progressive failure. Geomorphology 103, 5-16.

Pedrazzini, A., Froese, C.R., Jaboyedoff, M., Hungr, O., Humair, F., 2012. Combining digital elevation model analysis and run-out modeling to characterize hazard posed by a potentially unstable rock slope at Turtle Mountain, Alberta, Canada. Engineering Geology 128, 76-94.

Pedrazzini, A., Jaboyedoff, M., Froese, C.R., Langenberg, C.W., Moreno, F., 2011. Structural analysis of Turtle Mountain: origin and influence of fractures in the development of rock slope failures. Geological Society of London, Special Publications 351, 163-183.

Appendix 3 – Expert Panel Review

Expert Panel Review of Turtle Mountain Monitoring Program

Lars Harald Blikra, Chief Geologist, Åknes/Tafjord Early Warning Centre, Norway
Giovanni Crosta, Professor, University of Milano Bicocca, Italy
Jacques Locat, Professor, University of Laval, Quebec, Canada

October, 2014

This information is preliminary and is subject to revision. It is being provided to meet the need for scientific review of the Turtle Mountain Monitoring Program. The information is provided as a guidance document to suggest improvement on the monitoring program future to the Alberta Geological Survey/Alberta Energy Regulator. The expert panel shall not be held liable for any damages resulting from the authorized or unauthorized use of this information.

Report prepared for the Alberta Energy Regulator, Alberta Geological Survey:
Draft delivered: July 15, 2013
Final delivered: October 27, 2014

Prepared by:
Lars Harald Blikra, Chief Geologist, Åknes/Tafjord Early Warning Centre, Norway
Giovanni Crosta, Professor, University of Milano Bicocca, Italy
Jacques Locat, Professor, University of Laval, Quebec, Canada

Introduction

The Alberta Energy Regulator (AER) /Alberta Geological Survey (AGS) have appointed an expert panel to provide independent, internationally recognized review and advice on the Turtle Mountain Monitoring Program and its future tasks.

On July 3rd 2013, a one day workshop on the Frank Slide was held in Waterton, Alberta, to review ten years of monitoring activities. Presentations were given by AGS, University of Lausanne, various consultants, and the Frank Slide Interpretive Centre. On July 4th, a site visit to Turtle Mountain (TM) to have a close look at the monitoring system put in place over the last ten years.

One of the main objectives was to evaluate how the acquired knowledge about the Frank Slide could be used to revisit the early warning system approach and monitoring strategy. AGS has presented the following options for discussion:

(1) No change to the current situation,

(2) return to a monitoring aimed at characterizing and tracking the hazard (vigilance), and/or

(3) Discontinue monitoring. It appeared from the presentation by AGS that they would favour option 2. The expert panel team were asked to contribute to the discussion and provide our opinion on this issue.

Our brief report will address the following points;

1. Characterization and hazard
2. The implemented monitoring at Turtle Mountain and the current early warning system
3. Recommendations
    - for further characterization and hazard evaluation,
    - for real-time monitoring and early warning,
    - for changes in monitoring and management strategy, and
    - for organizational aspects and governmental affiliation/commitment.

Site characterization and hazard assessment

A series of technical and scientific papers and yearly status reports from AGS describe the work and findings from the characterization work of Turtle Mountain's instabilities. The latest summary of the hazard characterization is given by Moreno & Froese (2012) and Pedrazzini et al. (2011).

The characterization and hazard evaluation for the potential future rockslides from Turtle Mountain have been performed in collaboration with different international groups. They are published in high-level journals, and it is our opinion that this work is of high international quality and standard. In this report we will focus on some topics that are of importance for the final hazard evaluation:

(1) The geological and structural model for the instabilities,

(2) the estimated volumes and runout,

(3) the present day rate of movement and state of activity, and

(4) the possibility to predict the time of failure.

Geological and structural model

A geological model for large slope instabilities needs to be built by integrating different datasets, like structural geology (bedding, fractures), geomorphology, topography, displacement patterns and stability modelling. The structural data from Turtle Mountain is very well documented (Humair et al., 2013), but is very complex including the highly varied bedding attitude along the anticline and of fracture sets. This opens for several possibilities for structural control of possible large failures and at the same time predispose to a complex set of movement types in the upper scarp and crown area, making difficult a full interpretation of the evolution.

The papers and reports present a series of different possible instabilities on Turtle Mountain and most authors conclude that the scenarios from South Peak (upper and lower instability) are the most likely ones. Several profiles are presented from this area, but there seems to be a need for a long profile going through both the upper and lower instability of the South Peak, following the directions of the main displacement direction towards the northeast.

Displacement rate and pattern

Since 1903, various types of measurement devices have been used at the Frank Slide to measure the displacement of rock masses with the most significant effort taking place since 2003 (Froese et al. 2009). Movements have been analyzed in detail by Froese et al. (2009). The longest set of measurements is provided by a series of control points positioned and identified on large scale aerial photographs for displacement computation ranging from 1985 to 2005. These analyses give a displacement rate ranging from 0.9 to 3.2 mm/year. Local crackmeters have indicated movement of order at 1 mm per year (Figure 2).

Therefore, following ten years of detailed monitoring it is clear that the rate of various sliding mechanisms (wedge, toppling/sliding) identified on the slope can be considered as extremely slow using Cruden and Varnes classification (1996, i.e. displacement rate lower than 16 mm/year).

Observed fissures pattern surrounding the Frank Slide scarp is probably a direct result of slope re-adjustments following the initial 1903 slide. As well considering the partial occlusion of large tension cracks by superficial debris in this area. The instability zones identified along the escarpment of the Frank Slide can be considered as post-slide re-adjustment which could control various future failure scenarios. When considering the cumulated displacements as provided by the fracture opening, it seems clear that most of the movements leading to these fractures took place as part of the nearly immediate post-slide stress relief adjustment in the slope. The actual opening of these fissures should be considered, per se, as a sign of slide activity, but presently occurring at an extremely slow rate.

As a summary, a large effort has been done in the program to investigate the displacements on Turtle Mountain, including both remote sensing methods (photogrammetry, satellite- based and ground- based InSAR) and in-situ methods (GPS, total station, crackmeters, tiltmeters). The displacements documented on Turtle Mountain are very small compared to other monitored rockslides, and this makes the interpretation of the displacement data difficult. There appears to be some inconsistencies in the reported displacement directions in the presented models. This should be solved or explained so to have a more complete and definitive rockslide model. A summary map showing all displacement data should be prepared. This is important for the evaluation of the presented geological models related to the potential instabilities.

Slide volume

The 1903 slide mobilized a volume estimated at about 30 $*10^6$ m^3. After 10 years, a detailed morpho-structural analysis, combined to kinematic and displacement measurements, led to the establishment of various slide scenarios. According to these scenarios identified by AGS, the potential events could generate a maximum volume of 10 $*10^6$ m^3 coming from the upper and lower instability at South Peak. The potential runout of a slide originating from the South Peak has been estimated over time by means of different approaches, with the latest estimate showing a more restricted runout distance. However, all scenarios do indicate that slide debris would reach inhabited parts of the terrain below the slope and would reach the highway and railroad. Although the scenarios from the North Peak involve a much smaller volume, a runout analysis still remains to be performed for this sector.

Although the latest runout modeling carried by Hungr (2008) has been calibrated using the 1903 Frank Slide and the Jonas Creek Slide (Figure 1) one must remember that there are still uncertainties about various aspects such as:

- the transformation of the solid mass into a fluid-like material,
- the role of the type of initial sliding/falling mechanism on the post-failure behaviour of the moving mass, and
- the numerical model capabilities and limitations.

Therefore, regarding slide volume, the various scenarios appear realistic and it appears that no reason subsists for modifying the current land-use planning, unless proven otherwise by further analyses to be carried out by a competent consulting firm.

Predicting the timing of the event

It is known that increasing acceleration of movements can be observed several weeks and months before an actual event. A compilation of known rate of movements for various slides around the World is shown in Figure 3 and 4, together with the threshold values proposed for the Åknes rockslide in Norway and Turtle Mountain. The rate of movement indicative of a 'yellow' alert is in the two proposals suggested to be of 1.5 mm/day, i.e. c. 450 mm/year.

The rate of movement estimated over the last 25 years at Turtle Mountain is extremely low. This is far below other rockslides which are under early warning and not at a velocity close to the yellow alert. However, the large open fractures existing on the mountain behind the scarp of the 1903 event and the recorded displacements, even if limited, suggest that vigilance is still required.

In order to help identify a warning criterion, AGS developed a velocity curve based on international documented events, and placed the thresholds in the lower sector. Considering the current rate of movement and the expected rate leading to a yellow alert, it becomes clear that a large change needs to occur in terms of stability conditions in order to fail a large portion of the mountain. A quantification of hazard is extremely difficult for large-scale and complex landslides and the evaluation of the need of real-time early warning is often based on the rate of active displacements.

Considering the extremely low displacement rates, also seen in relation to other rockslides monitored internationally, a change from real-time monitoring to periodically monitoring checks of the instabilities would be adequate for handling the actual risk. The future monitoring could then take advantage of the acquired knowledge on the Frank Slide and exploitation of new remote sensing technologies.

The monitoring and early warning system

The ongoing monitoring system put in place over the last 10 years has greatly evolved to take advantage of the cooperation with other monitoring projects worldwide and the developing technologies.

In general, the system involves two types of data acquisition:

(1) Point source data (e.g. displacement at a given point obtain by a single instrument like GPS, crack meter, or simple target), and

(2) remotely sensed aerial/volumetric data obtained by scanner type instruments like terrestrial, airborne LiDAR, or ground-based Radar.

The monitoring system at the Frank Slide is of excellent quality. It has been set up following modern and correct technical standards and its development represents a serious effort made by the AGS to use the best available and suitable techniques also for the improving and renovation of the original instrumentation. Actually, by looking at the GPS system and the GB Radar, it is clear that the Frank Slide has been used as a test site for companies interested to develop monitoring tools. This again supports the idea that the characterization and monitoring work performed at the Frank Slide is of a very high standard.

All these instruments have generated an impressive amount of data that enabled AGS to finely evaluate the behaviour of Turtle Mountain. Moreover, as discussed below, all the movements observed at the Frank Slide are now integrated in order to get an improved understanding of the processes involved in the instability assessment and forecasting.

The entire early warning system developed by AGS is to be seen as world-leading, and has a systematic focus on roles and responsibilities. All routines connected to responsibilities and operation of the early warning system and during normal actions, and emergencies are well documented and reported (e.g. Moreno & Froese, 2009).

It is our opinion that the overall monitoring and the early warning system are well implemented for the Turtle Mountain Program. However, the implementation of the early warning system is based on the decision in 2005, when the AER through AGS took ownership and responsibility for the long-term monitoring, including the warning to the Alberta Emergency Management Agency.

At that time, the appraisal of the need of a real-time early warning system was relatively weakly based, but definitively required considering the field evidences only. The most recent data and understanding of the Turtle Mountain instabilities make a need of a re-evaluation of the hazard and thus the requirement for real-time early warning system.

Recommendations (Advices)

We were specifically asked to write a report that considers discussions and material from the workshop and that provides guidance for next monitoring and site management phase at Turtle Mountain. One of the key questions is the need of having a real-time early warning for Turtle Mountain.

In the following, we give some main recommendations linked to characterization, the need for real-time monitoring/early warning and on organizational issues.

Site characterization and hazard evaluation

An impressive work has been done in order to characterize and understand the instabilities at Turtle Mountain. In spite of this, some remaining questions are related to the geological model and the displacement pattern, which are important for the hazard evaluation and the long-term handling by state and local authorities.

We propose to continue the characterization phase by performing annual campaigns by using ground-based InSAR, which can cover the entire front of all the instabilities at Turtle Mountain. Some problems concerning data acquisition and the location of the system should be solved in order to maximize the resolution and the line of sight (LOS). Repeated LiDAR scans can also be considered.

Furthermore, as also suggested by AGS, a continued exploring of the use of finer resolution satellite based InSAR data should supplement the ground-based campaigns. This may be even more interesting as satellite InSAR images can be obtained at least few time per year or better.

We also suggest performing runout analyses for the scenarios proposed for the North Peak sector, although these are probably not that critical.

We recommend that the main conclusions and summary related to the geological/structural model and the displacement pattern be summarized in a short AGS report together with the proposed changes and plans for future handling, and for future decisions by the involved municipality.

Real-time monitoring and early warning

AGS proposed in the workshop a change of the monitoring schedule on Turtle Mountain from real-time monitoring to a new and updated characterization phase.

We agree with AGS proposal on the fact that there is a need to evolve towards a monitoring strategy adjusted to the acquired knowledge on the rate of movement of the critical parts of Turtle Mountain. Nevertheless, it must be kept in mind that the danger is still there and that the timing of a major catastrophic event may be decades down the road. In the meantime, vigilance must remain active and land-use planning must be ascertained to ensure a "no development zone" in the estimated runout zone, unless proven otherwise.

It is important to continue a basic monitoring (mostly remote) for a continued characterization of the Frank Slide in order to improve the understanding on the development of the instability. This will ensure a minimum monitoring so that, at any sign of acceleration in the rate of movement, a quick response could be established in order to ensure an adequate risk management. This means that there is a need for making a clear plan for the re-establishment or deployment of in-field monitoring systems if it should be required.

It is also recommended to continue some periodic GPS measurements (e.g. yearly or every second year campaigns), since the data is essential in order to get real displacement vectors to be compared with the InSAR data.

Organizational aspects

The Turtle Mountain Program has been so far very well organized. AGS has shown to be highly reliable on the roles and responsibility for the real-time and operational monitoring and early warning issues during such a long time span.

Despite the suggestions to reduce the real-time monitoring, it is still critical to continue the long-term characterization and periodic monitoring to ensure a control on the overall stability conditions.

It is important to stress the need for a more formal commitment by the Alberta Energy Regulator in order to ensure that AGS maintains the necessary long-term actions on the Turtle Mountain. This can be done by having a long-term plan that includes procedures for annual or semi-annual status reports and at an increased frequency in case of changes in the state of activity. Concerning this last point, it is important to define the steps to be undertaken in case of a progressive or rapid change in behavior of the unstable slope sectors.

Conclusions

The expert panel is generally impressed by the work performed by AGS on the Turtle Mountain Monitoring Program and the responsibility taken on issues related to real-time monitoring and early warning.

We agree with AGS that the future operations and management should be focused on refine characterization and that the real-time monitoring and early warning can be withdrawn.

This is mainly based on the conclusion that the active movements at the potential instabilities are extremely slow.

We recommend that a summary report be produced presenting an overview of the main findings and conclusions regarding stability and displacements, and which states the strategy for the new phase of the activities at Turtle Mountain.

We suggest that there should be a revisit and review after 5 years. Furthermore, we advise the Alberta Energy Regulator implements a formal commitment for AGS to ensure a sustainable long-term risk handling for the Turtle Mountain area.

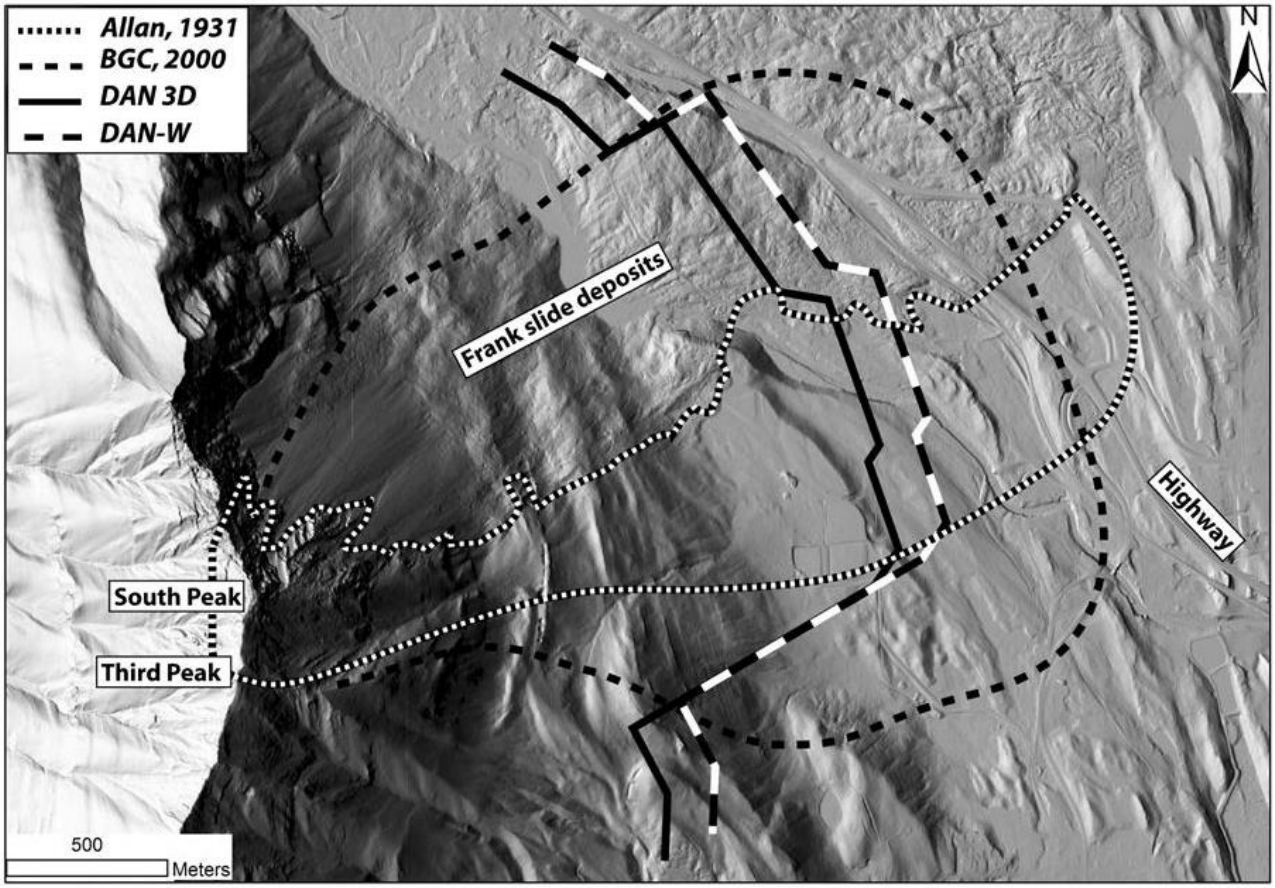

Figure 1. (Figure 23 of AGS OFR 2010 (2012-03)).

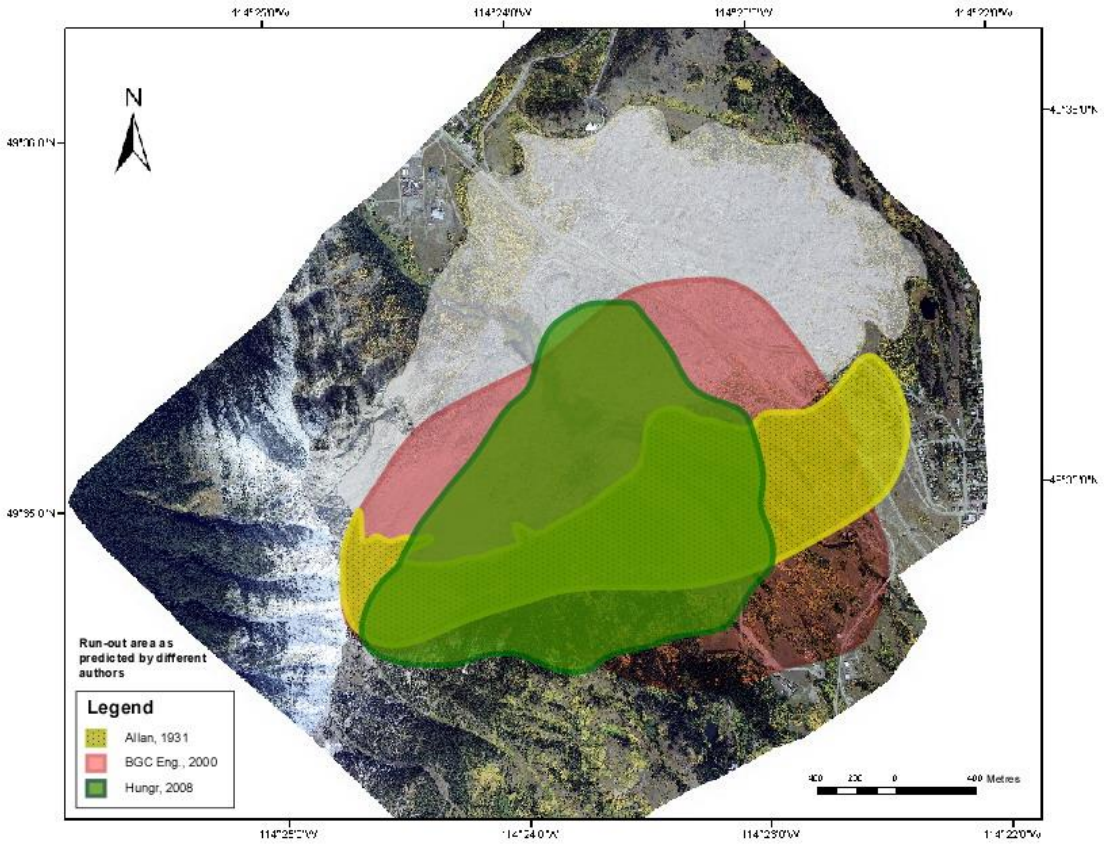

Alternate Figure 1. (Figure 3, Froese and Moreno, 2011).

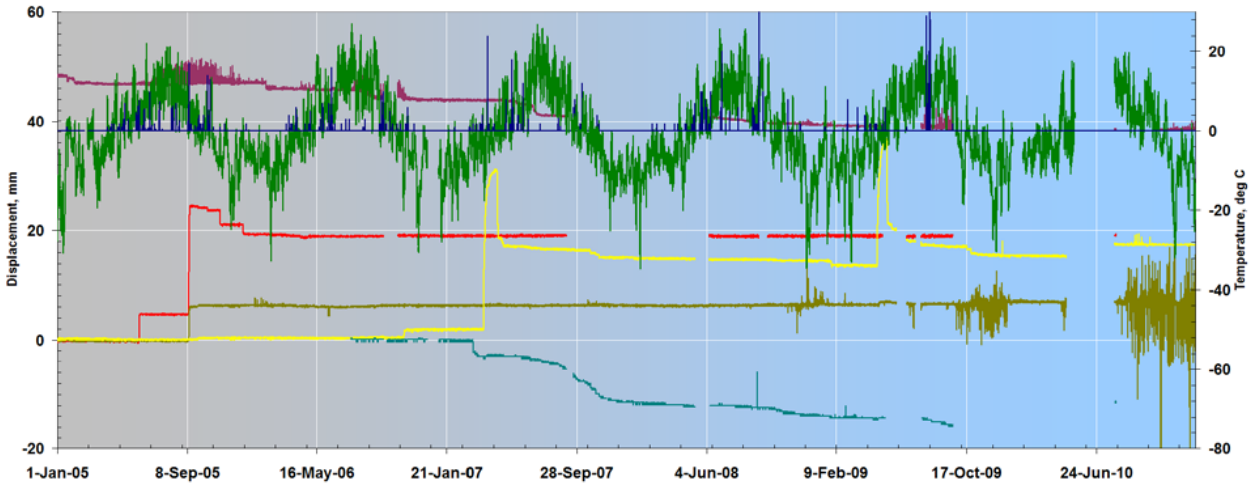

Figure 2. (Figure 10 of AGS OFR 2010 (2012-03)).

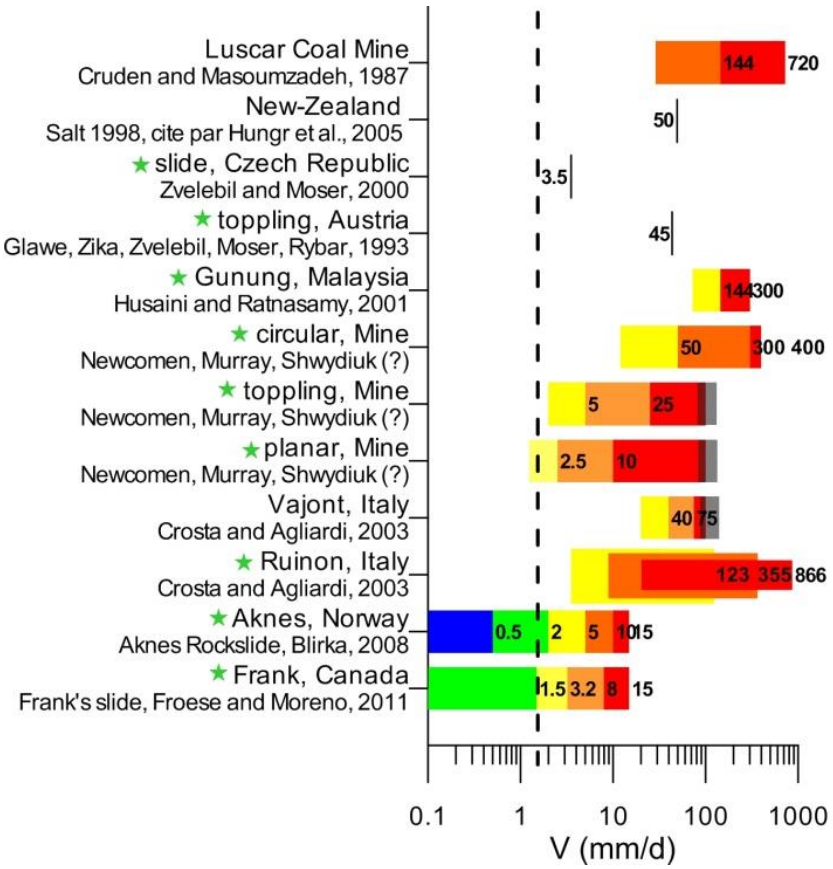

Figure 3. Different values of velocity criteria threshold for warning system found in literature. Colors have been adapted for this figure (some authors did not associate values with colors; from Locat et al. 2013).

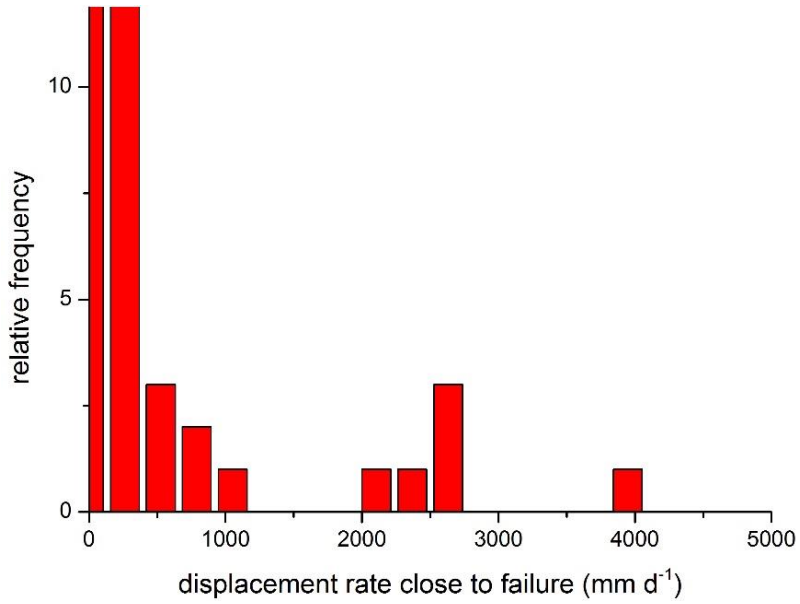

Figure 4. Histogram of relative frequency of displacement rate values close to the catastrophic collapse for a sample of 53 historical events (Crosta et al., 2013).

References

CRUDEN D.M. & VARNES D.J. (1996) *Landslide types and processes* in Turner & Schuster, *Landslides, Investigation and Mitigation*, Special Report 247, National Academy Press, Washington, D.C.

CROSTA, G.B., IMPOSIMATO, S., RODDEMAN, D. (2013). Monitoring and modelling of Rock Slides and Rock Avalanches. Italian journal of engineering geology and environment, 3-14 10.4408/IJEGE.2013-06.B-01.

FROESE, C., MORENO, F., JABOYEDOFF, M. and CRUDEN, D. (2009): 25 years of movement monitoring on the South Peak of Turtle Mountain: understanding the hazard; Canadian Geotechnical Journal, v. 46, p. 256–269.

FROESE, C., and MORENO, F. (2011): Structure and components for the emergency response and warning system on Turtle Mountain, Alberta, Canada. Nat Hazards, 1689-1712 10.1007/s11069-011-9714-y.

HUMAIR, F. and JABOYEDOFF, M. (2013): North Peak area stability analysis (Turtle Mountain): description and mechanisms of the unstable volumes; unpublished report, Faculty of Geosciences and Environment, University of Lausanne, Switzerland, 24 p.

HUNGR, O. (2008): Turtle Mountain, Frank, Alberta; Runout analyses of potential landslides on South and Third Peaks.; unpublished report prepared by Geotechnical Research Inc. for Alberta Geological Survey, 51 p.

LOCAT, J., CLOUTIER, C., and JABOYEDOFF, M., 2013. A risk evaluation approach for an active rock slide: the Gascons coastal rock slide, Québec. Proceedings of the 66th Canadian Geotechnical conference, Montréal, Paper 591, 8p.

MORENO, F. and FROESE, C. (2009b): ERCB/AGS roles and responsibilities manual for the Turtle Mountain Monitoring Project, Alberta, ERCB/AGS Open File Report 2009-06, 35 p.

MORENO, F. and FROESE, C. (2012): Turtle Mountain Field Laboratory: 2010 data and activity summary; Energy Resources Conservation Board, ERCB/AGS Open File Report 2012-03, 22 p.